

**Chromatographic and Spectroscopic Data of
Phytochemicals from *Cannabis sativa* Roots**



**A Dissertation submitted to the Department of Chemistry,
Quaid-i-Azam University, Islamabad**

In partial fulfilment of the requirement for the degree of

Master of Philosophy

In

Organic Chemistry

By

Qurat-ul-Ain

Department of Chemistry

Quaid-i-Azam University, Islamabad

2015



*I dedicate my dissertation work to my
Father, Mother, my beloved brothers Ibtisam and Muzaid
(late), to my cute sister Aseena and also to my dear husband Ali
Zaheer-ud-Din*

ACKNOWLEDGEMENTS

All praises to the **Allah Almighty**, who induced me with intelligence, knowledge and wisdom. Peace and blessings of Allah be upon the Holy Prophet, who exhorted his followers to seek for knowledge from cradle to grave.

I am highly indebted to my supervisor, **Dr. Muhammad Farman**, Assistant Professor, for motivating me to undertake these studies and also for his continuous support during my M. phil study, for his patience, motivation, enthusiasm and immense knowledge. His guidance helped me in all the time of research work.

My sincere thank goes to Chairman Department of Chemistry, QAU, **Prof. Dr. Amin Badshah and Prof. Dr. Shahid Hameed** for providing me all the facilities during my research work. I am also thankful to all teaching and nonteaching staff of the chemistry department for their support.

I would like to thank my lab fellows specially **Ms. Saba, Ms. Noreen, Ms. Aaminah Jamil, Ms. Madiha Aqsa, Sadia Ameer, Komal Ifitkhar and Sofia Basharat** for their moral support, generosity and encouragement throughout this research work. I would like to express my appreciation to all my class fellows and friends for their kindness and moral support. Thanks for friendship and beautiful memories.

Last but not least, my deepest gratitude goes to my beloved **Father and Mother** for their unconditional support, both financially and emotionally throughout my degree, also special thanks to my brothers **Ibtsam-ur-Rehman and Muyaid-ur-Rehman (late)** and also to my beloved sister **Aleena Rehman**. I am also grateful to my mamon **Prof. Zaheer-ud-din**, and my teacher **Ms. Tasneem** for their endless love, prayers and encouragement. I also dedicate this dissertation to my husband **Ali Zaheer-ud-Din**, who has offered unwavering support and encouragement. Thank you very much.

Qurat-ul-Ain

Contents

List of Abbreviations	i-
List of Figures	iii
List of Tables	viii
List of Schemes	ix
Abstract	xiii
Chapter 1 Introduction	01
1.1 Literature Survey of <i>Cannabis Sativa</i>	03
1.1.1 Phytochemical Constituents	03
1.1.1.1 Fatty acids	03
1.1.1.2 Glycoproteins	03
1.1.1.3 Flavonoids	03
1.1.1.4 Terpenoids	04
1.1.1.5 Cannabinoids	04
1.1.2 Extractions	09
1.1.3 Biosynthesis	10
1.1.4 Hemp Fiber	10
1.1.5 Hemp Biomass	11
1.1.6 Hemp as Poison	12
1.1.7 Microelements of <i>Cannabis</i>	12
1.1.8 Storage of <i>Cannabis</i>	13
1.1.9 Oil and Flour of <i>Cannabis</i>	13
1.1.10 Pharmacological Activities	13
1.1.10.1 Antileishmanial Activities	13
1.1.10.2 Antitumor Drug	13
1.1.10.3 Antioxidant Activity	14
1.1.10.4 Antiprotozoal Activity	14
1.1.10.5 Chemopreventive Effect	14
1.1.10.6 Antineoplastic	14
1.1.10.7 Anticonvulsant	14

1.1.10.8	Antipanic Effect	14
1.1.10.9	Antiinflammatory	14
1.1.10.10	Anxiolytic Effect	15
1.1.10.11	Antispasticity	15
1.1.10.12	Antiemetic	15
1.1.10.13	Antipsychotic	15
1.1.11	Concluding Remarks	16
Chapter 2	Materials and Methods	17
2.1	Choice of plant	17
2.2	Taxonomic Ranking and Description of <i>C. sativa</i>	17
2.3	Family	17
2.4	Trivial Names	18
2.5	Geographical Distribution	18
2.6	Morphological Description	18
2.7	Extraction	18
2.7.1	Maceration followed by Ultrasonication	19
2.7.1.1	Analysis by GC-MS	19
2.7.1.2	Analysis by HPLC-DAD-ESI-MS	20
2.7.2	Soxhlet Extraction	20
2.7.2.1	Analysis by GC-MS	21
2.7.2.2	Analysis by HPLC-MS	21
2.8	Preliminary Qualitative Analysis	21
2.8.1	Acid Hydrolysis	21
2.8.1.1	Procedure for Acid Hydrolysis	21
2.8.1.2	Analysis of Sugars	21
2.8.1.3	Analysis of Aglycones	22
2.8.1.4	Analysis by HPLC-DAD-ESI-MS	22
2.8.2	Alkaline Hydrolysis	22
2.8.2.1	Procedure for Alkaline Hydrolysis	22
2.8.2.1.1	Analysis of Ether Layer	23
2.8.2.1.2	Analysis by HPLC-DAD-ESI-MS	23
2.9	Qualitative Analysis	23

2.9.1	HPLC-DAD-ESI-MS Profiling	23
2.9.1.1	Instrumentation	24
2.9.1.2	Stationary Phase	24
2.9.1.3	Gradient Elution Program	25
2.9.1.4	Mobile Phase	25
2.9.1.5	Sample Preparation	25
2.10	GC-MS Profiling	26
2.10.1	Instrumentation	26
2.10.2	Sample Preparation	27
2.11	Chromatographic Technique	27
2.11.1	Selection of Column Packing	27
2.11.1.1	Cellulose	27
2.11.1.2	Silica	27
2.11.2	Column Chromatography 1	28
2.11.3	Column Chromatography 2	28
2.12	Isolation of Cannabinoids	29
2.12.1	Procedure for isolation of Cannabinoids	29
2.12.2	Purification	29
2.12.3	Spraying Reagents	30
2.12.4	Duquenois Levine Reagent	30
2.12.4.1	Procedure	30
Chapter 3	Results and Discussions	31
3.1	Acid and Alkaline Hydrolysis	31
3.1.1	Results of Acid Hydrolysis for Sugar Identification	31
3.1.1.1	TLC	31
3.1.2	Results of Alkaline hydrolysis	32
3.1.2.1	TLC	32
3.2	Results and Discussions of GC-MS analysis	34
3.3	Volatile Compounds of CS-E extract	38
3.3.1	CS-E1	38
3.3.2	CS-E2	39
3.3.3	CS-E3	41

3.3.4	CS-E4	43
3.3.5	CS-E5	44
3.3.6	CS-E6	46
3.3.7	CS-E7	48
3.3.8	CS-E8	50
3.3.9	CS-E9	51
3.4	Volatile Compounds of CS-ET-SOX Extract	53
3.4.1	CS-E10	54
3.4.2	CS-E11	55
3.4.3	CS-E12	56
3.4.14	CS-E13	58
3.5	Volatile Compounds of CS-H Extract	60
3.5.1	CS-H1	60
3.5.2	CS-H2	61
3.5.3	CS-H3	62
3.5.4	CS-H4	64
3.5.5	CS-H5	66
3.5.6	CS-H6	67
3.6	Volatile Compound of CS-A Extract	70
3.6.1	CS-A1	70
3.7	Volatile Compounds of CS-PE Extract	72
3.7.1	CS-PE1	72
3.7.2	CS-PE2	73
3.7.3	CS-PE3	74
3.7.4	CS-PE4	74
3.7.5	CS-PE5	77
3.7.6	CS-PE6	78
3.7.7s	CS-PE7	80
3.8	Results of HPLC-DAD-ESI-MS analysis	85
3.9	HPLC	85
3.10	DAD	85
3.11	ESI-MS	88

3.12	Compounds Identified from CA-E Extracts	92
3.12.1	Chromatographic Profiling of CA-E Extracts	92
3.12.1.1	CA-E1	93
3.12.1.2	CA-E2	95
3.12.1.3	CA-E3	97
3.12.1.4	CA-E4	99
3.12.1.5	CA-E5	101
3.12.1.6	CA-E6	103
3.12.1.7	CA-E7	105
3.12.2	Chromatographic Profiling of CA-A Extracts	108
3.12.2.1	CS-A1	108
3.12.2.2	CS-A2	111
3.12.2.3	CS-A3	113
3.12.3	Chromatographic Profiling of CA-Ex-Sox	116
3.12.3.1	CA-EX1	117
3.12.3.2	CA-EX2	119
3.12.3.3	CA-EX3	122
3.12.3.4	CA-EX4	124
3.12.4	Chromatographic Profiling of Ca-AH	126
3.12.4.1	Ca-AH1	126
3.12.4.2	Ca-AH2	128
3.12.4.3	Ca-AH3	131
3.12.4.4	Ca-AH4	133
3.12.4.5	Ca-AH5	135
3.12.4.6	Ca-AH6	137
3.12.4.7	Ca-AH7	139
3.12.4.8	Ca-AH8	141
3.12.4.9	Ca-AH9	143
3.13	HPLC-DAD-ESI-MS Analyses of Cannabinoids	146
3.13.1	C-1	146
3.13.2	C-2	147
3.13.3	C-3	149

3.13.4	C-4	151
3.13.5	C-5	153
3.13.6	C-6	155
3.13.7	C-7	157
3.13.8	C-8	159
3.13.9	C-9	159
3.14	Column Chromatographic Results	162
3.14.1	Cannabinoid Isolation Results	162
3.14.2	Results of Duquenois Levine Reagents	164
3.15	Conclusions	166
	References	169

List of Abbreviations

TEMPO	2,2,6,6-Tetramethylpiperidine-1-oxyl radical
AcOH	Acetic Acid
CBC	Cannabichromene
CBCA	Cannabichromenic acid
CBL	Cannabicyclol
CBLA	Cannabicyclic acid
CBD	Cannabidiol
CBDA	Cannabidiolic acid
CBG	Cannabigeriol
CBGA	Cannabigerolic acid
CBN	Cannabinol
CBNA	Cannabinolic acid
C ₄ H	Cinnamic acid-4-hydroxylase
Δ^8 -THC	Delta-8-tetrahydrocannabinol
Δ^9 -THC	Delta-9-tetrahydrocannabinol
THCA	Delta-9-tetrahydrocannabinolic acid
THCA-C4	Delta-9-tetrahydrocannabinolic acid-C4
THV	Delta-9-tetrahydrocannabivarin
THVA	Delta-9-tetrahydrocannabivarinic acid
DEAE	Diethylaminoethyl
DAD	Diode-Array-Detector
DPAG	Dorsal Periaqueductal Grey
ESI	ElectroSpray Ionization
EtOAc	Ethylacetate
FIRSST	Feedstock Impregnation Rapid and Sequential Steam Treatment
Fig.	Figure
FID	Flame Ionization Detection

GC-MS	Gas Chromatography Mass Spectrometry
Gla	Galactose
Glc	Glucose
HS-SPME	Headspace Solid Phase Microwave Extraction
HHB	Hemp Hurd Biomass
HCC	Hepatocellular Carcinoma
HPLC	High Performance Liquid Chromatography
HDI	Hydrogen Deficiency Index
i.d	Internal Diameter
LC	Liquid Chromatography
<i>m/z</i>	Mass to Charge ratio
min.	Minute
MS	Multiple Sclerosis
OA	Olivetolic acid
OAC	Olivetolic Acid Cyclase
PAL	Phenylalanine Ammonia Lyase
PS 2	Photosystem 2
PTLC	Preparative TLC
t_R	Retention time
RP Column	Reverse Phase Column
Rha	Rhamnose
TLC	Thin Layer Chromatography
TIC	Total Ion Current
2D-TLC	Two Dimensional Thin Layer Chromatography
UV	Ultraviolet
Xyl	Xylose

List of Figures

- Fig. 1** (a) Aerial Parts (b) Roots of *Cannabis sativa*
- Fig. 2.1** Soxhlet Extractor
- Fig. 2.2** Brown Color Crystals of acid hydrolysate
- Fig. 2.3** Mechanism of Cannabinoids with Duquenois Levine reagent
- Fig. 3.1** TLC Chromatogram of Sugar constituents from *Cannabis sativa* roots visualized under Short wavelength UV light (254nm) using Aniline hydrogen phthalate reagent
- Fig. 3.2** 2-D TLC Chromatogram of Phenolic acids from *C. sativa* roots under short wavelength UV light (254nm)
- Fig. 3.3** TIC profile of CS-E extract
- Fig. 3.3.1** 1-Ethyl-3,5-dimethylbenzene
- Fig. 3.3.2** Methyl Derivative of Cannabidivarin
- Fig. 3.3.3** Cannabinol
- Fig. 3.3.4** Bicyclo[3.1.0]hexan-2-one
- Fig. 3.3.5** Ethyltridecanoate
- Fig. 3.3.6** N-Methyl-2,7,15-eicosatrienoic acid
- Fig. 3.3.7** Linoleic acid methyl ester
- Fig. 3.3.8** 3,4-Dichloro-6-nitrophenol
- Fig. 3.3.9** Lanosterol
- Fig. 3.4** TIC profile of CS-ET-SOX
- Fig. 3.4.1** 1-Methyl-2-(1-methylethyl)benzene
- Fig. 3.4.2** Hexylethanoate
- Fig. 3.4.3** 2,4,5-Trimethyl-1, 3-dioxolane
- Fig. 3.4.4** 4,14-Dimethyl-Ergosta-8,22-dien-3-ol
- Fig. 3.5** TIC profile of CS-H extract
- Fig. 3.5.1** Undecane
- Fig. 3.5.2** N-(3-acetyl-2-methyl-4-quinolinyl) acetamide
- Fig. 3.5.3** Methyl- 9, 12-octadecadienoate
- Fig. 3.5.4** Methyl octadecanoate
- Fig. 3.5.5** Methyl docosanoate

-
- Fig. 3.5.6** Tetrahydrocannabinol
- Fig. 3.6** TIC profile of CS-A extract
- Fig. 3.6.1** Cannabidiol
- Fig. 3.7** TIC profile of CS-PE extract
- Fig. 3.7.1** 3-Methyldecane
- Fig. 3.7.2** Propylbenzene
- Fig. 3.7.3** Butylcyclohexane
- Fig. 3.7.4** *n*-Propyltoulene
- Fig. 3.7.5** *n*-Amylcyclohexane
- Fig. 3.7.6** Naphthalene
- Fig. 3.7.7** Iodoctane
- Fig. 3.8** DAD spectra in the range of 190-300nm obtained in HPLC
- Fig. 3.8.1** Absorbing portion of flavonoids skelton
- Fig. 3.8.2** Ion nomenclature for Flavonoids
- Fig. 3.8.3** Cleavages at the glycosidic-*O*-linkage
- Fig. 3.8.4** Products ions formed by cross ring cleavage of Monosaccharides
- Fig. 3.9** Chromatographic Profiling of Compound with code CA-E
- Fig. 3.9.1** DAD and ESI-MS Spectrum of Compound with Code CA-E1
- Fig. 3.9.2** 1-*O*-[β -D-glucopyranosyl-(1 \rightarrow 4)- β -D-xylopyranosyl-(1 \rightarrow 4)- β -D-xylopyranosyl]-*p*-hydroxybenzoate
- Fig. 3.9.3** DAD and ESI-MS Spectrum of Compound with Code CA-E2
- Fig. 3.9.4** THC-1-*O*- β -D-(6-acetylglucopyranosyl-(1 \rightarrow 4)-rhamnopyranoside)
- Fig. 3.9.5** DAD and ESI-MS Spectrum of compound with code CA-E1
- Fig. 3.9.6** 1-*O*-[β -D-glucopyranosyl-[1 \rightarrow 4]- α -L-rhamnopyranosyl] syringate
- Fig. 3.9.7** DAD and ESI-MS Profiling of Compound with code CA-E4
- Fig. 3.9.8** 1-*O*-[β -D-xylopyranosyl-(1 \rightarrow 4)- β -D-xylopyranosyl]gallate
- Fig. 3.9.9** DAD and ESI-MS Spectrum of Compound with Code CA-E5
- Fig. 3.9.10** Tetrahydrocannabinol-1-*O*- β -
D[rhamnopyranosyl(1 \rightarrow 4)rhamnopyranosyl(1 \rightarrow 4)rhamnopyranoside
]
- Fig. 3.9.11** DAD and ESI-MS Spectrum of compound with code CA-E6
- Fig. 3.9.12** THVA-1-*O*- β -D-[rhamnosyl-(1 \rightarrow 4)-glucosyl-(1 \rightarrow 4)-rhamnosyl-
-

- (1→4)-glucoside]
- Fig. 3.9.13** DAD and ESI-MS Spectrum of Compound with Code CA-E7
- Fig. 3.9.14** THCA-C4-1-*O*-β-
D[glucopyranosyl(1→4)rhamnopyranosyl(1→4)xylopyranoside]
- Fig. 3.10** Chromatographic Profiling of Compound with Code CS-A
- Fig. 3.10.1** DAD and ESI-MS Spectrum of Compound with code CS-A1
- Fig. 3.10.2** Δ⁽⁸⁾-Tetrahydrocannabinol-1-*O*-β-*D*-
[xylopyranosyl(1→4)glucopyranosyl(1→4)glucopyranosyl(1→4)rhamnopyranoside]
- Fig. 3.10.3** DAD and ESI-MS of compound with code CA-A2
- Fig. 3.10.4** Luteolin-1-*O*-β-*D*[xylopyranosyl(1→4)rhamnopyranoside]
- Fig. 3.10.5** DAD and ESI-MS Spectrum of compound with code CA-A3
- Fig. 3.10.6** THCA-C4-1-*O*-β-
D[glucopyranosyl(1→4)glucopyranosyl(1→4)xylopyranoside]
- Fig. 3.11** Chromatographic Profiling of CA-Ex-Sox
- Fig. 3.11.1** DAD and ESI-MS Spectrum of compound with code CA-EX1
- Fig. 3.11.2** Cannabinol -1-*O*-β-
D[xylopyranosyl(1→4)xylopyranosyl(1→4)glucopyranosyl(1→4)rhamnopyranoside]
- Fig. 3.11.3** DAD and ESI-MS Spectrum of compound with code CA-EX2
- Fig. 3.11.4** Luteolin-1-*O*-β-
D[xylopyranosul(1→4)xylopyranosyl(1→4)xylopyranosyl(1→4)glucopyranoside]
- Fig. 3.11.5** DAD and ESI-MS Spectrum of compound with code CA-EX3
- Fig. 3.11.6** 6-Hydroxytricetin-7-*O*-β-
D[xylopyranosyl(1→4)rhamnopyranosyl(1→4)glucopyranosyl]
- Fig. 3.11.7** DAD and ESI-MS Spectrum of compound with code CA-EX4
- Fig. 3.11.8** Cannabinol-1-*O*-β-
D[glucopyranosyl(1→4)xylopyranosyl(1→4)xylopyranoside]
- Fig. 3.12** Chromatographic Profiling of Compound with Code Ca-AH
- Fig. 3.12.1** DAD and ESI-MS Spectrum of Compound with Code Ca-AH1
- Fig. 3.12.2** Syringic acid-1-*O*-β-*D*-[glucopyranosyl(1→4)xylopyranoside]

-
- Fig. 3.12.3** DAD and ESI-MS Spectrum of Compound with code Ca-AH2
- Fig. 3.12.4** Cannabinol-1-*O*- β -
D[rhamnopyranosyl(1 \rightarrow 4)xylopyranosyl(1 \rightarrow 4)glucopyranoside]
- Fig. 3.12.5** DAD and ESI-MS Spectrum of compound with code Ca-AH3
- Fig. 3.12.6** Cannabichromene -1-*O*- β -D-glucoside
- Fig. 3.12.7** DAD and ESI-MS Spectrum of Compound with Code Ca-AH4
- Fig. 3.12.8** Tetrahydrocannabivarinic acid -1-*O*- β -
D[glucopyranosyl(1 \rightarrow 4)xylopyranoside]
- Fig. 3.12.9** DAD and ESI-MS Spectrum of Compound with Code Ca-AH5
- Fig. 3.12.10** Cannabinol-1-*O*- β -
D[xylopyranosyl(1 \rightarrow 4)rhamnopyranosyl(1 \rightarrow 4)rhamnopyranoside]
- Fig. 3.12.11** DAD and ESI-MS Spectrum of Compound with Code CA-AH6
- Fig. 3.12.12** Luteolin-7-*O*-rhamnoside
- Fig. 3.12.13** DAD and ESI-MS Spectrum of compound with Code Ca-AH7
- Fig. 3.12.14** Cannabichromenic acid-1-*O*- β -
D[xylopyranosyl(1 \rightarrow 4)glucopyranosyl(1 \rightarrow 4)rhamnopyranoside]
- Fig. 3.12.15** DAD and ESI-MS Spectrum of Compound with Code CA-AH8
- Fig. 3.12.16** Tetrahydrocannabinolic acid (C4)-1-*O*- β -
D[rhamnopyranosyl(1 \rightarrow 4)glucopyranosyl(1 \rightarrow 4)xylopyranoside]
- Fig. 3.12.17** DAD and ESI-MS Spectrum of Compound with Code CA-AH9
- Fig. 3.12.18** Quercetin-4'-methylether-3-*O*- β -
D[rhamnopyranosyl(1 \rightarrow 4)xylopyranosyl(1 \rightarrow 4)rhamnopyranosyl(1 \rightarrow 4)glucopyranoside]
- Fig. 3.13** TLC plates using three different solvent
- Fig. 3.14** Preparative TLC on silica gel plates
- Fig. 3.15** Products obtained after PTLC
- Fig. 3.16** Results of Duquenois Levine reagent test
- Fig. 3.17** DAD and ESI-MS Spectrum of Compound with code C-1
- Fig. 3.17.1** Cannabichromene-1-*O*- β -D-glucoside
- Fig. 3.18** DAD and ESI-MS Spectrum of Compound with code C-2
- Fig. 3.18.1** Tetrahydrocannabinol-1-*O*- β -D-glucoside
- Fig. 3.19** DAD and ESI-MS Spectrum of compound with code C-3
-

-
- Fig. 3.19.1** Cannabinol-1-*O*- β -D-
[glucopyranosyl(1 \rightarrow 4)rhamnopyranosyl(1 \rightarrow 4)glucopyranosyl(1 \rightarrow 4)
glucopyranoside]
- Fig. 3.20** DAD and ESI-MS Spectrum of Compound with code C-4
- Fig. 3.20.1** Cannabinolic acid-1-*O*- β -D-
[glucopyranosyl(1 \rightarrow 4)glucopyranosyl(1 \rightarrow 4)glucopyranoside]
- Fig. 3.21** DAD and ESI-MS spectrum of Compound with code C-5
- Fig. 3.21.1** THC-1-*O*- β -D-rhamnopyranoside
- Fig. 3.22** DAD and ESI-MS Spectrum of Compound with code C-6
- Fig. 3.22.1** Tetrahydrocannabinol-1-*O*- β -D-
[xylopyranosyl(1 \rightarrow 4)glucopyranosyl(1 \rightarrow 4)glucopyranoside]
- Fig. 3.23** DAD and ESI-MS Spectrum of Compound with code C-7
- Fig. 3.23.1** Tetrahydrocannabinol-1-*O*- β -
D[rhamnopyranosyl(1 \rightarrow 4)rhamnopyranosyl(1 \rightarrow 4)glucopyranoside]
- Fig. 3.24** DAD and ESI-MS Spectrum of compound with code C-9
- Fig. 3.24.1** Cannabinol-1-*O*- β -
D[rhamnopyranosyl(1 \rightarrow 4)glucopyranosyl(1 \rightarrow 4)rhamnopyranoside]

List of Tables

- Table 1** Types of Cannabinoids
- Table 2.1** Taxonomic Ranking of *Cannabis sativa*
- Table 2.2** Morphological Description of *Cannabis sativa*
- Table 2.4** Mobile Phase Composition of HPLC-DAD-ESI-MS
- Table 3.1** Sugars Identified from Acid Hydrolysis
- Table 3.2** Identified Phenolic acids from Alkaline Hydrolysis
- Table 3.3** List of Compounds Identified by GC-MS Extracts
- Table 3.4** List of Compounds Identified by HPLC-DAD-ESI-MS
- Table 3.5** UV Absorption range for Flavonoids
- Table 3.6** Absorption Maxima and Molecular Masses of Phenolic acids
- Table 3.7** List of Isolated Cannabinoids
- Table 3.8** Detection of Cannabinoids by Duquenois Levine Reagent

List of Schemes

- Scheme 3.1.1** Fragmentation Scheme of 1-Ethyl-3,5-dimethylbenzene
- Scheme 3.1.2** Fragmentation Scheme of Methyl Derivative of Cannabidivarin
- Scheme 3.1.3** Fragmentation Scheme of Cannabinol
- Scheme 3.1.4** Fragmentation Scheme of Bicyclo[3.1.0]hexan-2-one
- Scheme 3.1.5** Fragmentation Scheme of Ethyltridecanoate
- Scheme 3.1.6** Fragmentation Scheme of N-Methyl-2,7,15-eicosatrienoic acid
- Scheme 3.1.7** Fragmentation Scheme of Linoleic acid ethylester
- Scheme 3.1.8** Fragmentation Scheme of 3,4-Dichloro-6-nitrophenol
- Scheme 3.1.9** Fragmentation Scheme of Lanosterol
- Scheme 3.2.1** Fragmentation Scheme of 1-Methyl-2-(1-methylethyl)benzene
- Scheme 3.2.2** Fragmentation Scheme of Hexylethanoate
- Scheme 3.2.3** Fragmentation Scheme of 2,4,5-Trimethyl-1,3-dioxolane
- Scheme 3.2.4** Fragmentation Scheme of 4,14-Dimethyl-Ergosta-8,22-dien-3-ol
- Scheme 3.3.1** Fragmentation Scheme of Undecane
- Scheme 3.3.2** Fragmentation Scheme of N-(3-acetyl-2-methyl-4-quinolinyl)acetamide
- Scheme 3.3.3** Fragmentation Scheme of Methyl-9,12-octadecadienoate
- Scheme 3.3.4** Fragmentation Scheme of Methyloctadecanoate
- Scheme 3.3.5** Fragmentation Scheme of Methyldocosanoate
- Scheme 3.3.6** Fragmentation Scheme of Tetrahydrocannabinol
- Scheme 3.4.1** Fragmentation Scheme of Cannabidiol
- Scheme 3.5.1** Fragmentation Scheme of 3-Methyldecane
- Scheme 3.5.2** Fragmentation Scheme of Propylbenzene
- Scheme 3.5.3** Fragmentation Scheme of Butylcyclohexane
- Scheme 3.5.4** Fragmentation Scheme of *n*-Propyltoluene
- Scheme 3.5.5** Fragmentation Scheme of *n*-Amylcyclohexane
- Scheme 3.5.6** Fragmentation Scheme of Naphthalene
- Scheme 3.5.7** Fragmentation Scheme of Iodoctane
- Scheme 3.6.1** Fragmentation Scheme of 1-*O*-[β -D-xylopyranosyl-(1 \rightarrow 4)- β -D-xylopyranosyl-(1 \rightarrow 4)- β -D-glucopyranosyl]-*p*-Hydroxybenzoate

-
- Scheme 3.6.2** Fragmentation Scheme of $\Delta^{(8)}$ -THC-1-*O*- β -(6- β -D-acetylglucopyranoside-[1 \rightarrow 4]- α -L-rhamnopyranoside).
- Scheme 3.6.3** Fragmentation Scheme of Syringoate-1-*O*-[β -D-glucopyranosyl-(1 \rightarrow 4)- α -L-rhamnopyranoside]
- Schem 3.6.4** Fragmentation Scheme of Galloate-1-*O*-[β -D-xylopyranosyl-(1 \rightarrow 4)- β -D-xylopyranoside]
- Scheme 3.6.5** Fragmentation Scheme of Tetrahydrocannabinol-1-*O*-[α -L-rhamnopyranosyl-(1 \rightarrow 4)- α -L-rhamnopyranosyl-(1 \rightarrow 4)- α -L-rhamnopyranoside]
- Scheme 3.6.6** Fragmentation Scheme of THVA-1-*O*-[α -L-rhamnopyranosyl-(1 \rightarrow 4)- β -D-glucopyranosyl-(1 \rightarrow 4)- α -L-rhamnopyranosyl-(1 \rightarrow 4)- β -D-glucopyranoside]
- Scheme 3.6.7** Fragmentation Scheme of THCA-C4-1-*O*-[β -D-glucopyranosyl-(1 \rightarrow 4)- α -L-rhamnopyranosyl-(1 \rightarrow 4)- β -D-xylopyranoside]
- Scheme 3.7.1** Fragmentation Scheme of $\Delta^{(8)}$ -Tetrahydrocannabinol-1-*O*-[β -D-xylopyranosyl-(1 \rightarrow 4)- β -D-glcopyranosyl-(1 \rightarrow 4)- β -D-glucopyranosyl-(1 \rightarrow 4)- α -L-rhamnopyranoside]
- Scheme 3.7.2** Fragmentation Scheme of Luteolin-4-*O*-[β -D-xylopyranosyl-(1 \rightarrow 4)- α -L-rhamnopyranoside]
- Scheme 3.7.3** Fragmentation Scheme of THCA-C4-1-*O*-[β -D-glucopyranosyl-(1 \rightarrow 4)- β -D-glucopyranosyl-(1 \rightarrow 4)- β -D-xylopyranoside]
- Scheme 3.8.1** Fragmentation Scheme of Cannabinol -1-*O*-[β -D-xylopyranosyl-(1 \rightarrow 4)- β -D-xylopyranosyl-(1 \rightarrow 4)- β -D-glucopyranosyl-(1 \rightarrow 4)- α -L-rhamnopyranoside]
- Scheme 3.8.2** Fragmentation Scheme of Luteolin-1-*O*-[β -D-xylopyranosul-(1 \rightarrow 4)- β -D-xylopyranosyl-(1 \rightarrow 4)- β -D-xylopyranosyl-(1 \rightarrow 4)- β -D-glucopyranoside]
- Scheme 3.8.3** Fragmentation Scheme of 6-Hydroxytricetin-7-*O*-[β -D-xylopyranosyl-(1 \rightarrow 4)- α -L-rhamnopyranosyl-(1 \rightarrow 4)- β -D-glucopyranosyl]
- Scheme 3.8.4** Fragmentation Scheme of Cannabinol-1-*O*-[β -D-glucopyranosyl-(1 \rightarrow 4)- β -D-xylopyranosyl-(1 \rightarrow 4)- β -D-xylopyranoside]
-

-
- Scheme 3.9.1** Fragmentation pattern of Syringoate-1-*O*-[β -D-glucopyranosyl-(1 \rightarrow 4)- β -D-xylopyranoside]
- Scheme 3.9.2** Fragmentation pattern of Cannabinol-1-*O*-[α -L-rhamnopyranosyl-(1 \rightarrow 4)- β -D-xylopyranosyl-(1 \rightarrow 4)- β -D-glucopyranoside]
- Scheme 3.9.3** Fragmentation scheme of Cannabichromene -1-*O*- β -D-glucopyranoside
- Scheme 3.9.4** Fragmentation pattern of Tetrahydrocannabivarinic acid -1-*O*-[β -D-glucopyranosyl-(1 \rightarrow 4)- α -L-xylopyranoside]
- Scheme 3.9.5** Fragmentation Scheme of Cannabinol-1-*O*-[xylopyranosyl(1 \rightarrow 4)rhamnopyranosyl(1 \rightarrow 4)rhamnopyranoside]
- Scheme 3.9.6** Fragmentation Scheme of Luteolin-7-*O*- α -L-rhamnopyranoside
- Scheme 3.9.7** Fragmentation Scheme of Cannabichromenic acid-1-*O*-[β -D-xylopyranosyl-(1 \rightarrow 4)- β -D-glucopyranosyl-(1 \rightarrow 4)- α -L-rhamnopyranoside]
- Scheme 3.9.8** Fragmentation Scheme of Tetrahydrocannabinolic acid (C4)-1-*O*-[α -L-rhamnopyranosyl-(1 \rightarrow 4)- β -D-glucopyranosyl-(1 \rightarrow 4)- β -D-xylopyranoside]
- Scheme 3.9.9** Fragmentation Scheme of Quercetin-4'-methylether-3-*O*-[α -L-rhamnopyranosyl-(1 \rightarrow 4)- β -D-xylopyranosyl-(1 \rightarrow 4)- α -L-rhamnopyranosyl-(1 \rightarrow 4)- β -D-glucopyranoside]
- Scheme 3.10.1** Cannabichromene-1-*O*- β -D-glucopyranoside
- Scheme 3.10.2** Tetrahydrocannabinol-1-*O*- β -D-glucopyranoside
- Scheme 3.10.3** Cannabinol-1-*O*-[β -D-glucopyranosyl-(1 \rightarrow 4)- α -L-rhamnopyranosyl-(1 \rightarrow 4)- β -D-glucopyranosyl-(1 \rightarrow 4)- β -D-glucopyranoside]
- Scheme 3.10.4** Cannabinolic acid-1-*O*-[β -D-glucopyranosyl-(1 \rightarrow 4)- β -D-glucopyranosyl-(1 \rightarrow 4)- β -D-glucopyranoside]
- Scheme 3.10.5** Tetrahydrocannabinol-1-*O*- α -L-rhamnopyranoside
- Scheme 3.10.6** Tetrahydrocannabinol-1-*O*-[β -D-xylopyranosyl-(1 \rightarrow 4)- β -D-glucopyranosyl-(1 \rightarrow 4)- β -D-glucopyranoside]

Scheme 3.10.7 Tetrahydrocannabinol-1-*O*-[α -L-rhamnopyranosyl-(1 \rightarrow 4)- α -L-rhamnopyranosyl-(1 \rightarrow 4)- β -D-glucopyranoside]

Scheme 3.10.8 Cannabinol-1-*O*-[α -L-rhamnopyranosyl-(1 \rightarrow 4)- β -D-glucopyranosyl-(1 \rightarrow 4)- α -L-rhamnopyranoside]

Abstract

Cannabis sativa commonly called "Bhang" is an endemic species of Central Asia of Himalayas. Its roots have been widely used in the ethnomedicine for arthritis and in drugs like Nabilone, Sativex, Dronabinol and Rimonabant. In addition to the social aspects of the use of drug and its abuse potential, the issue of approving it as a medicine is further complicated by the complexity of the chemical makeup of the plant.

This manuscript discusses the chemical constituents of the roots with particular emphasis on the Cannabinoids responsible for the drug's psychological properties. The present work describes a sample preparation by Maceration and Soxhlet Extraction followed by hydrolytic studies to identify sugars and phenolic acids.

A simple method is presented for the preparative isolation of seven major Cannabinoid glycosides involving Preparative Thin Layer Chromatography (PTLC) using solvent system *n*-Hexane : Diethyl-ether (1:1) as mobile phase and 60F₂₅₄ (Merck) Silica gel as stationary phase.

Chromatographic and spectroscopic data was used to provide footing for the structural elucidation of cannabinoids, flavonoids, phenolic acids, esters, hydrocarbons, steroids, benzene derivatives, alcohols, heterocycles and carboxylic acids. These phytochemical constituents were studied by GC-MS and hyphenated technique HPLC-MS. Information gleaned from GC-MS analyses lead to the discovery of esters, hydrocarbons, psychoactive cannabibnoids, steroids and carboxylic acids. While HPLC-MS analyses allowed the identification of phenolic acids, Cannabinoids and flavonoid glycosides derivatives. Psychoactive cannabinoid glycosides were first time identified from the roots of *C. sativa*. Detailed picture of phytochemical constituents provided a strong evidence for the utilization of roots for medicinal purpose, drug discovery and also in green chemistry.

Introduction

The genus *Cannabis* belongs to family *Cannabaceae* of order *Urticales*. Two subsp. of *Cannabis*, namely *C. sativa subsp. sativa* and *C. sativa subsp. indica* and each subsp. was further classified into wild and cultivated varieties (var.) as follows:

C. sativa subsp. sativa var. sativa (cultivated)

C. sativa subsp. sativa var. spontanea (wild)

C. sativa subsp. indica var. indica (cultivated)

C. sativa subsp. indica var. kafiristanica (wild)

In 1597 Herbal list, Gerarde lists the following common names for plant: *hempe* (English), *kemp* (Bradanders), *Zarnerhanff* (Dutch), *Canape* (Italian), *Cananio* (Spanish), *Chanvre* (French), *kannabis* (Greek) and *Cannabis* (Latin).

The *Cannabis* is expressed by **Bloomquist (1971)** signify "cane like", while *sativa* signify "planted or sown" and it indicates that plant is propagated from seeds not from perennial roots. **Haney and Bazzaz (1970)** observed that *Cannabis* plants can control the development of contending weeds, perhaps through the unpredictable terpenes and sesquiterpenes.

Cannabis sativa as shown in **Fig. 1 (a)** is a yearly herb, which develops throughout the warm season. It is generally dioecious, male and female blooms are generated on partitioned plants and fertilization happens predominantly by wind. The male plant dies soon after pollination while female plants persist until the onset of harsh climate. *Cannabis* has taproots something like one tenth of the length of stalk and stature fluctuate from 1-20 feet as shown in **Fig. 1 (b)**. Plants of both genders have comparative presence upto blooming season, despite of fact that male plants may be more slender than female. Both genders have compound green leaves with 3-15 leaflets arranged in palmate fashion *i.e.*, emanating from a solitary point at the end of stalk.

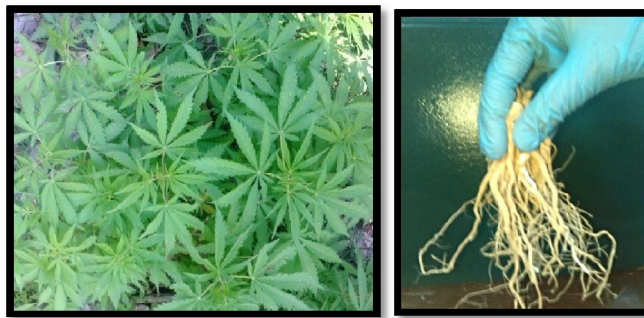


Fig. 1 (a) Aerial Parts (b) Roots of *Cannabis sativa*

Haney and Bazzaz (1970) reported intriguing perceptions while gathering the wild *Cannabis* plants along roads and interstates in United States, that just 41% were male as contrasted with 55% of all plants. **Harrison (1957)** exhibited that presence of low level carbon monoxide for brief time can result in a movement of sex declaration from male to female.

1.1 Literature Survey of *Cannabis sativa*

1.1.1 Phytochemical Constituents

C. sativa synthesized a bewildering variety of phytochemicals and derivatives of phytochemical constituents. Literature survey of *C. sativa* showed that it contains a wide variety of phytochemical constituents like terpenoids, cannabinoids, phytocannabinoids, endocannabinoids, synthetic cannabinoids, natural cannabinoids, flavonoids, fatty acids and glycoproteins.

1.1.1.1 Fatty Acids

Ross et al. (1996) studied chemical composition of fatty acids by gas liquid chromatography coupled with mass spectrometry in 24 different samples of *C. sativa*. Saturated and unsaturated fatty acids were found to be present in *C. sativa* seeds. Fatty acids like linolenic acid, palmitoleic acid, oleic acid, stearic acid, arachidic acid and behenic acid were also reported in *Cannabis*.

1.1.1.2 Glycoproteins

Hillestad et al. (1977) isolated 2-acetamido-2-deoxyglucose, 2-acetamido-2-deoxygalactose, galacturonic acid, galactose, arabinose, mannose and glucose from *C. sativa* by extraction with water and chromatography on DEAE-cellulose. The main part of non reducing end group was arabinofuranosyl units. The hexoses were usually linked as (1→3) and (1→4) units.

1.1.1.3 Flavonoids

Ross et al. (2005) examined two flavonoid glycosides from methanolic extracts. The two flavonoid glycosides that were distinguished kaempferol-3-*O*-sophoroside and quercetin-3-*O*-sophoroside by spectroscopic strategies utilizing high field 2-D NMR.

Ibrahim et al. (2010) explained the cannflavin *B*-7-sulphate, 6"-*S*,7"-dihydroxy cannflavin(A)-7-sulphate, Cannflavin(*B*)-7-*O*-β-*D*-4"-*O*-methylglucopyranoside etc. were produced from the microbial metabolism of cannflavin A and B, two biologically active flavonoids obtained from *C. sativa*.

Cannabis contains flavonoids like kaempferol, quercetin, vitexin, isovitexin, apigenin and luteolin were also discovered in *Cannabis*.

1.1.1.4 Terpenoids

Sixty five compounds were identified by **Rothschild et al. (2005)** by Coupled Gas Chromatography and Mass Spectrometry. 25 sesquiterpenoids, 20 monoterpenes and 20 biogenetic compounds were discovered. The five major components of monoterpenes were β -myrcene, β -ocimene, terpenoline, β -pinene and limonene.

Therapeutic agents like terpenoids; limonene, linalool, pinene, linalool, β -caryophyllene oxide and phytol were also extracted. Phytocannabinoid and terpenoid interactions could be used for the treatment of inflammation; anxiety, depression, cancer, fungal, bacterial, addiction and epilepsy were reported by **Russo and Ethan (2011)**.

1.1.1.5 Cannabinoids

Cannabinoids are a diverse class of chemical compounds that are found in *Cannabis sativa* as shown in **Table 1**. These include endocannabinoids, phytocannabinoids, natural cannabinoids and synthetic cannabinoids. On the basis of carboxylic acids attached to Cannabinoids, Cannabinoids are acidic as well as neutral.

Endocannabinoids

Endocannabinoids are substances produced within the body that activate cannabinoid receptors. Arachidonylethanolamine (Anandamide) 2-Arachidonoylglycerol, 2-Arachidonoyl glyceryl ether (noladin ether) and Virodhamine are the types of endocannabinoids ligand.

Gamage et al. (2012) revealed that Δ^9 -Tetrahydrocannabinol used to treat nausea and stimulate appetite in AIDS patient. THC effects are mediated through endocannabinoids which promotes energy balance through appetite stimulation.

Sun et al. (2012) has revealed the adverse effect of *Cannabis* in female fertility like prematuration, preimplantation parturition etc.

Phytocannabinoids

C. sativa has ability to stimulate appetite especially for sweet food. **Cota et al. (2003)** elucidated the interactions of cannabinoid system with metabolic pathway in the control of food intake.

Phytocannabinoids are the substances that are found in *Cannabis* and some other plants. The most abundant cannabinoid is Δ^9 -Tetrahydrocannabinol (THC), psychoactive compound of *Cannabis*. Δ^9 -Tetrahydrocannabinol, Cannabidiol, Cannabicitran, Cannabicyclol, Cannabidiol, Cannabichromene, Cannabigerol, 9,10-Epoxycannabitrol, 10-*O*-Ethylcannabitroil were recently discovered Cannabinoids by **Ross et al. (2005)**.

Eleven new cannabinoid esters from *C. sativa* were isolated by **Ahmed et al. (2008)**. These structures were 4-terpenyl cannabinolate, bomyl Δ^9 -Tetrahydrocannabinolte, α -Cadinyl Cannabigerolate, Fenchyl Δ^9 -tetrahydrocannabinolate etc.

Politia et al. (2008) studied hot and cold water extracts as well as ethanolic water extracts of *Cannabis* to understand that how these extracts differ from each other. Polarity and temperature of solvents affect the total amount of Δ^9 -THC.

Zulfiqara et al. (2012) isolated cannabisol a dimer of Δ^9 -Tetrahydrocannabinol with methylene bridge from *C. sativa*. This structure was confirmed by GC-MS and NMR spectroscopy.

Holland et al. (2012) reported chemiluminescence by the reaction of acidic potassium permanganate with cannabinoids. He highlighted the light producing reactions of cannabinoids with resorcinol and major phenolics in cannabinoids by using potassium permanganate. Changing the alkyl substituents on phenolic ring has great effect on emission intensity.

Synthetic Cannabinoids

Synthetic cannabinoids are the substances that are manufactured chemically and are used in treatment of diseases like cancer.

Within the Pharmaceutical industry, cannabinoid medicines like Marinol (synthetic THC product) used for nausea treatment in cancer patients, Nabilone with antiemetic properties, used for vomiting treatment and Sativex (THC and CBD rich extracts) used by Sclerosis patients were discovered by **Stott *et al.* (2004)**.

The effect of synthetic Cannabinoids WIN55, 212-2 on the human hepatocellular carcinoma (HCC) BEL-7402 was determined by **Hong *et al.* (2013)**. HCC is the common cancer in china. WIN can reduce cell viability and proliferation of BEL-7402. The upregulation of PPAR γ expression and the activation of PPAR γ DNA binding initiated the WIN induced apoptosis.

Natural Cannabinoids

Elsohly (2005) reported the total number of natural compounds were 423 in 1985 and 483 in 1995. The following classes have been identified in *Cannabis*, vitamins, two new flavonoids Kaempferol-3-*O*-sophoroside and Quercetin-3-*O*-sophoroside, steroids, terpenes, lactones, esters, fatty acids, aldehydes, ketones, hydrocarbons and simple alcohols.

Identification of Cannabinoids

Cannabinoids were identified by various techniques like High Performance Liquid Chromatography, Gas Liquid Chromatography, Column Chromatography, Centrifugal Partition Chromatography, Flash Chromatography and Ethephon treatment.

High Performance Liquid Chromatography (HPLC) was used by **Turner and Mahlberg (1982)** for the isolation of acidic and neutral cannabinoids. Hewlett Packard 1084B liquid chromatography with single wavelength at 254 nm UV detectors was used. Eluting solvents were water and acetonitrile. He also optimized conditions for cannabinoid extraction in two clones of *Cannabis sativa* by using gas-liquid chromatography and high performance liquid chromatography. Extraction temperature did not affect the profiling of *Cannabis*. When the leaves were dried at 37°C high ratio of acid to neutral cannabinoids were derived. Non-dried leaves also yielded high acid to neutral forms.

Rustichelli et al. (1998) quantified the presence of neutral and acidic cannabinoids in plant tissue extracts by coupling with HPLC-MS without derivitization. HPLC was performed by using four liquid quaternary pump with analytical HPLC detector set at 220 nm, eluting solvent consisting of methanol/water.

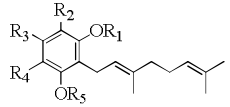
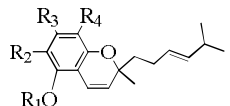
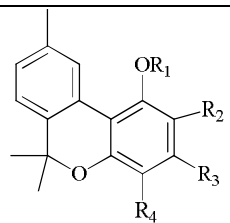
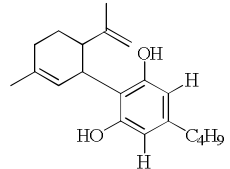
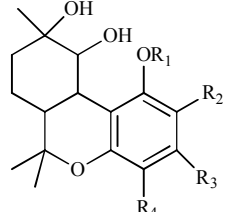
Hazekamp et al.(2004) used Centrifugal Partition Chromatography (CPC) for the preparative isolation of seven different cannabinoids from the *C. sativa*. More than 90% pure Cannabidiolic acid (CBDA), Cannabigerolic acid (CBGA), Δ^9 -*trans*-Tetrahydrocannabinolic acid (THCA), Cannabidiol (CBD), Cannabiniol (CBN), Cannabigerol (CBG), Δ^9 -*trans* Tetrahydrocannabinol (THC) were isolated by using gas chromatography.

Lachenmeier et al. (2004) has determined Cannabinoids in food samples and distinguished between drug type and fiber type *C. sativa* by using Headspace Solid Phase Microwave Extraction (HS-SPME) and alkaline hydrolysis.

The isolation of Δ^9 -Tetrahydrocannabinolic acid from the *Cannabis* plant by using two flash chromatography systems were explained by **Wohlfarth et al. (2011)**. In system 1, normal silica based column using cyclohexane and acetone as mobile phase was used, by loading 1800 mg *Cannabis* extract yielding 99.8% 623 mg of THCA. Second system was based on reverse phase using C-18 column with formic acid and methanol as mobile phase. By loading 300 mg *Cannabis* extract yielding 98.8% pure 51 mg THCA. In both systems UV absorbance was maintained at 207 and 209 nm.

Lavoie et al. (2012) investigated Fast Blue B and Duquenois-Levine test for the identification of cannabinoids in forensics laboratory.

THC content of leaf in male and female plant increases by treatment with ethephon was revealed by **Mansouri et al. (2013)**. Chlorophyll a and b level in male and female plant increases by treatment with lowest level of ethephon. Highest level of tocopherol is also observed in male and female plants when treated with ethephon.

Cannabinoid	Structure	Name of Cannabinoids	R ₁	R ₂	R ₃	R ₄	R ₅
Cannabigerol		Cannabigerol	H	H	C ₅ H ₁₁	H	H
		Cannabigerolic acid	H	COOH	C ₅ H ₁₁	H	H
		Cannabigerolmonomethyl ether	H	H	C ₅ H ₁₁	H	CH ₃
		Cannabigerolic acid monomethylether	H	COOH	C ₅ H ₁₁	H	H
		Cannabigerovaricin	H	COOH	C ₃ H ₁₁	H	H
Cannabichromene		Cannabichromene	H	H	C ₅ H ₁₁	H	--
		Cannabichromenic acid	H	COOH	C ₅ H ₁₁	H	--
		Cannabichromevarin	H	H	C ₃ H ₇	H	--
Cannabinol		Cannabinol	H	H	C ₅ H ₁₁	H	--
		Cannabinolic acid	H	COOH	C ₅ H ₁₁	H	--
		Cannabivarin	H	H	C ₃ H ₇	H	--
		Cannabinol (C ₄)	H	H	C ₄ H ₉	H	--
Cannabidiol		Cannabidiol	H	H	C ₅ H ₁₁	H	H
		Cannabidiolic acid	H	COOH	C ₅ H ₁₁	H	H
		Cannabidiolcol	H	H	CH ₃	H	H
		Cannabidivarin	H	H	C ₃ H ₇	H	H
		Cannabidiol (C ₄)	H	H	C ₄ H ₉	H	H
Cannabitriol		Cannabitriol	H	H	C ₅ H ₁₁	H	--

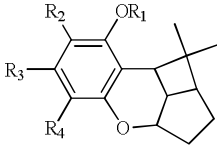
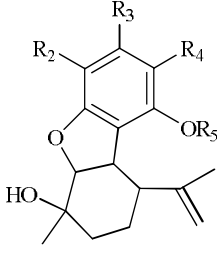
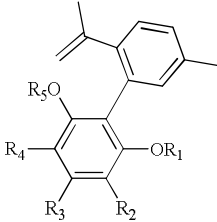
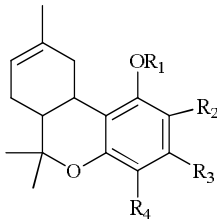
Cannabicyclol		Cannabicyclol	H	H	C ₅ H ₁₁	H	--
		Cannabicycloic acid	H	COOH	C ₅ H ₁₁	H	--
		Cannabicyclovarin	H	H	C ₃ H ₇	H	--
Cannabielsoin		Cannabielsoin	--	H	C ₅ H ₁₁	H	H
		Cannabielsoic acid A	--	COOH	C ₅ H ₁₁	H	H
Cannabinodiol		Cannabinodiol	H	H	C ₅ H ₁₁	H	H
		Cannabinodivarin	H	H	C ₃ H ₇	H	H
Δ^8 -Tetrahydrocannabinol		Δ^8 -Tetrahydrocannabinol	H	H	C ₅ H ₁₁	H	--
		Δ^8 -Tetrahydrocannabinolic acid	H	COOH	C ₅ H ₁₁	H	--

Table 1 Types of Cannabinoids

1.1.2 Extraction

Solid Phase Microextraction combined with GC-MS was used for the extraction of Swiss marijuana samples from different regions. High temperature (150°C) was used to reduce analysis time and increase sensitivity. **Ilias *et al.* (2005)** reported that relatively long desorption time (3 min.) was required for complete transfer of fiber into injection port of chromatograph.

Petrova *et al.* (2012) demonstrated the ability of transfer zinc, copper, arsenic and cadmium from roots to shoot, that increases the phytoextraction efficiency.

Except arsenic all the metalloids were accumulated in roots, while EDTA has a positive effect on metalloid mobility.

Tomita *et al.* (2013) extracted the oil by using supercritical carbon dioxide from hemp seed. The oil was extracted between 40-80°C temperature, pressure of 20-40 Mpa and CO₂ flow rate of 3 mL/min. The fatty acid profile was evaluated by using GC-FID (Gas Chromatography Flame Ionization Detection).

1.1.3 Biosynthesis

Olivetolic acid (OA) is considered to be a first intermediate in cannabinoid biosynthetic pathway described by **Gagnea *et al.* (2012)**. Glandular trichomes of female *Cannabis* are considered to be a primary site of biosynthetic pathway. Olivetolic acid cyclase (OAC) demonstrates cannabinoid pathway and polyketide biosynthesis in plants and animals.

Docimo *et al.* (2013) reported the phenylpropanoid pathway using phenylalanine ammonia lyase (PAL), cinnamic acid-4-hydroxylase (C₄H) and 4-coumarate COA ligase (4Cl) as first three steps.

1.1.4 Hemp Fiber

FIRSST (Feedstock Impregnation Rapid and Sequential Steam Treatment) was performed by **Lavoie *et al.* (2012)** for the production of fibers and biomolecules, lead to the isolation of lignin, hemicellulose and cellulose.

Puangsin *et al.* (2013) oxidized hemp bast holocellulose fiber using TEMPO (2,2,6,6-Tetramethylpiperidine-1-oxyl radical) by adding NaClO levels in water at pH 10. Cellulose is considered as major renewable carbon resource on earth Nanofabricated cellulose fibers are prepared by TEMPO mediated oxidation of hemp bast holocellulose by applying various conditions.

Jaraboa *et al.* (2012) investigated the pulp obtained from hemp core using ethanolamine at 60°C. It resulted in the best mechanical properties and high retention solids for fiber cement production.

Marrota et al. (2013) understand the mechanical behavior of plant fiber as a best reinforcement material in polymeric matrix composites. Nanoindentation investigation has also been carried out with hemp stem *insitu*. X ray diffraction patterns highlight the amorphous matrix polymer rate in hemp. Biochemical analysis highlights the nanostructural and matrix pectins distribution.

Use of hemp as a thermal insulation for building materials were analyzed by **Zampori et al. (2013)**. Hemp is suitable in building applications due to its good hydrothermal properties and acoustical insulation properties.

Behnaz et al. (2013) reported hemp fiber for reinforcing polymeric composites because of high strength, stiffness and aspect ratio. Scanning electron microscopy was used to study fiber/matrix interface.

1.1.5 Hemp Biomass

Yang et al. (2010) explained the process of *trans* esterification and hydrogenation for biodiesel production in *Cannabis*. SrO supported with 10% CuO was used for *trans* esterification with biodiesel yield of 96%.

Kreugera et al. (2011) developed pretreatment steam methods for the production of ethanol and methane with and without prehydrolysis of cellulose enzyme.

Ethanol production from hemp hurd by performing enzymatic hydrolysis converts lignocelluloses into ethanol. Improved environmental performance was observed by using ethanol based fuel such as global warming *etc.* demonstrated by **Garcia et al. (2012)**.

Cannabis is a renewable source for the production of biofuels investigated by **Rehman et al. (2013)**. It is a potential crop in Pakistan to meet its energy demand for the production of biofuel.

Abraham et al. (2013) studied locally available hemp biomass, *Cannabis sativa* for the production of fermentable sugars. Hemp Hurd Biomass (HHB) was treated by using five different pretreatments that are dilute H₂SO₄, NaOH, alkaline peroxide, hot

water and at end again with dilute H₂SO₄. This results in degradation and loosening of HHB that facilitates enzymatic saccharifications.

1.1.6 Hemp as Poison

Tetrahydrocannabinol (THC) is a major psychoactive constituent of *Cannabis* analyzed by **Fitzgerald *et al.* (2013)**. Hashih contains higher degree of THC and is extracted from the top of flowering plant. Canine intoxication symptom includes epilepsy, insomnia, muscle spasm, parkinsons disease, anxiety and depression. Higher dosage may cause tachypnea, ataxia, insomnia *etc.* Gas Chromatography and Mass Spectrometry is used for THC detection.

Macedo *et al.* (2013) investigated the insect fragment that was associated with hemp drug. Insect that was associated with seizure of *Cannabis* shows the effect of illicit drug.

1.1.7 Microelements of *Cannabis*

Arru *et al.* (2004) investigated the copper localization in *Cannabis sativa* grown in hydroponic copper rich culture with the aim to decontaminate the polluted soil. X ray microanalysis combined with electron microscopy was used to investigate the localization of copper in *Cannabis*.

Linger *et al.* (2005) studied the effect of cadmium concentration on the photosynthesis and growth of *C. sativa*. 50-100 mg of cadmium concentration in stem and leaves had a strong effect on plant growth, while hemp roots showed a high degree of cadmium tolerance. Cadmium shows negative effect on water splitting process, antenna and energy distribution of photo system (PS 2). 17mg of Cadmium per kg of soil, could not affect the hemp growth and photosynthetic apparatus.

Shi *et al.* (2011) has revealed that *Cannabis* can be grown in Cadmium contaminated soil for the biodiesel production. Hemp can be considered as a best candidate for new strategy of phytoremediation of Cd contaminated soil.

1.1.8 Storage of *Cannabis*

Stability of cannabinoids in hemp after long time was discussed by **Trofin *et al.* (2011)**. The contents of CBN increases during the storage and is more pronounced when stored in light at 22°C after this placed in darkness at 4°C.

1.1.9 Oil and Flour of *Cannabis*

Mycotoxin analysis shows the presence of aflatoxin, B1, B2, G1, G2 and ochratoxin. Hemp oil contains a higher content of diethylhexylphthalate. Hemp flour is the source of micronutrients such as iron, manganese and zinc as described by **Fusari *et al.* (2013)**. Due to polyunsaturated compounds, hemp seed oil is used in detergents, soaps, printer and inks *etc.*

1.1.10 Pharmacological Activities

Members of the genus *Cannabis* have been investigated thoroughly for their pharmacological activities which are given below:

1.1.10.1 Antileishmanial Activity

Radwan *et al.* (2008) reported new compounds that are 5-Methoxycannabigerolic acid, Cannabispirane, β -Cannabispiranol and Dehydrocannabinifuran shows antimicrobial as well as antileishmanial activity.

1.1.10.2 Antitumor Drug

Cannabinoids and derivatives limit cell proliferation and induce death of tumor cells as described by **Pisanti *et al.* (2009)**. Cannabinoid provides a novel strategy to treat cancer cells.

Cannabinoid inhibitory effects on cancer cells were reported by **Calvaruso *et al.* (2012)**. He highlighted the different routes of cell death in tumor. Cannabinoids can induces cell death in different types of cancer.

1.1.10.3 Antioxidant

Tang et al. (2009) described the antioxidant activities of hydrolysates that were obtained from Hemp enzymatic hydrolysis, showed the varying DPPH radical scavenging properties, chelating abilities and reducing power.

1.1.10.4 Antiprotozoal Activity

Ibrahim et al. (2010) unveiled five metabolites from the microbial metabolism of cannflavin A and B. Antibacterial and antiprotozoal activity was shown by all these metabolites.

1.1.10.5 Chemopreventive Effect

Cannabidiol shows chemopreventive effects, pharmacological effects and reduces cell proliferation. Cannabidiol reduces endocannabinoid level and reduces the oxidative damage of DNA explained by **Aviello et al. (2012)**.

1.1.10.6 Antineoplastic

Lopesa et al. (2012) has reported antineoplastic psychotropic cannabinoid, Δ^9 -Tetrahydrocannabinol that causes induction of apoptosis and reduction of cellular metabolism.

1.1.10.7 Anticonvulsant

Cannabidiol (CBD) was identified as anticonvulsant and non-psychotomimetic constituent of *Cannabis sativa* discovered by **Campos et al. (2013a)**. CBD suppressed epileptiform activity in brain cells.

1.1.10.8 Antipanic Effect

Nonpsychotomimetic constituent of *Cannabis* is cannabidiol that promotes antipanic effect. Treatment with CBD induces the antipanic effects by acting on 5HT1A receptors in DPAG (Dorsal Periaqueductal Grey) determined by **Borelli et al. (2013)**.

1.1.10.9 Antiinflammatory *Cannabis* has positive impact on inflammatory bowel disease. Cannabigerol (CBG) a nonpsychotropic *Cannabis* derived cannabinoid reduces the colon weight, colon length ratio and myeloperoxidase activity determined by **Borellia et al. (2013)**.

Cannabidiol nonpsychotropic constituent of *Cannabis sativa* has anti-inflammatory or immunosuppressive properties. Adenosine A_{2A} receptors involved in antiinflammatory effects of CBD. As A_{2A} antagonist ZM241385 blocks the protective effect of CBD in the initial stages of inflammation reported by **Mecha et al. (2013)**.

1.1.10.10 Anxiolytic Effect

Campos et al. (2013b) Cannabidiol (CBD) exerts promising effect on mental health of human like inhibition of anxiety and depression. CB1 cannabinoid receptors are involved in the anxiolytic effect of CBD.

1.1.10.11 Antispasticity

Efficacy of Cannabinoids has importance in the treatment of spasticity in Multiple sclerosis (MS) patients. MS related spasticity in Germany was cured by using Sativex (1:1 mixture of Tetrahydrocannabinol and Cannabidiol) reported by **Husseni et al. (2012)**.

1.1.10.12 Antiemetic

Müller et al. (2013) investigated that *Cannabis* extract Nabiximol and Tetrahydrocannabinol is used for the treatment of anorexia, nausea and vomiting. In Tourette syndrome, evidences shows that *Cannabis* is used for the treatment of behavioral problems as well as for the suppression of tics.

1.1.10.13 Antipsychotic

Cannabinoids due to its antipsychotic like properties is a best alternative treatment of Schizophrenia. Pharmacological profiles of CBD were investigated by **Dieana (2013)** has similar effect as that of antipsychotic drug. In Tourette syndrome, evidences shows that *Cannabis* is used for the treatment of behavioral problems.

1.1.11 Concluding Remarks

Humans have put *C. sativa* to work as medicine and mind altering drug for thousands of year. Still there are endless useful products in *C. sativa* that still await discovery. *C. sativa* have proven to be a rich well spring of novel complexes like cannabinoids with an elevated amount of structural differences and a wide range of organic compounds. Thorough study of *C. sativa* uncovered that it holds tremendous assortment of phytochemical constituents like unsaturated fats, flavonoids, glycoproteins, terpenoids, cannabinoids and so on. However, there is large number of reported phytochemicals that were extracted from the *C. sativa* aerial part yet there is a space for investigating phytochemicals in *C. sativa* roots. It is not out of ordinary in this connection that new phytochemicals from *C. sativa* roots may be brought to surface by a characterization device of GC-MS and by a touchy method of HPLC-DAD-ESI-MS. HPLC has been proven to be a breakthrough method to accelerate and streamline the analyses of phytochemical constituents of *C. sativa*, by allowing quick, efficient identification and quantification. The point of study concentrates on the phytochemical examination, MS profiling, and bioevaluation of *C. sativa* roots.

Materials and Methods

2.1 Choice of Plant

Cannabis sativa is a source of wide variety of phytochemicals and derivatives of phytochemical constituents like fatty acids, glycoproteins, flavonoids, terpenoids and cannabinoids, which have been explored, reported and documented in the literature review. Today plant selection is not only for the yield of phytochemical constituents, but also for the *Cannabis* ability to overcome diseases, climatic stresses and the hazards caused by mankind. Ethnopharmacology and fascinating plant folklore leads to medicinal potential like antimalarial, antitumor, antileishmanial diseases *e.t.c.* Unfortunately, systematic and well conducted research on the *C. sativa* roots is comparatively low. For these reason roots of *C. sativa* was selected to unveil the hidden phytochemicals.

2.2 Taxonomic Ranking and Description of *Cannabis sativa*

The taxonomic ranking of *C. sativa* is as follows;

Kingdom	Plantae
Class	Angiosperma
Order	Urticales
Family	Cannabaceae
Genus	<i>Cannabis</i>
Specie	<i>Sativa</i>

Table 2.1 Taxonomic Ranking of *Cannabis sativa*

2.3 Family

The genus *Cannabis* belongs to family Cannabaceae (often called Cannabinaceae, Cannabidaceae or even Cannaboidaceae) of order urticales. The family Cannabaceae contains only two genera-*Cannabis* and *Humulus*.

2.4 Trivial Names

Gerarde in his 1597 Herbal, lists the following common European names for *Cannabis* : *Hempe* (English), *Kemp* (Brabanders), *Zarner hanff* (Dutch), *Chanvre* (French), *Canapé* (Italian), *Kannabis* (Greek), *Cananio* (Spanish) and *Cannabis* (Latin).

2.5 Geographical Distribution

History of *Cannabis* is complex and it has not been possible to describe the geographical origin of plant. Himalayas have been proposed as its native habitat. But there is a general agreement that *Cannabis* is Asiatic in origin and ranges from Caspian sea and Southern Russia to North India.

2.6 Morphological Description

Plant body	Plant body vary in height from 1-20 feet (1-6 m)
Stem	Angular, furrowed, hollow and can be branched or unbranched, depending on the proximity of neighbouring plants.
Leaves	Compound green leaves composed of 3-15 leaflets or blades with toothed margins. Leaves are arranged in pairs with alternate and spiral arrangement.
Leaflets	Leaflets are arranged in a palmate fashion <i>i.e.</i> , radiating from a single point at the end of a stalk. Leaflets are 6-11 cm long and between 2 to 15 mm wide.
Roots	Tap roots, about one-tenth the length of stalk, and with small branches diversifying out from the main root.

Table 2.2 Morphological Description of *Cannabis sativa*

2.7 Extraction

After the selection of envisaged target plant material, it was then necessary to define and to choose the most efficient methodologies to be employed in the extraction process. This selection was usually directly related and even limited by the selection of the most suitable solvents and solvent mixtures. According to **Pan *et al.* (2003)** extraction is a separation process used in the separation of substances from

matrix. It may be solid phase extraction and liquid liquid extraction. It uses two immiscible phases to separate a solute from one phase to another. The distribution of a solute between two phases is an equilibrium condition described by partition theory.

The selection of the extraction methodologies, must taken in consideration not only the technological/engineering specificities, clear advantages and disadvantages of each technique, but also other quite important issues such as ; available technologies, required extraction yield, thermal and chemical stability of compounds. Following extraction methods were used for the isolation of chemical constituents from *C. sativa*.

2.7.1 Maceration followed by Ultrasonication

Maceration followed by ultrasonication was performed with four different solvents *i.e.*, *n*-hexane, acetone, pet-ether and chloroform.

250g of *C. sativa* roots were soaked in a conical flask in 4 different solvents 750ml of each *i.e.*, *n*-hexane, acetone, pet-ether and chloroform. Then the extract was kept for about 10 days at room temperature. After that ultrasonic bath was used for the extraction, that allows variation of temperature and amplitude. Working frequency was set at 33 kHz. When the extraction was complete, the extract was filtered on double layer of filter paper Whatman No. 21 and collected in a flask. The residue was taken back and re-extracted three times using fresh solvent each time with the same condition as above. Then the washings were added to the extract. Then the combined extracts were transferred to round bottom flask and evaporated using a rotary evaporator under vacuum.

2.7.1.1 Analysis by GC-MS

1mg of sample with code CS-H (*C. sativa* root extract of *n*-hexane), CS-E (*C. sativa* root extract of ethanol), CS-A (*C. sativa* root extract of Acetone) and CS-PE (*C. sativa* root extract of pet-ether) was dissolved in 1ml *n*-hexane then 1 μ l was injected into GC-MS for analysis.

2.7.1.2 Analysis by HPLC-DAD-ESI-MS

1mg of sample with code CS-E (*C. sativa* root extract of ethanol) and CS-A (*C. sativa* root extract of Acetone) was dissolved in 1mL of ethanol then 1 μ L was injected into HPLC-DAD-ESI-MS instrument for analysis.

2.7.2 Soxhlet Extraction

Soxhlet extraction technique was employed for the extraction and separation of chemical constituents of *C. sativa* roots. A general full factorial design with two factors (extraction time and extractor solvent) was implemented. Soxhlet extraction was performed at 9hrs. extraction time with ethanol solvent.

10g of *C. sativa* roots were placed inside a thimble made from thick filter paper, which was loaded into the main chamber of the soxhlet extractor. The ethanol (30ml) was taken as extracting solvent in a distillation flask and the soxhlet extractor was then placed onto this flask. The soxhlet was then equipped with condenser. The soxhlet chamber containing the solid material was slowly filled with warm solvent. The time period for soxhlet extraction experiment was 9hrs. Desired compound was then dissolved in a warm solvent. Repeat this experiment thrice under the same working conditions. Then the extracts were transferred to round bottom flask and evaporated using a rotary evaporator under vacuum as shown in **Fig. 2.1**.



Fig. 2.1 Soxhlet Extractor

2.7.2.1 Analysis by GC-MS

1mg of sample with code CS-E-Sox (*C. sativa* roots Ethanolic extracts by Soxhlet extraction) was dissolved in 1ml of *n*-hexane then 1 μ L was injected into GC-MS instrument for analysis.

2.7.2.2 Analysis by HPLC-DAD-ESI-MS

1mg of sample with code CS-E-Sox (*C. sativa* roots Ethanolic extracts by Soxhlet extraction) was dissolved in 1mL of ethanol then 1 μ L was injected into LC-DAD-ESI-MS instrument for analysis.

2.8 Preliminary Qualitative Analysis

2.8.1 Acid Hydrolysis

Acid hydrolysis was used for the identification of sugars and aglycones moiety.

2.8.1.1 Procedure for Acid Hydrolysis

20g *C. sativa* roots were soaked in 120 mL of 2M HCl. The contents were refluxed on boiling water bath at 100°C for 6 hrs and then cooled. The hydrolysate was filtered and filtrate was extracted thrice with 50 mL diethyl ether in separating funnel respectively to recover aglycones whereas sugars remained in aqueous phase. The aqueous and diethyl ether layers were separated. Then these layers were concentrated *in vacuo*.

2.8.1.2 Analysis of Sugars

Concentrated aqueous layer was analyzed by TLC and LC-DAD-ESI-MS method for the detection of sugars.

Standard solutions of xylose, arabinose, glucose and galactose were taken as reference for the identification of sugars in aqueous phase. The solutions were prepared by dissolving 50mg of each sugar in 10ml of distilled water. 10% isopropyl alcohol was added as preservatives.

Sugars were identified by using TLC employing precoated silica gel 60 F₂₅₄ (Merck) impregnated with 2M NaH₂PO₄ as stationary phase, binary solvent system acetone : water (9:1) as mobile phase and standard solutions as reference. Aliquots (4 μ L) of reference standards were then applied at points along the baseline of silica gel plates which were then developed in ascending mode.

Aniline hydrogen phthalate was prepared by dissolving 0.92mL of aniline and 1.6g of phthalic acid in 49mL BuOH, 49mL ether and 2.0mL of distilled water.

For the visibility of sugar spots, aniline hydrogen phthalate was sprayed on chromatogram as spraying reagent. The chromatogram was then heated in an oven at 100°C for 1hr. till brownish spots appeared.

2.8.1.3 Analysis of Aglycones

Aglycones were analyzed by GC-MS analysis of diethyl ether layer. 1mg of sample with code CS-DE-Ah (*C. sativa* diethyl ether layer acid hydrolysis) was dissolved in 1mL of *n*-hexane and 1 μ L was injected into GC-MS for analysis.

2.8.1.4 Analysis by HPLC-DAD-ESI-MS

The concentrated aqueous layer sample was submitted for LC-MS analysis. 1mg of sample with code Ca-Ah-H₂O (*C. sativa* Acid Hydrolysis Aqueous Layer) was dissolved in 1mL of ethanol and 1 μ L was injected into the GC-MS instrument for analysis.

2.8.2 Alkaline Hydrolysis

Alkaline Hydrolysis was carried out for the qualitative analysis of phenolic acids present in *C. sativa* roots.

2.8.2.1 Procedure for Alkaline Hydrolysis

10g *C. sativa* roots were soaked in 50mL of 2M NaOH under nitrogen atmosphere to avoid the oxidation of phenolic acids. The contents were then kept for 4 hrs. at room temperature. The orangish yellow filtrate was then acidified with conc. HCl. For the separation of acids, the acidified solution was extracted with ethyl

acetate. For obtaining phenolic acids, the ethyl acetate layer was extracted with 5% NaHCO₃, leaving other phenolics in ethyl acetate layer. The acids were then recovered by acidifying the NaHCO₃ layer and re-extracting with ethyl acetate.

2.8.2.1.1 Analysis of Ether layer

Residue obtained after the evaporation of ethyl acetate layer was dissolved in distilled MeOH and was subjected to Two Dimensional TLC (2D TLC) and LC-MS analysis.

2D TLC analysis was carried out for the analysis of phenolic acids. Precoated silica gel 60F₂₅₄ (Merck) was used as stationary phase and binary solvents Chloroform : Acetic acid (9:1) and Toluene : Ethyl acetate (5.5:4.5) as mobile phase in one and two dimensions respectively.

For the visualization of spots on TLC plate, 10% Folin-ciocalteu spraying reagent was used. Catechol or hydroquinones with phenolic acids gave blue color with this reagent in visible region.

2.8.2.1.2 Analysis by HPLC-MS

1mg of sample with code Ca-alk-Eth (*C. sativa* alkaline hydrolysis ethyl acetate layer) was dissolved in MeOH and 1 μ L was injected into the LC-MS instrument for analysis.

2.9 Qualitative Analysis

Qualitative analysis of *C. sativa* extract was carried out by employing the following techniques.

2.9.1 HPLC-DAD-ESI-MS Profiling

Hyphenation of chromatographic and separation methods holds a great value in a modern natural product analysis. It ensures superior resolution and analysis of natural products like cannabinoids, phenolic compounds and flavonoids.

2.9.1.1 Instrumentation

HPLC-DAD-ESI-MS with following parameters were used.

The HPLC profiles were acquired on an Agilent 1200 LC system, consisting of a G1322A solvent degasser, a G1311A quaternary solvent pump and G1329A autosampler. The column was kept at constant temperature by using a HPLC (4.6 × 150 mm) stainless-steel column. The column was of type Agilent Eclipse XRD C-18 (5 μ m). Light absorption and emission were detected by a G1315 UV-diode array detector (DAD). The system consisted of Edward E1M18 Pump A22304199, having Nitrogen generator N-118 LA and 6310 Ion trap LC/MS G2445D SL. UV spectra were measured online by DAD in the range of 195-400 nm. Electrospray ionization (ESI) was used in the ionization mode.

HPLC system	Agilent 1200 LC system Degasser G1322A. Quaternary Pumps G1311A. Auto-sampler G1329A and Column compartment G316A. Nitrogen generator N-118 LA. Edward E1M18 Pump A22304199, 6310 Ion trap LC/MS G2445D SL, Chem. Station for LC. 3D system Rev.B.01.03 [2004].
Column	HPLC column (4.6×150mm) stainless-steel column packed with Agilent Eclipse XRD C-18 (5 μ m).
DAD	Diode Array Detector G1315.
Wavelengths	Detects at 190nm, 254nm, 320nm, and 380nm.
Ionization mode in MS	Electrospray in positive ion mode.
Mass range	(<i>m/z</i>) 50-2200.

2.9.1.2 Stationary Phase

By using Reverse Phase (RP) column, HPLC used in the separation of different classes of phenolic compounds was considerably enhanced. In RP-HPLC column the stationary phase comprises porous silica beads to which various alkyl groups are covalently bonded like RMe₂SiCl, where R is the straight chain alkyl group such as C₁₈H₃₇. Separation of compounds in RP-HPLC column takes place on

the basis of their hydrophobicity. The stationary phase is relatively hydrophobic and the mobile phase is hydrophilic with respect to sample. Retention was the result of the differential hydrophobic interactions of the sample molecules and the hydrophobic functionalities of the stationary phase. As a result hydrophilic molecules having little affinity with stationary phase was eluted first and the hydrophobic molecules were eluted at later retention time.

2.9.1.3 Gradient Elution Program

Gradient elution program was applied for the analyses of phenolic compounds. The composition of mobile phase was changed from hydrophilic to hydrophobic. For the analysis of complex mixtures or samples containing dissimilar components required modification of mobile phase, so that all components of mixture were eluted. With the aim of improving resolution and shortening the time of resolution, gradient elution has been widely used in the field of natural products.

2.9.1.4 Mobile Phase

A binary mobile phase was used consisting of deionized water (Solvent A) and HPLC grade acetonitrile (Solvent B). In order to suppress the ionization of phenolic hydroxyl groups, 0.1% formic acid was used as a modifier. The flow rate of mobile phase was 0.5 mL/min. From 0-20 min. the mobile phase was isocratic (same composition), and then concentration of mobile phase composition was varied (gradient) with time as follows:

Time (min.)	% of B
0	10
10	10
20	20
30	40
40	50
45	60
50	70
60	10

2.9.1.5 Sample Preparation

For HPLC-DAD-ESI-MS analysis, 1mg of sample with code CAH (*C. sativa* *n*-Hexane extract), CAE (*C. sativa* ethanol extract), CAA (*C. sativa* acetone extract) was dissolved in 1mL of ethanol then 1 μ L was injected into the instrument after the compatibility test for HPLC. For this purpose each sample was mixed with few drops of water and acetonitrile. If the solutions remained clear that samples were appropriate for HPLC analyses.

2.10 GC-MS

For the analysis of volatile compounds in the *C. sativa* extract, GC-MS was performed. Some compounds were identified by comparison with NIST (Mass spectral library).

2.10.1 Instrumentation

To obtain GC retention times, molecular weights and fragmentation spectra, GC-MS analyses were performed on Agilent Technologies GC-MS instrument with model no. 6890N coupled with mass selective detector model no. 5973. The GC was fitted with column; Agilent JW Scientific DB-5MS column (30 m \times 0.25 mm i.d. \times 0.25 μ m film thickness). The oven temperature was programmed from 120-280 $^{\circ}$ C with regular increase of 12 $^{\circ}$ C per min. Helium was used as carrier gas at pressure of 60-85 *psi*. Injection volume was 1 μ L and sample was injected manually. Sample was injected manually and Splitless injectors were used. The injection and detector port temperatures were maintained at 120 $^{\circ}$ C respectively. Electron impact (EI) mode was used in ionization with electron energy of 70eV.

GC-MS with following instrumental parameters were used.

GC	Agilent Technologies GC-MS instrument. GC with model no. 6890N was used.
Injection volume	1 μ L
Injector	Splitless

Injection	Manually
Gas temperature	120°C
Carrier gas (mobile phase)	Helium
Ramping temperature	120-280°C with regular increase of 12°C per min.
Column (Stationary phase)	Agilent JW Scientific DB-5MS column (30m×0.25mm i.d.×0.25μm film thickness)
MS	Mass selective detector model no. 5973
Ionization mode	Electron Impact (EI)
Electron energy	70 eV
Mass range (<i>m/z</i>)	0-1000

2.10.2 Sample Preparation

1mg of sample with code CAH, CAE and CAA (*Cannabis n*-hexane, ethanol, and acetone) was dissolved in 1mL of *n*-hexane and 1μL was injected into GC-MS instrument for analyses.

2.11 Chromatographic Techniques

2.11.1 Selection of Column Packing

Cellulose and Silica was commonly used packing material in column chromatography.

2.11.1.1 Cellulose

Cellulose was used for column packing. It was ideal for the separation of glycosides from one another or from aglycones and also for the separation of less polar aglycones.

2.11.1.2 Silica

Silica was used for the separation of less polar aglycones *e.g.*, isoflavones, flavanones, methylated flavones and flavonols. First of all, prewash the column with

strong HCl to remove traces of iron, which causes flavonoids to adhere strongly to the column packing.

Aqueous layer of acid hydrolysis of *C. sativa* roots were brown precipitates (crystal like brown sugars). Column chromatography was performed using cellulose as stationary phase and distilled water as mobile phase to separate colored components as shown in **Fig. 2.2**.

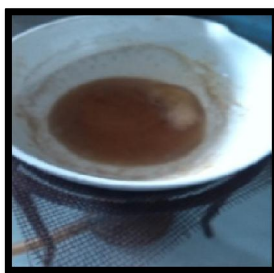


Fig. 2.2 Brown Crystals of Acid Hydrolysate

2.11.2 Column Chromatography 1

Prior to use, cellulose was suspended in the distilled water overnight. Slurry was prepared by dissolving 25g of cellulose in 45mL of water. It was packed in a 25cm×25mm id column and equilibrated with 500mL water with a slow flow rate of 2mL in 10-15 minutes. So, flash chromatography by applying nitrogen pressure was preferred, that also provided inert atmosphere. Sample (brown colored crystals) was dissolved in distilled water. Then the sample was loaded on to the column. At the end of adsorption, the column was eluted with water to remove non-adsorbed impurities.

2.11.3 Column Chromatography 2

Silica gel was used as stationary phase with water as eluent. It was suspended in the distilled water for 1 day. Then slurry was prepared by dissolving 25g of silica gel in 45mL of water. Then slurry was packed in 25cm×25mm id column and equilibrated with distilled water with a better flow rate of 5mL/min. Sample was then loaded on to the column. At the end of adsorption, column was eluted with water to remove non-adsorptive impurities.

2.12 Isolation of Cannabinoids

Cannabinoids are a group of C₂₁ terpenophenolic compounds, including carboxylic acids and analogues that are typically present in *C. sativa*. The major compound of this group includes Δ^9 -Tetrahydrocannabinolic acid, Cannabidiolic acid, Cannabinolic acid and minor compounds Cannabigerolic acid and Cannabichromenic acid.

The root of *C. sativa*, as an underground part of the plant was scientifically overlooked. Although the stem, flowers, seeds and leaves of *C. sativa* received an overwhelming amount of attention that unveiled the presence of higher contents of Cannabinoids. Almost nothing was so far published on the roots of *C. sativa*. **Pelt (2008)**. Roots are the primary storage organs of plant. Due to higher contents of lipids and sugars in roots of *C. sativa*, concentration of Cannabinoids was very much less in the root as compared to aerial part. Hence for obtaining the standards of Cannabinoids, these were isolated from the aerial part of *C. sativa*. Research on the *Cannabis* plant demanded reference compounds in the form of purified *Cannabis* constituents. For reference compound, the biggest obstacle was the availability of sufficient amount of highly purified compound. Many isolation methods or routes were discussed so far for the isolation of Cannabinoids but most of these methods were inefficient, time consuming or not suitable for preparative isolation. A simple and advanced method was presented for the preparative isolation of Cannabinoids from *C. sativa* plant material.

2.12.1 Procedure for Isolation of Cannabinoids

253g of *C. sativa* plant material was pulverized in a mortar. The powder obtained was stirred with a mixture of Chloroform : Methanol (1:1, V/V) (800 mL) in a beaker and filtered by suction. The solvent was removed completely from the filtrate *in vacuo*. The dark brown oil (3g) that remained was dissolved in Methanol : Water (9 : 1 V/V) (75 mL) and extracted with *n*-hexane (4×40mL). The combined hexane phases were reduced to dryness *in Vacuo*. The orange oil that remained (2 g) was dissolved in ethyl acetate (100mL) and extracted with saturated NaHCO₃ solution

(7×30mL). The aqueous phase was discarded. The ether was removed from the organic phase *in Vacuo*. 2g of oil remained.

2.12.2 Purification

Oil was further purified by preparative TLC on self made plates [Layer prepared with Merck Silica gel for preparative TLC at a thickness of 1 mm], and eluent was *n*-Hexane : Diethyl ether (1:1,V/V). The ether was removed *in vacuo* and the remaining material was subjected to the same procedure again.

2.12.3 Spraying reagents

Duquenois Levine reagent was commonly used as spraying reagent for the detection of Cannabinoids.

2.12.4 Duquenois Levine reagents

Add 2gms of vanillin and 2.5mL of acetaldehyde in 100mL of ethanol.

2.12.4.1 Procedure

Add 2-3mL of sample in a glass test tube, then 10 drops of Duquenois Levine reagent. After shaking 10 drops of concentrated hydrochloric acid was added and tube was shaken again. Color after the addition of hydrochloric acid was noted. 20 drops of chloroform was added and test tube was vortexed, then allowed to settle and separated into two layers. Any color that transferred to organic layer was noticed.

The mechanism of reaction of Cannabinoids with this reagent was given below as shown in **Fig. 2.3**.

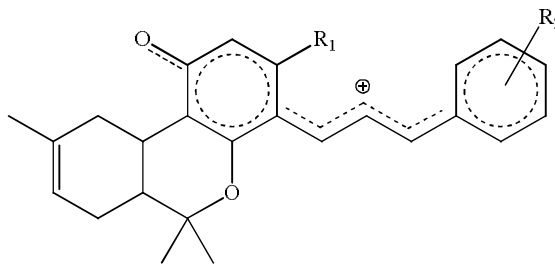


Fig. 2.3 Mechanism of Cannabinoids with Duquenois Levine reagent.

3.1 Acid and Alkaline Hydrolysis

3.1.1 Results of Acid Hydrolysis for Sugars Identification

Acid hydrolysis was used for the identification of sugars by TLC and LC-MS.

3.1.1.1 TLC

Sugars were identified by TLC using precoated silica gel 60 F₂₅₄ (Merck) impregnated with 2M NaH₂PO₄ as stationary phase, binary solvent system acetone : water (9:1) as mobile phase and standard solution as reference. Spot 1 was rhamnose, its reported R_f value is 0.89 and observed R_f value is 0.87. Spot 2 was xylose, reported R_f value is 0.78 and observed R_f value is 0.66. Spot 3 represented Arabinose, its reported R_f value is 0.66 and observed R_f value is 0.58. Spot 4 was due to glucose, its observed R_f value is 0.49 and reported R_f value is 0.53. Spot 5 was galactose, reported R_f value is 0.33 and observed R_f value is 0.28. Spot 6 showed the sample of acid hydrolysate as shown in **Table 3.1**. Brownish spots were appeared after spraying with aniline hydrogen phthalate viewing under short wavelength UV light (254 nm) as shown in **Fig. 3.1**

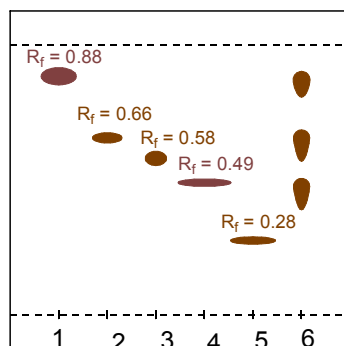


Fig. 3.1 TLC chromatogram of sugar constituents from *C. sativa* roots spraying with aniline hydrogen phthalate reagent (see spot colours above) viewing under short wavelength UV light (254 nm)

Track assignment: 1=Rhamnose, 2= xylose, 3= Arabinose, 4= Glucose, 5= Galactose, 6= Sample of acid hydrolysate

Standord sugars	R _f ×100	Sugars identified in aqueous solution
Rhamnose	88	+
Xylose	79	+
Arabinose	66	-
Glucose	53	+
Galactose	33	-

+ Indicates the presence of sugar/-Indicates absence of sugar

Table 3.1 Sugars identified from Acid Hydrolysis

3.1.2 Results of Alkaline hydrolysis

Alkaline hydrolysis was performed for the identification of Phenolic acids in *C. sativa* roots extract by TLC and HPLC.

3.1.2.1 TLC

Phenolic acids of benzoic, Cinnamic, syringic and salicylic acid was commonly found as derivatives in *C. sativa* plant extracts and were frequently encountered as acyl groups attached to flavonoids and cannabinoid glycosides. For analysis, these are readily cleaved from glycosides with alkali.

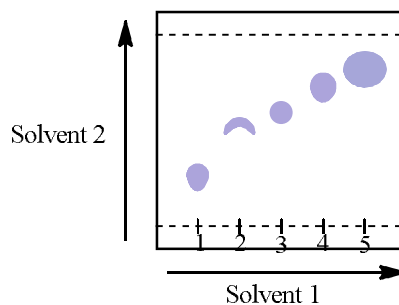


Fig. 3.2 2D-TLC chromatogram of phenolic acids from *C. sativa* roots (a) short wavelength UV light (254 nm)

Track assignment: (1) Salicylic acid, (2) Syringic acid, (3) *p*-Hydroxy benzoic acid, (4) 2,5 Dihydroxy benzoic acid, (5) Gallic acid

2D TLC was performed for phenolic acid separation using 10% acetic acid in chloroform (1:9) in 1D solvent system and 45 % ethylacetate in toluene (4.5:5.5) in 2D solvent system. In 1D solvent system calculated R_f values were 0.8, 0.76, 0.59,

0.57 and 0.51 for 5, 4, 3, 2 and 1 spots respectively. In 2D TLC calculated R_f values were 0.89, 0.756, 0.60, 0.30 and 0.27 for 5, 4, 3, 2 and 1 spots as shown in **Table 3.2**. Light bluish spots were appeared when viewed chromatogram under short UV wavelength (254nm) as shown in **Fig. 3.2**. Position and R_f value of spots were found in agreement with Salicylic acid, Syringic acid, *p*-Hydroxy benzoic acid, 2,5-Dihydroxybenzoic acid and Gallic acid.

Spot	R_f value		Identified Phenolic acid
	CHCl ₃ :AcOH 1:9	Toluene:ETOAc 11:9	
1	0.51	0.27	Salicylic acid
2	0.57	0.30	Syringic acid
3	0.59	0.60	<i>p</i> -Hydroxy benzoic acid
4	0.76	0.756	2,5-Dihydroxy benzoic acid
5	0.8	0.89	Gallic acid

Table 3.2 Identified Phenolic Acids from Alkaline Hydrolysis

3.2 Results and Discussions of GC-MS Analyses

GC-MS was proven to be a quick, efficient identification and quantification technique. Information gleaned from GC-MS retention time and MS spectra lead to the discovery of hydrocarbons, alcohols, esters, cannabinoids, carboxylic acids, aromatic compounds, hetrocyclic and triterpenoids with the help of NIST library match. 30 different compounds were identified through GC-MS analyses from extracts of *C. sativa* roots in different solvents. In ethanolic extract of *C. sativa* roots two Cannabinoids (methyl derivative of Cannabidivarin and Cannabinol) were first time identified eluted at retention time 2.127 and 3.031 min. Retention time of Cannabinoids in GC-MS were quite similar but their separation was good enough to distinguish them **Hazekamp et al., (2007)**. Two steroids were also first time identified from ethanolic extract. In *n*-hexane and acetone extracts of *C. sativa* roots two important Cannabinoids were also detected first time *i.e.*, Δ^9 -Tetrahydrocannabinol and Cannabidiol. Cannabidiol was differ from Cannabichromene and Cannabicyclol by the formation of just one peak at m/z 246 due to Retro-Diels-Alder cleavage. Similarly, base peak of Cannabinoids did not corresponded to the molecular ion peak, but to a fragment indicating that these Cannabinoids were easily fragmented by GC-MS **Hazekamp et al., (2007)**. Only the neutral Cannabinoids were detected by GC-MS analyses because at high temperature decarboxylation of acidic Cannabinoids converted it into their neutral form **Novotny et al., (1976)**. While in pet ether extracts of *C. sativa* roots only the hydrocarbons were detected. List of compounds identified by GC-MS CS extracts are enlisted in **Table 3.3**.

Table 3.3 List of compounds identified by GC-MS extracts

Compd. Code	TIC Time (min.)	Mol. Ion peak (m/z)	Molecular Formula	IUPAC Name	Significant Fragments (m/z)
CS-E1	2.126	134	C ₁₀ H ₁₄	1-Ethyl-3,5-dimethylbenzene	119, 104, 95, 65
CS-E2	2.127	298	C ₂₀ H ₂₆ O ₂	Methyl derivative of Cannabidivarin	199, 177, 134, 119
CS-E3	3.031	310	C ₂₁ H ₂₆ O ₂	Cannabinol	238, 223, 294, 281
CS-E4	3.963	96	C ₆ H ₈ O	Bicyclo[3.1.0]hexan-2-one	68, 54
CS-E5	11.437	242	C ₁₅ H ₃₀ O ₂	Ethyl tridecanoate	213, 185, 129, 101, 88
CS-E6	13.04	319	C ₂₁ H ₃₇ NO	N-methyl-2,7,15-eicosatrienoic acid	207, 150, 124, 95, 67
CS-E7	13.056	308	C ₂₀ H ₃₆ O ₂	Linoleic acid methylester	279, 263, 150, 109, 81
CS-E8	15.842	207	C ₆ H ₃ Cl ₂ NO ₃	3,4-Dichloro-6-nitrophenol	179, 149, 109, 79
CS-E9	21.107	426	C ₃₀ H ₅₀ O	Lanosterol	426, 400, 342, 355, 337, 327

CS-E10	2.121	134	C ₁₀ H ₁₄	1-Methyl-2-(1-methylethyl)benzene	119, 118, 104, 91
CS-E11	2.956	144	C ₆ H ₁₂ O ₂	Hexyl ethanoate	115, 101, 59
CS-E12	2.965	116	C ₂ H ₄ O ₂	2,4,5-Trimethyl-1,3-dioxolane	101, 72, 46
CS-E13	17.650	426	C ₃₀ H ₅₀ O	4,14-Dimethylergosta-8,22-dien-3-ol	411, 393, 327, 299, 281
CS-H1	2.453	156	C ₁₁ H ₂₄	Undecane	57, 85, 113
CS-H2	10.801	242	C ₁₄ H ₁₄ N ₂ O ₂	N-(3-acetyl-2-methyl-4-quinolinyl)acetamide	227, 199, 184,
CS-H3	12.499	294	C ₁₉ H ₃₄ O ₂	Methyl-9,10-octadecadienoate	263, 221, 196, 177, 123, 88
CS-H4	12.701	298	C ₁₉ H ₃₈ O ₂	Methyl octadecanoate	255, 213, 185, 157, 129, 74
CS-H5	16	354	C ₂₃ H ₄₆ O ₂	Methyl docosanoate	311, 228, 186, 143, 74
CS-H6	16.282	314	C ₂₁ H ₃₀ O ₂	Δ ⁽⁹⁾ -Tetrahydrocannabinol	258, 243, 299, 231, 163
CS-A1	16.300	314	C ₂₁ H ₃₀ O ₂	Cannabidiol	246, 243, 299, 207, 176

CS-PE1	2.021	156	C ₁₁ H ₂₄	3-Methyldecane	99, 85, 71, 55
CS-PE2	2.161	120	C ₉ H ₁₂	Propylbenzene	105, 91, 77
CS-PE3	2.184	140	C ₁₀ H ₂₀	Butylcyclohexane	111, 83, 55
CS-PE4	2.384	134	C ₁₀ H ₁₄	<i>n</i> -Propyltoluene	119, 105, 91
CS-PE5	2.825	154	C ₁₁ H ₂₂	<i>n</i> -Amylcyclohexane	83, 55, 41
CS-PE6	3.420	128	C ₁₀ H ₈	Naphthalene	102, 74, 51
CS-PE7	8.427	240	C ₈ H ₁₇ I	Iodoctane	127, 99, 85, 71, 57

3.3-Volatile compounds of CS-E extract

From ethanolic extracts of *C. sativa* root 9 compounds were identified. The TIC profile is given in **Fig. 3.3**.

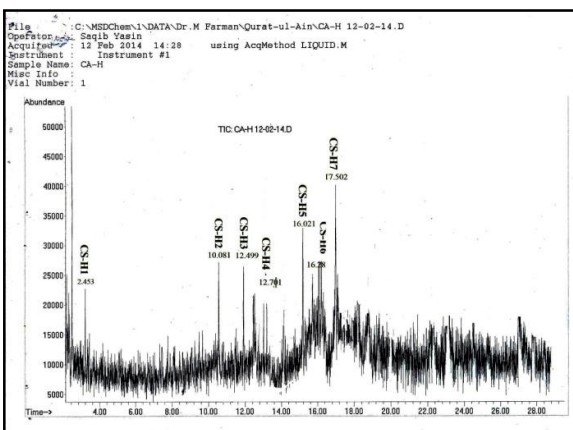


Fig. 3.3 TIC Profile of CS-E Extract

3.3.1 CS-E1

Explanation

The signal at retention time 2.126 min. in the HPLC profile of ethanolic extract of *C. sativa* roots was assigned a code CS-E1. Low retention time indicated that more volatile components were eluted out first as they are carried through the column by the carrier gas at lower temperature (**Greaves and Roboz 2014**). In digital bar graph, length of line corresponded to the signal intensity. Peak at this retention time did not corresponded to highly intense signal. Molecular ion peak appeared at m/z 134. From m/z 134 to m/z 119 loss of 15 mass unit indicated the loss of methyl. Loss of 28 mass unit from m/z 119 to m/z 91 manifested the presence of ethyl moiety. Peak at m/z 91 displayed the tropilium cation. So, benzene ring was confirmed. The tropilium ion eliminated the neutral acetylene molecule to give a peak at m/z 65. Loss from m/z 65 to m/z 51 indicated the loss of 14 mass unit as shown in **Scheme 3.1**.

From rule of thirteen, molecular formula came out to be $C_{10}H_{14}$. HDI calculated was 4, 3 satisfied by 3 double bonds and 1 was satisfied by cyclic ring. So, identified compound is 1-Ethyl-3,5-dimethylbenzene as shown in **Fig.3.3.1**. This compound matched with NIST library (72%).

Identified Compound

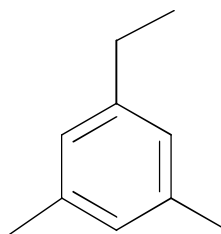
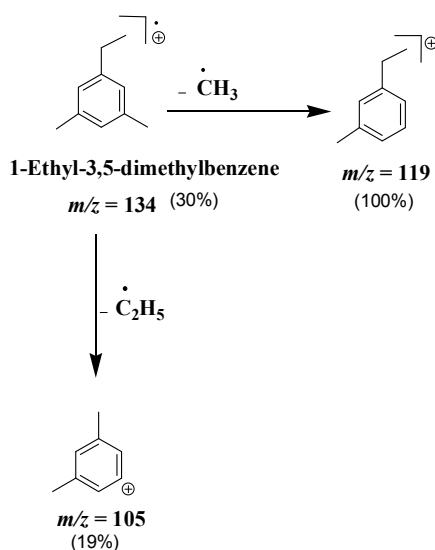


Fig. 3.3.1:1-Ethyl-3, 5-dimethylbenzene (CS-E1)

Fragmentation Scheme



Scheme 3.1.1 Fragmentation Scheme of 1-Ethyl-3, 5-dimethylbenzene

3.3.2 CS-E2

Explanation

The signal at retention time 2.127 min. in the HPLC profile of ethanolic extract of *C. sativa* roots was assigned a code CS-E2. Lower retention time inferred the presence of volatile compounds (**Greaves and Roboz 2014**). Molecular ion peak appeared at m/z 298. As molecular ion peak was with an even mass, odd number of nitrogen atoms were absent stated by nitrogen rule. So, amides, amines, nitriles or nitro group containing odd nitrogen atoms were absent (**Pavia and Coworkers 2011**). From m/z 298 to m/z 193, loss of 105 mass unit may be due to neutral ethyl benzene

or methyl tropilium. Cleavage of 16 mass unit manifesting the loss of oxygen or NH_2 . Loss of 43 from m/z 177 inferred the presence of propyl radical. Cleavage of 15 mass unit from m/z 134 to m/z 119 may be due to methyl radical loss. The fragment ion peak at m/z 91 from m/z 119 corresponded to 28 unit which may be due to CO or ethene. Peak at m/z 91 unveiled the presence of tropilium cation. No M-1, M-29 or m/z 29 confirmed the absence of aldehyde. Amines were also absent as confirmed by nitrogen rule. 26 mass unit loss from m/z 91 to m/z 65 may be due to ethyne. Oxygen atom loss from m/z 193 to m/z 177 and radical cation appeared at m/z 177. Base peak at m/z 119 was justified by the loss of methyl radical from m/z 134 as shown in **Scheme 3.2**. Base peak did not corresponded to the molecular ion peak, but to a fragment indicated that these fragments are easily fragmented by GC-MS (**Hazekamp et al., 2007**). Only the alkanes, alkenes or oxygen atom's presence were confirmed.

Molecular formula calculated from rule of 13 was $\text{C}_{22}\text{H}_{34}$. Due to the presence of oxygen moiety, molecular formula was modified by the insertion of two oxygen moieties and it became $\text{C}_{20}\text{H}_{26}\text{O}_2$. Hydrogen deficiency index (HDI) calculated by using formula $\{X+1-(1/2)y+(1/2)z\}$ where X represents number of carbon atom, Y represents hydrogen atom and Z represents hetroatom other than carbon and hydrogen. HDI came out to be 8, 6 satisfied by 6 double bonds and 2 was satisfied by 2 cyclic rings. By consolidating all the information obtained from retention time and fragmentation pattern, identified compound was methylcannabidivarin as shown in **Fig. 3.3.2**.

Identified Compound

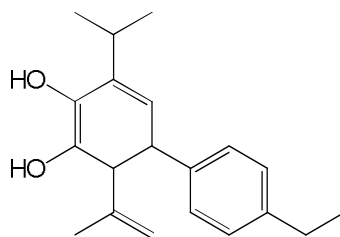
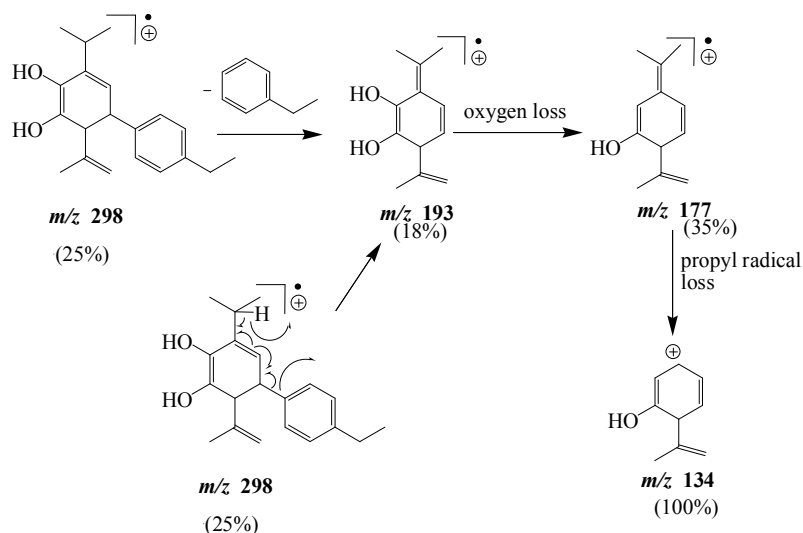


Fig. 3.3.2: Methyl Derivative of Cannabidivarin (CS-E2)

Fragmentation Scheme



Scheme 3.1.2 Fragmentation of Methyl Derivative of Cannabidivarin

3.3.3 CS-E3

Explanation

The signal at retention time 3.031 min. in the HPLC profile of ethanolic extract of *C. sativa* roots was assigned a code CS-E3. As temperature ramped with 120-280°C with regular increase of 12°C per minute, volatile compounds were eluted out first (**Greaves and Roboz 2014**). Molecular ion peak appeared at m/z 310. As molecular ion peak was of even number, odd number of nitrogen atoms were absent as explained by nitrogen rule (**Pavia and Coworkers 2011**). From m/z 310 to m/z 294 loss of 16 mass unit may be due to oxygen moiety. 29 mass unit loss from m/z 310 to m/z 281 may infer ethyl radical or CHO of aldehyde. From m/z 281 to m/z 251, loss of 30 mass unit may be due to presence of primary amines (CH_2NH_2^+) or NO^+ . 43 mass unit difference from m/z 281 to m/z 238 may be due to $\text{CH}_2=\text{CHO}$ radical of aldehydes or propyl radical. Cleavage of 72 mass unit from m/z 310 to m/z 238 displayed the neutral loss of pentane. From m/z 238 to m/z 223 cleavage of 15 mass unit inferred the loss of methyl radical. 27 mass unit difference from m/z 223 to m/z 196 may be due to HCN. From m/z 238 to m/z 196 may inferred the $\text{CH}_2=\text{CO}$ radical of aldehydes and ketones. Loss of 32 mass unit from m/z 196 to m/z 164 may be exhibited by methanol. 57 mass unit difference from m/z 196 to m/z 139 unveiled the loss of butyl radical. 44

mass unit difference from m/z 139 to m/z 95 may be revealed by McLafferty cleavage of aldehydes. Again the difference of 32 mass unit betrayed the loss of methanol from m/z 115 to m/z 83. Another methyl radical loss was inferred from m/z 83 to m/z 68. One more significant peak at m/z 83 was due to $C_5H_7O^+$ and the loss of $C_{16}H_{19}O$ radical. Fragment ion peak at m/z 238, due to neutral loss of pentane was also reported by (Novotny *et al.*, 1976). Peak at m/z 138 was exhibited by $C_9H_{14}O$ radical cation and by neutral loss of $C_{12}H_{12}O$ as shown in **Scheme 3.3**. Odd number of nitrogen atom was absent as indicated from nitrogen rule. So, amines, amides or nitriles containing odd number of nitrogen atoms were absent. Base peak did not correspond to molecular ion peak, but to fragment indicated that these compounds were easily fragmented by GC-MS (Hazekamp *et al.*, 2007). No M-1 peak, confirmed the absence of aldehydes. No loss of 17 (OH), 45 (CO_2H) or appearance of peak at 45 mass unit indicated that carboxylic acids were also absent. M-15, M-29 or M-43 betrayed the loss of alkyl chain. From rule of thirteen, molecular formula came out to be $C_{23}H_{34}$. By the insertion of two oxygen moieties, modified formula became $C_{21}H_{26}O_2$. HDI came out to be 9, that were satisfied by 6 double bonds and 3 cyclic rings. Retention times of Cannabinoids in GC were quite similar, but their separation was quite enough to distinguish them (Hazekamp *et al.*, 2007). Keeping in mind all the information obtained from above fragmentation scheme and retention time, identified Compound was Cannabinol as shown in **Fig. 3.3.3**.

Identified Compound

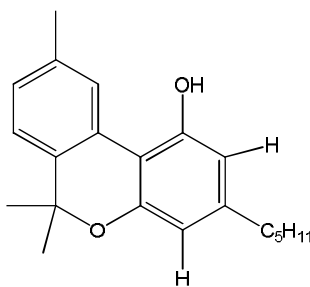
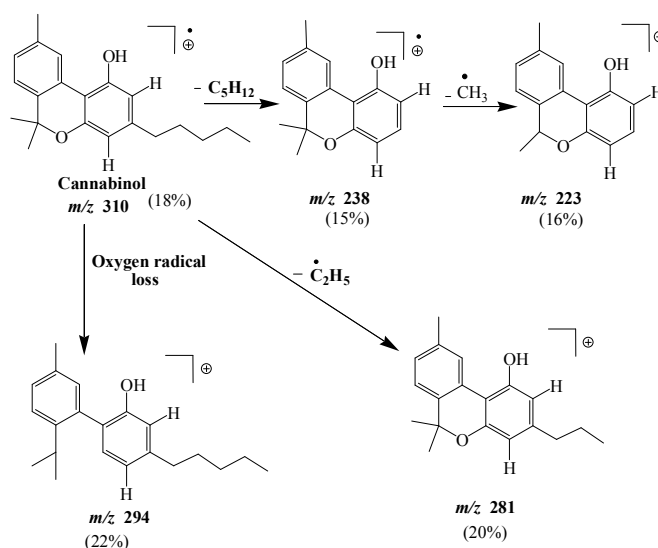


Fig. 3.3.3: Cannabinol (CS-E3)

Fragmentation Scheme



Scheme 3.1.3 Fragmentation Scheme of Cannabinol

3.3.4 CS-E4

Explanation

The signal at retention time 3.963 min. in the HPLC profile of ethanolic extract of *C. sativa* roots was assigned a code CS-E4. More volatile components were eluted out first as they are carried through the column by the carrier gas at low temperature (Greaves and Roboz 2014). Molecular ion peak appeared at m/z 96. As molecular ion peak was with an even number, so nitrogen rule (containing odd number of nitrogen atom) was ruled out (Pavia and Coworkers 2011). From m/z 96 to m/z 81 loss of 15 mass unit which indicated the loss of methyl radical. 28 mass unit difference from m/z 96 to m/z 68 may be due to CO or ethene loss. From m/z 55 to m/z 27 28 mass unit loss inferred the presence of CO and ethene. From m/z 55 to m/z 39 difference of 16 mass unit manifested the presence of oxygen moiety. Loss of 28 mass unit from m/z 55 to m/z 27 betrayed the loss of ethene as shown in Scheme 3.4. From rule of thirteen, molecular formula came out to be C_7H_{12} . By the insertion of one oxygen moiety modified molecular formula became C_6H_8O . By collecting all the information obtained from retention time and fragmentation pattern, identified

compound was Bicyclo [3.1.0]hexan-2-one as shown in **Fig. 3.3.4**. This compound showed 42% resemblance with NIST library.

Identified Compound

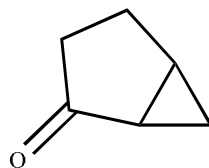
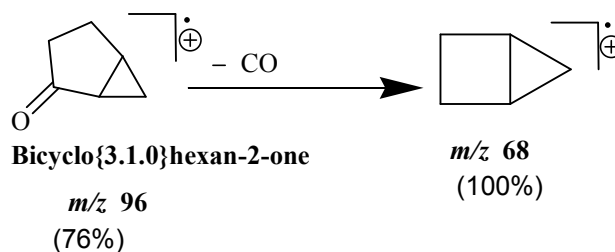


Fig. 3.3.4: Bicyclo[3.1.0]hexan-2-one (CS-E4)

Fragmentation Scheme



Scheme 3.1.4 Fragmentation Scheme of Bicyclo[3.1.0]hexan-2-one

3.3.5 CS-E5

Explanation

The signal at retention time 11.437 min. in the HPLC profile of ethanolic extract of *C. sativa* roots was assigned a code CS-E5. Length of line at given retention time corresponded to high signal intensity. Temperature ramped at 120-280°C with the regular increase of 12°C per minute infer the elution of volatile components first followed by less volatile components (**Greaves and Roboz 2014**). Molecular ion peak appeared at m/z 242. As molecular ion peak was with an even mass showed that odd number of nitrogen atoms were absent, stated by nitrogen rule (**Pavia and Coworkers 2011**). Amides, amines, nitriles or nitro groups containing odd nitrogen atoms were absent. From m/z 242 to m/z 227 inferred the loss of 15 mass unit may be due to methyl. 29 mass unit difference may be due to ethyl loss from m/z 242 to m/z 213. 16 mass unit loss may be due to oxygen or methane. Difference of 14 mass unit

may be due to methylene loss from m/z 199 to m/z 185, revealed the presence of alkyl chain. Difference of 56 mass unit may be due to butane loss from m/z 241 to m/z 185. Loss of 84 might be due to hexane from m/z 241 to m/z 157. Difference of 28 mass unit from m/z 185 to m/z 157 may be due to CO moiety or ethene. 46 mass unit difference from m/z 157 to m/z 111 might be due to NO_2 or $(\text{H}_2\text{O} + \text{CH}_2=\text{CH}_2)$. 41 mass unit loss from m/z 129 to m/z 88 inferred allylic radical. 42 mass unit difference from m/z 111 to m/z 69 may be due to CH_2CHO radical of aldehydes or ketones. Again the loss of 14 mass unit betrayed the methylene from m/z 69 to m/z 55. From m/z 101 to m/z 69 may be due to methanol loss. M-1 or M-29 peak was absent which displayed the absence of aldehydes. No loss or appearance of peak at m/z 43 confirmed the absence of ketones. M-17 or M-45 peak was absent, carboxylic acids were also absent. Base peak at m/z 88 was due to the McLafferty cleavage of ethyl-esters. This cleavage confirmed the presence of γ hydrogen on γ carbon atom (**Pavia and Coworkers 2011**). The fragment ion peak at m/z 213 was due to loss of ethyl radical. Peak at m/z 185 was due to loss of ethene from m/z 213. Again loss of ethene from m/z 185 peak appeared at m/z 157. Fragment ion peak at m/z 185 was due to cleavage of C_4H_9 radical as shown in **Scheme 3.5**. Peak at m/z 101 was due to loss of ethene from m/z 129. So, Ester moiety was confirmed from McLafferty cleavage. This ester was already reported in literature (**Elsohly 2006**). From rule of thirteen, molecular formula came out to be $\text{C}_{18}\text{H}_{26}$. Due to presence of two oxygen moieties modified molecular formula became $\text{C}_{15}\text{H}_{30}\text{O}_2$. HDI calculated was 1, satisfied by 1 carbonyl moiety of ester. Keeping in mind all the information obtained from retention time and fragmentation pattern, identified compound was Ethyl tridecanoate as shown in **Fig. 3.3.5**.

Identified Compound

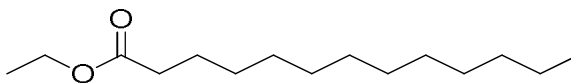
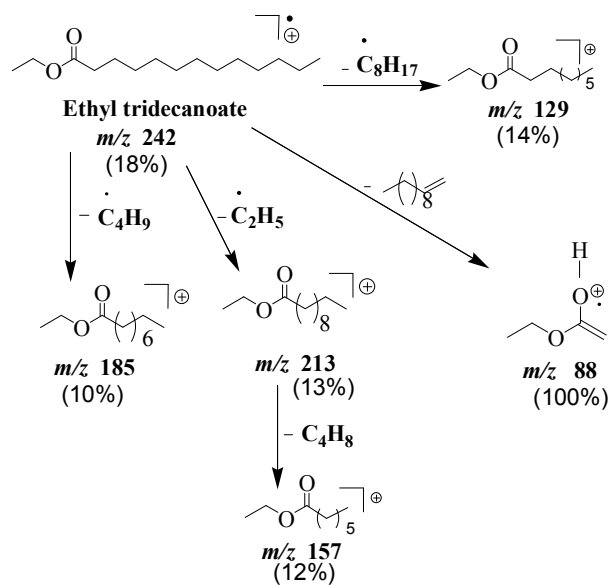


Fig. 3.3.5: Ethyltridecanoate (CS-E5)

Fragmentation Scheme



Scheme 3.1.5 Fragmentation Scheme of Ethyl tridecanoate

3.3.6 CS-E6

Explanation

The signal at retention time 13.044 min. in the HPLC profile of ethanolic extract of *C. sativa* roots was assigned a code CS-E6. Molecular ion peak was with an odd mass, it contained odd number of nitrogen atom as stated by nitrogen rule (**Pavia and Coworkers 2011**). Amides, amines, nitriles or nitro functionality containing odd nitrogen atoms were present. From m/z 319 to m/z 293 difference of 27 mass unit may be due to ethyne or nitriles. Loss of 56 mass unit from m/z 319 to m/z 263 might be due to butane. Loss of 32 mass unit from m/z 263 to m/z 231 may be because of methanol. Loss of 74 mass unit from m/z 281 to m/z 207 might be because of McLafferty cleavage of methyl esters. The fragment mass at m/z 231 from m/z 187, displayed loss of 44 mass unit may be due to α cleavage of amides. From m/z 231 to m/z 160, 71 mass unit may due to pentyl loss. From m/z 207 to m/z 150 difference of 57 mass unit may be due to butyl radical loss. Difference of 15 mass unit from m/z 150 to m/z 135 may be because of methyl radical loss. Loss of 26 mass unit from m/z 150 to m/z 124 may be due to ethyne loss. 41 mass unit difference from m/z 150 to

m/z 109 may be because of ethyl radical loss. 29 mass unit loss inferred the ethyl loss from m/z 124 to m/z 95. Loss of 42 mass unit from m/z 109 to m/z 67 may be because of CH_2CHO radical of aldehydes or ketones. Difference of 28 mass unit from m/z 109 to m/z 81 might be because of ethene loss. Loss of 14 mass unit from m/z 109 to m/z 95 may be due to nitrogen. M-1 or M-29 peak was absent, aldehydes were also absent. No peak at m/z 30 revealed the absence of amines. No peak at m/z 43 which betrayed the absence of ketones. No loss of 46 (NO_2) or peak at m/z 30 which was due to NO confirmed the absence of nitro functionality. Loss of 27 mass unit due to HCN loss was also absent. So, nitriles were also absent. The fragment ion peak at m/z 207 inferred loss of octene from m/z 319. Peak at m/z 150 was due to the loss of butyl radical. The fragment ion peak at m/z 124 corresponded the loss of ethyne from m/z 150. Hydrogen radical loss from m/z 124, peak appeared at m/z 123. Peak at m/z 95 was due to the loss of ethene from m/z 123 as shown in **Scheme. 3.6**. From m/z 95, 28 mass unit was due to the loss of CO and base peak appeared at m/z 67. From above fragmentations one nitrogen atom, carbonyl moiety and alkyl chain was confirmed. From rule of thirteen, molecular formula came out to be $\text{C}_{24}\text{H}_{31}$. By insertion of one nitrogen atom and one oxygen moiety modified molecular formula became $\text{C}_{21}\text{H}_{37}\text{NO}$. By consolidating all the information obtained from retention time and fragmentation scheme, identified compound was *N*-methyl-2,7,15-eicosatrienoic acid as shown in **Fig. 3.3.6**.

Identified Compound

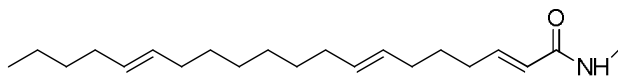
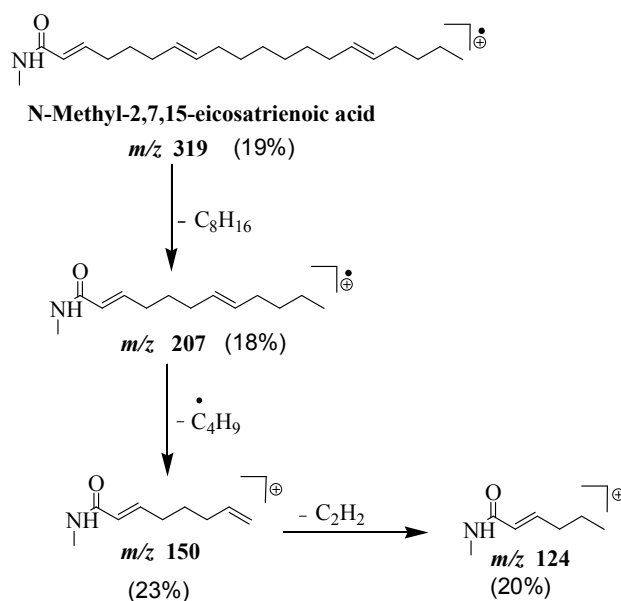


Fig. 3.3.6: *N*-Methyl-2,7,15-eicosatrienoic acid (CS-E6)

Fragmentation Scheme



Scheme 3.1.6 Fragmentation Scheme of N-Methyl-2,7,15-eicosatrienoic acid

3.3.7 CS-E7

Explanation

The signal at retention time 13.056 min. in the HPLC profile of ethanolic extract of *C. sativa* roots was assigned a code CS-E7. 27 mass unit difference from m/z 308 to m/z 281 may be due to HCN loss. From m/z 308 to m/z 263 45 loss inferred the loss of ethoxy or CO_2H of carboxylic acid. From m/z 263 to m/z 247 loss of 16 mass unit displayed the loss of oxygen moiety. 60 mass unit loss from m/z 281 to m/z 221 might be because of the McLafferty cleavage of carboxylic acid. From m/z 247 to m/z 206 loss of 41 mass unit might be due to allylic radical. Loss of 15 mass unit indicated methyl radical from m/z 221 to m/z 206. Loss of 42 mass unit inferred the loss of CH_2CO radical from m/z 206 to m/z 164. 35 mass unit loss indicated chloride ion loss from m/z 150 to m/z 185. Peak at m/z 279 revealed loss of ethyl radical. Loss of ethoxy displayed peak at m/z 263. Loss of $C_7H_{13}O$ radical from m/z 263 gave peak at m/z 150 as shown in **Scheme 3.7**. Allylic radical loss of 41 mass unit from m/z 150 gave peak at m/z 109. Base peak at m/z 81 was satisfied from m/z 109 by the neutral

loss of ethene. Methylene radical cleavage from m/z 81 gave peak at m/z 67. Alkyl chloride showed M+2 peak of approximately one third the intensity of molecular ion peak. As there was no M+2 peak of one third intensity, chloride was absent. No loss of 29 mass unit (CHO) confirmed the absence of aldehyde. No loss of 17 mass unit (OH or CO₂H) confirmed the absence of carboxylic acid. Loss of ethoxy (45) with no loss of OH (17) confirmed the presence of ethyl esters. From rule of thirteen, molecular formula came out to be C₂₃H₃₂. By the insertion of two oxygen moieties, modified molecular formula became C₂₀H₃₆O₂. Calculated HDI came out to be 3, which was satisfied by 2 double bonds and one carbonyl moiety. With the view of this content, identified compound was Linoleic acid methyl ester as shown in **Fig. 3.3.7**.

Identified Compound

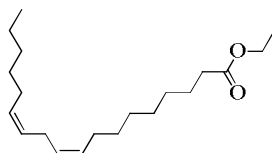
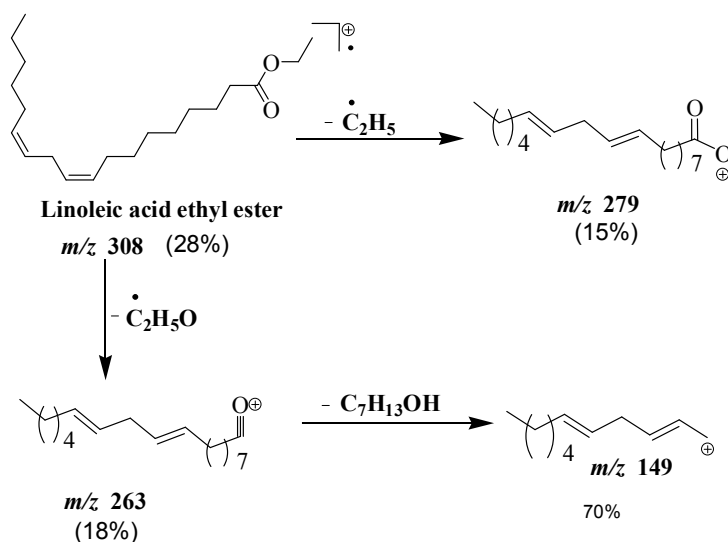


Fig. 3.3.7: Linoleic acid ethyl ester (CS-E7)

Fragmentation Scheme



Scheme 3.1.7 Fragmentation Scheme of Linoleic acid ethylester

3.3.8 CS-E8

Explanation

The signal at retention time 15.842 min. in the HPLC profile of ethanolic extract of *C. sativa* roots was assigned a code CS-E8. Molecular ion peak appeared at m/z 207. As molecular ion peak was with an odd mass, compound containing odd number of nitrogen atoms were present stated by nitrogen rule (**Pavia and Coworkers 2011**). Amines, amides, nitro or nitriles containing odd nitrogen atoms were present. 28 mass unit loss from m/z 207 to m/z 179 might be due to ethene loss or CO moiety. 41 mass unit difference from m/z 207 to m/z 166 may be because of allylic radical loss. The fragment ion peak at m/z 149 was due to 17 mass unit loss from m/z 166. Difference of 17 mass unit may be due to NH_3 or OH of phenol or carboxylic acid. 18 mass unit difference from m/z 149 to m/z 131 might be because of water loss. Loss of 32 mass unit from m/z 117 to m/z 149 might be due to methanol. Peak at m/z 105 inferred presence of methyl tropylium cation, benzoyl cation or benzoate ester. Peak at m/z 91 was due to presence of tropylium cation that manifested the presence of benzene ring. Loss of 35 mass unit from m/z 166 to m/z 131 might be due to loss of chloride ion. Presence of strong M+2 peaks revealed the presence of alkyl chloride or alkyl bromide. As M+ 2 peaks was approximately one third the intensity of the molecular ion peak, unveiled the presence of alkyl chloride. In addition to M+2 peak, distinct M+4 peak was also present that betrayed the presence of chlorine moiety. Loss of 46 mass unit from m/z 207 to m/z 161 might be due to loss of NO_2 as shown in **Scheme 3.8**. No loss of 30 mass unit or appearance of peak at m/z 30 revealed the absence of amines. No loss of 27 mass units that confirmed HCN loss. So, nitriles were also absent. M-1 or peak at m/z 29 due to aldehyde was absent. So, aldehydes were also absent. From all above calculations one benzene ring, two chlorine atoms, one hydroxyl and one nitro group were confirmed. From rule of thirteen, molecular formula came out to be $\text{C}_{15}\text{H}_{27}$. By insertion of two chlorine atoms, one nitrogen atom and three oxygen atoms modified molecular formula became $\text{C}_6\text{H}_3\text{Cl}_2\text{NO}_3$. Identified compound was 3,4-Dichloro-6-nitrophenol as shown in **Fig. 3.3.8**, that were characterized using combined interpretation of retention time and fragmentation pattern.

Identified Compound

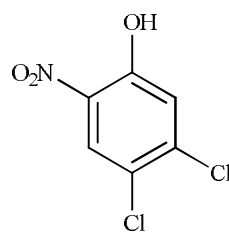
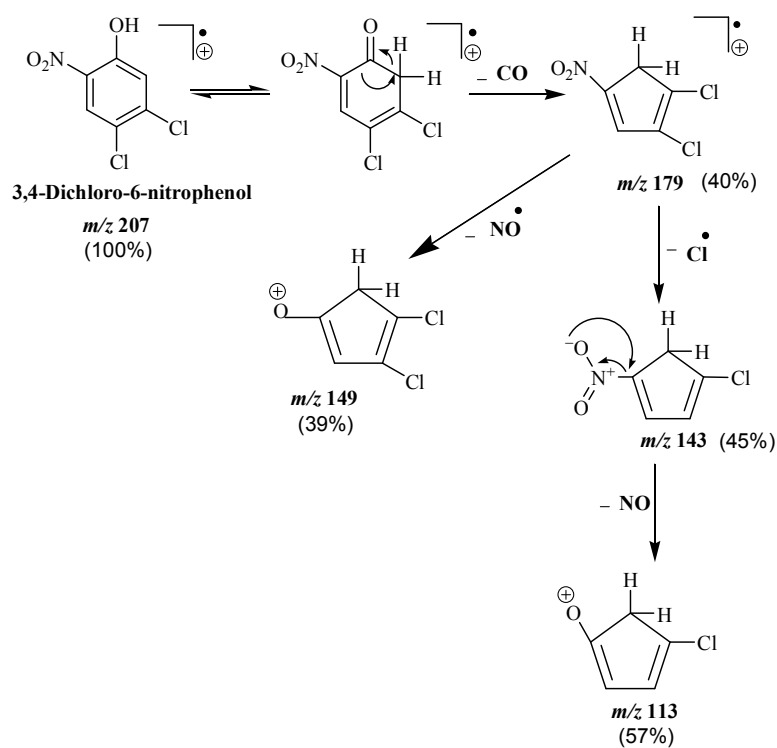


Fig. 3.3.8: 3, 4-Dichloro-6-nitrophenol (CS-E8)

Fragmentation Scheme



Scheme 3.1.8 Fragmentation Scheme of 3,4-Dichloro-6-nitrophenol

3.3.9 CS-E9

Explanation

The signal at retention time 21.107 min. in the HPLC profile of ethanolic extract of *C. sativa* roots was assigned a code CS-E9. This retention time corresponded to high intensity signal. As the column was heated progressively (ramped), less volatile components of a mixture were eluted out in sequence (**Greaves**

and Roboz 2014). Molecular ion peak appeared at m/z 426. As molecular ion peak was with an even mass, odd number of nitrogen atom was absent as stated by nitrogen rule (**Pavia and Coworkers 2011**). So, amines, amides, nitriles or nitro containing odd N atoms were absent. 26 mass unit difference from m/z 426 to m/z 400 inferred the loss of ethyne. 71 mass unit loss manifested pentyl radical loss from m/z 355 to m/z 426. Difference of 28 mass unit may be due to loss of CO and ethene from m/z 355 to m/z 327. 18 mass unit difference may be due to water loss from m/z 303 to m/z 285. 57 mass unit may be due to butyl radical loss from m/z 303 to m/z 246. Peak at m/z 208 was due to $C_{15}H_{28}$ cation and neutral loss of $C_{15}H_{22}O$. 43 mass unit cleavage may be due to propyl radical loss from m/z 178 to m/z 135. No cleavage of 29 mass unit or M-1 peak, aldehydes were absent. Allylic cleavage inferred that cycloalkene type moieties may be present. Peak at m/z 342 betrayed the loss of neutral hexane as shown in **Scheme 3.9**. Loss of methyl radical was manifested from m/z 342 to m/z 327. Fragment ion peak at m/z 285 was due to the cleavage of propene from m/z 327. Cleavage of 18 mass units indicated the water loss. From above evidences, cycloalkenes, hydroxyl group and alkyl chain were indicated. From rule of thirteen, molecular formula came out to be $C_{32}H_{42}$. By insertion of one oxygen atom modified molecular formula became $C_{30}H_{50}O$. Calculated HDI was 6, satisfied by 2 double bonds and 4 cyclic rings. In view of all this calculations, identified compound was Lanosterol as shown in **Fig. 3.3.9**.

Identified Compound

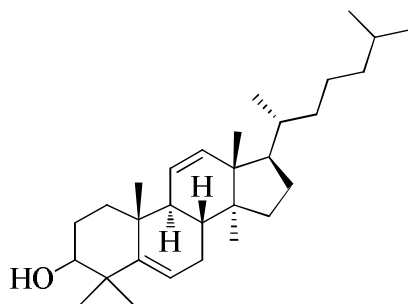
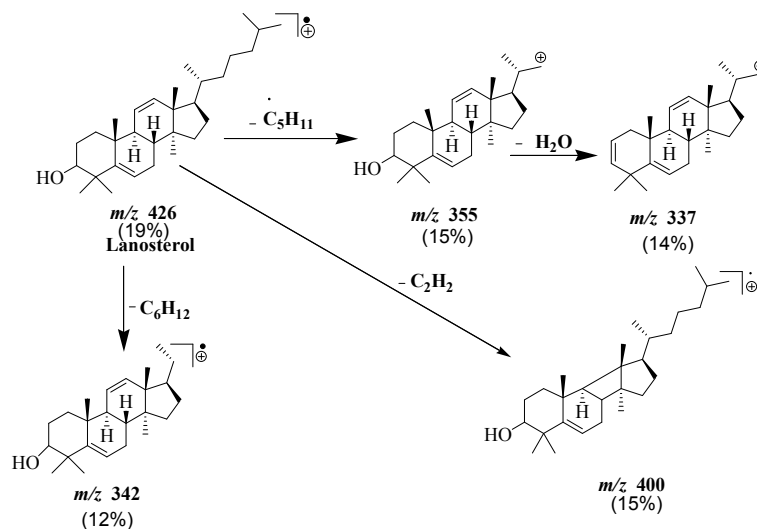


Fig. 3.3.9: Lanosterol (CS-E9)

Fragmentation Scheme



Scheme 3.1.9 Fragmentation Scheme of Lanosterol

3.4 Volatile Compounds of CS-ET-SOX Extract

3 compounds were identified from *Cannabis sativa* soxhlet extraction using ethanol as solvent. TIC profile is given in Fig. 3.2

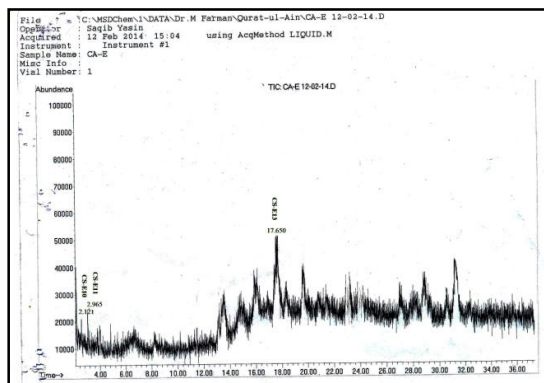


Fig. 3.4 TIC Profile of CS-ET-SOX

3.4.1 CS-E10

Explanation

The signal at retention time 2.121 min. in the HPLC profile of ethanolic extract of *C. sativa* roots was assigned a code CS-E10. Molecular ion peak appeared at m/z 134. Lower retention time inferred the presence of volatile compounds. From m/z 134 to m/z 119 loss of 15 mass unit may be due to ethyl radical. 14 mass unit loss may be due to methylene from m/z 119 to m/z 105. Peak at m/z 105 may be due to methyl tropilium or benzoyl cation. Loss of 14 mass unit from m/z 105 to m/z 91 may be due to loss of methylene. Peak at m/z 91 might be because of tropilium cation. Loss of 14 mass unit from m/z 91 to m/z 77 might be because of methylene. Fragment ion peak at m/z 77 might be due to presence of benzene ring as shown in **Scheme 3.10**. From above fragmentations no indication of M-1 or M-29 peak, aldehydes were absent. M-17 or M-45 peak was missing, carboxylic acids were also absent. As molecular ion peak was with an even mass, odd number of nitrogen atoms were absent stated by nitrogen rule (**Pavia and Coworkers 2011**). So, amines, amides, nitriles or nitro moiety containing odd N atoms were absent. No loss of hydroxyl group, only benzene or alkyl chain was indicated. Molecular formula generated by using rule of thirteen was $C_{10}H_{14}$. Hydrogen deficiency index calculated was 4, satisfied by 3 double bonds and 1 cyclic ring. By consolidating all the information gleaned from above calculations, identified compound was 1-Methyl-2-(1-methylethyl)benzene as shown in **Fig. 3.4.1**.

Identified Compound

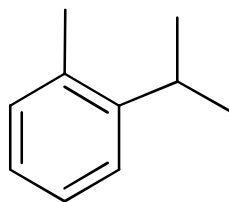
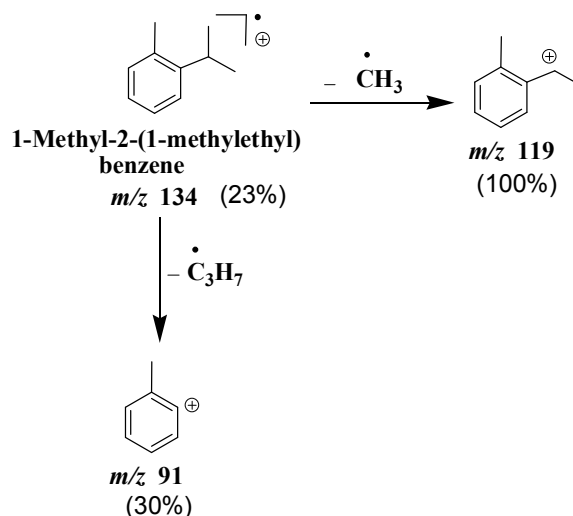


Fig. 3.4.1: 1-Methyl-2-(1-methylethyl)benzene (CS-E10)

Fragmentation Scheme



Scheme 3.2.1 Fragmentation Scheme of 1-Methyl-2-(1-methylethyl)benzene

3.4.2 CS-E11

Explanation

The signal at retention time 2.956 min. in the HPLC profile of ethanolic extract of *C. sativa* roots was assigned a code CS-E11. More volatile components were eluted out first as they are carried through the column by the carrier gas. From m/z 144 to m/z 115, 29 mass unit difference may be due to ethyl radical or CHO loss of aldehydes. Loss of 14 mass unit from m/z 115 to m/z 101 may be due to loss of methylene radical. 43 mass unit loss from m/z 144 to m/z 101 may be due to loss of CH_3CO radical of aldehydes, ketones or due to propyl radical. From m/z 101 to m/z 72 loss of 29 mass unit again because of ethyl radical. From m/z 144 to m/z 72, cleavage of 72 mass unit might be due to loss of pentane. Appearance of peak at m/z 72 or loss of 72 inferred that there was symmetry in the compound. Loss of 46 mass unit from m/z 101 to m/z 55 might be because of nitro moiety loss. 17 mass unit cleavage from m/z 72 to m/z 55 might be due to loss of hydroxyl group. As molecular ion peak was with an even mass, odd number of nitrogen atoms were absent. So, amines, amides, nitriles or nitro moieties were absent (Pavia and Coworkers 2011). No M-1 peak that

inferred absence of aldehydes. M-29, M-43 indicated the presence of alkyl chain. 43 mass unit loss from m/z 144 to m/z 101 unveiled the presence of CH_3CO . Peak at m/z 59 might be due to CH_3CO_2^+ of methyl esters as shown in **Scheme 3.11**. So, the ester moiety was confirmed. From rule of thirteen, molecular formula came out to be C_8H_{20} . By insertion of two oxygen moiety modified molecular formula became $\text{C}_6\text{H}_{12}\text{O}_2$. Hydrogen deficiency index calculated was 1, satisfied by 1 CO. By collecting all the information obtained from retention time and fragmentation pattern, identified compound was hexyl ethanoate as shown in **Fig. 3.4.2**.

Identified Compound

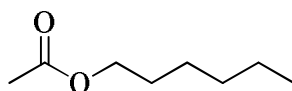
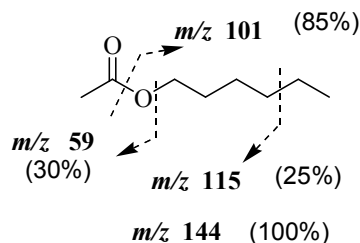


Fig. 3.4.2: Hexyl ethanoate (CS-E11)

Fragmentation Scheme



Scheme 3.2.2 Fragmentation Scheme of Hexyl ethanoate

3.4.3 CS-E12

Explanation

The signal at retention time 2.965 min. in the HPLC profile of ethanolic extract of *C. sativa* roots was assigned a code CS-E12. Molecular ion peak appeared at m/z 116. From m/z 101 to m/z 84, 17 mass unit loss may be due to hydroxyl moiety loss. Peak at m/z 84 inferred presence of hexene moiety. Loss of 29 mass unit from m/z 101 to m/z 72 may be because of ethyl radical loss. Again 17 mass unit loss from m/z 72 to m/z 55 might be because of hydroxyl moiety. Fragment ion peak at m/z 59 may be due to the McLafferty cleavage of amide. Loss of 18 mass unit from m/z 84 to

m/z 66 may be due to water. 42 mass unit difference from m/z 101 to m/z 59 may be due to CH_2CHO radical of aldehydes or ketones. From m/z 101 to m/z 55, 46 mass unit might be due to nitro loss. M-1 or M-29 peak was absent that confirmed the absence of aldehydes. No peak at M-43 or m/z 43, ketones were also absent. There was no loss of 16 mass unit due to NH_2 or α cleavage of amide at m/z 44 that inferred the absence of amide. No loss of 46 mass unit due to nitro or 30 mass unit due to nitroso, nitro moiety was also absent. No peak at m/z 30 due to $\text{CH}_2=\text{NH}_2^+$ that also revealed the absence of amines. From rule of thirteen, molecular formula came out to be C_8H_{20} . Loss of water manifested the presence of oxygen moiety. By insertion of two oxygen moiety, modified molecular formula became $\text{C}_6\text{H}_{12}\text{O}_2$. Hydrogen deficiency index calculated was 1, satisfied by 1 cyclic ring. The fragment ion peak at m/z 101 was due to the loss of methyl radical from m/z 116. Base peak at m/z 72 was due to the loss of $\text{C}_2\text{H}_4\text{O}$ radical as shown in **Scheme 3.12**. Peak at m/z 56 was due to the loss of $\text{C}_2\text{H}_4\text{O}_2$. With the view of all above information, identified compound was 2,4,5-Trimethyl-1,3-dioxolane as shown in **Fig. 3.4.3**.

Identified Compound

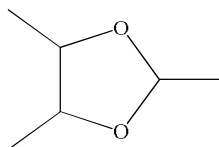
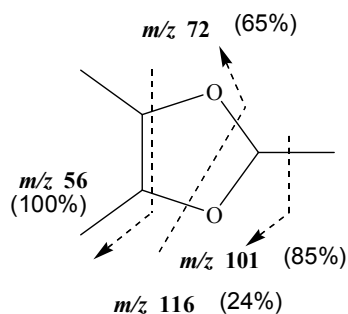


Fig. 3.4.3: 2, 4, 5-Trimethyl-1,3-dioxolane (CS-E12)

Fragmentation Scheme



Scheme 3.2.3 Fragmentation Scheme of 2,4,5-Trimethyl-1,3-dioxolane

3.4.4 CS-E13

The signal at retention time 17.650 min. in the HPLC profile of ethanolic extract of *C. sativa* roots was assigned a code CS-E13. Molecular ion peak appeared at m/z 426. As molecular ion peak was with an even mass, odd number of nitrogen atoms were absent as stated by nitrogen rule. Amides, amines, nitriles or nitro groups containing odd nitrogen atoms were absent. From m/z 426 to m/z 411, 15 mass unit loss might be due to methyl radical. Difference of 32 mass unit may be because of methanol loss from m/z 411 to m/z 379. 71 mass unit loss from m/z 426 to m/z 355 may be because of pentyl radical. Again loss of 32 mass unit may be due to methanol from m/z 355 to m/z 323. Difference of 43 mass unit from m/z 323 to m/z 280 may infer presence of propyl radical or CH_2CHO radical of aldehydes. 35 mass unit difference from m/z 280 to m/z 245 might be due to chloride radical. Cleavage of 30 mass unit may be due to NO loss of nitro functionality. Difference of 46 mass unit may be because of nitro loss from m/z 229 to m/z 183. Cleavage of 19 mass unit from m/z 163 to m/z 144 may be because of fluoride. 44 mass unit loss may be because of propane cleavage from m/z 163 to m/z 119. 14 mass unit difference may be because of methylene loss from m/z 119 to m/z 105. Peak at m/z 105 may be because of methyl tropilium cation and benzoyl cation. Loss of 26 mass unit from m/z 105 to m/z 79 may be due to ethyne loss. Difference of 18 mass unit was due to water, that confirmed the presence of hydroxyl group. The fragment ion peak at m/z 411 betrayed the loss of methyl radical from m/z 426. Loss of water from m/z 411 and fragment ion peak appeared at m/z 393. The fragment ion peak at m/z 327 was due to loss of hexene from m/z 426. Peak at m/z 299 was due to loss of ethene from m/z 327 as shown in **Scheme 3.31**. Loss of water from m/z 299, peak appeared at m/z 281. By applying rule of thirteen, molecular formula came out to be $\text{C}_{32}\text{H}_{42}$. Modified molecular formula became $\text{C}_{30}\text{H}_{50}\text{O}$ by insertion of one oxygen atom. Calculated HDI was 6, satisfied by 4 cyclic rings and 2 double bonds. So, identified compound was 4,14-Dimethylergosta-8,22-dien-3-ol as shown in **Fig. 3.4.4**.

Identified Compound

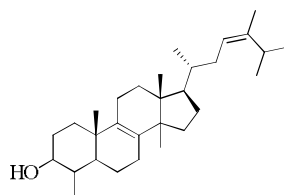
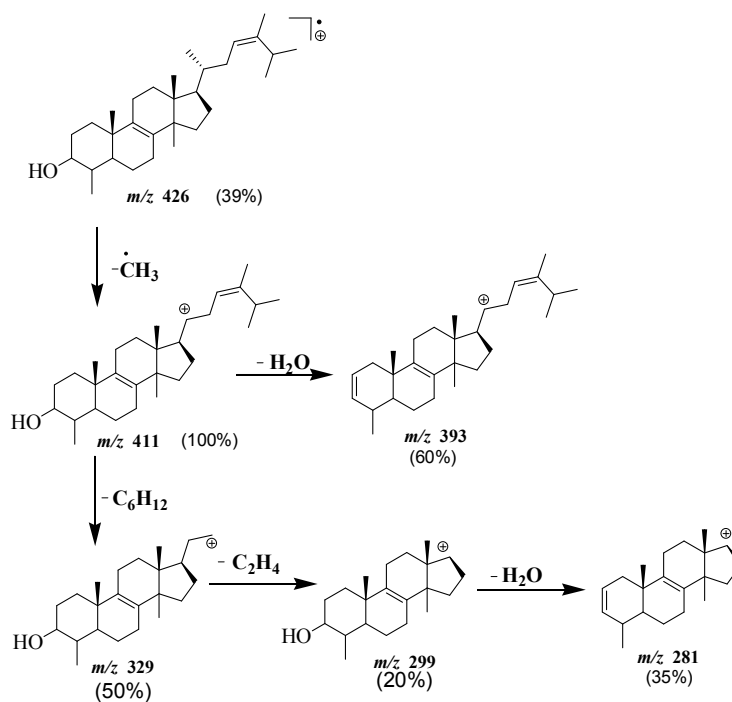


Fig. 3.4.4: 4,14-Dimethyl-Ergosta-8,22-dien-3-ol (CS-E13)

Fragmentation Scheme



Scheme 3.2.4 Fragmentation Scheme of 4,14-Dimethyl-Ergosta-8,22-dien-3-ol

3.5 Volatile compounds of CS-H extract

10 compounds were identified from *C. sativa* *n*-hexane extracts. TIC profile is given in **Fig. 3.5**.

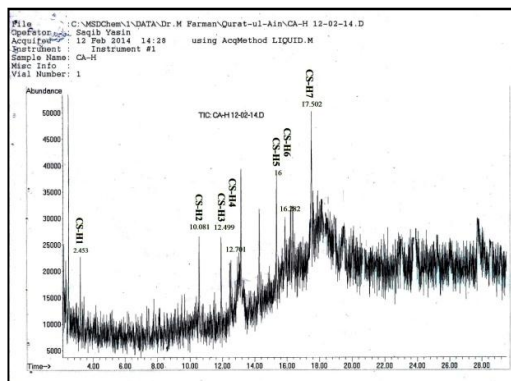


Fig. 3.5 TIC profile of CS-H extract

3.5.1 CS-H1

Explanation

The signal at retention time 2.453 min. in the HPLC profile of *n*-hexane extract of *C. sativa* roots was assigned a code CS-H1. Molecular ion peak appeared at m/z 156. This spectrum consisted of odd mass separated by 14 mass units, corresponding to the difference of CH_2 group. From m/z 158 to m/z 113 loss of 43 mass unit which manifested the loss of propyl radical. Appearance of peak at m/z 99 inferred the presence of heptylium cation. Loss of 57 mass unit from m/z 156 to m/z 99 unveiled the loss of butyl radical. Peak at m/z 85 displayed the presence of hexylium cation. Loss of 71 mass unit from m/z 85 to m/z 156 indicated the loss of pentyl radical as shown in **Scheme 3.13**. Base peak at m/z 57 indicated the presence of secondary butylium cation. As there is a general rule of chemistry that secondary carbocation is more stable than a primary carbocation.

From rule of thirteen, molecular formula came out to be $\text{C}_{11}\text{H}_{24}$. Calculated HDI was zero which indicated no unsaturation or cyclic compounds. By consolidating all the information obtained from retention time and fragmentation pattern, identified compound was undecane as shown in **Fig. 3.5.1**.

Identified Compound

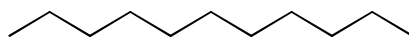
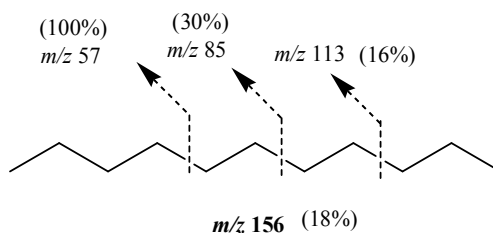


Fig. 3.5.1: Undecane (CS-H1)

Fragmentation Scheme



Scheme 3.3.1 Fragmentation Scheme of undecane

3.5.2 CS-H2

Explanation

The signal at retention time 10.801 min. in the HPLC profile of *n*-hexane extract of *C. sativa* roots was assigned a code CS-H2. Molecular ion peak appeared at m/z 242. From m/z 242 to m/z 227 loss of 15 mass unit inferred methyl. Loss of 28 mass unit from m/z 227 to m/z 199 unveiled the loss of ethene or CO. Difference of 57 mass unit from m/z 185 to m/z 242 might be due to propyl radical loss. One more loss of 28 mass unit from m/z 185 to m/z 157 manifested the loss of CO. Loss of methyl radical was inferred from m/z 199 to m/z 185. From m/z 116 to m/z 171, loss of 41 mass unit might be due to allylic radical. Loss of 42 mass unit from m/z 185 to m/z 143 displayed the loss of CO+N or may be due to CH₂CO radical. Peak at m/z 91 unveiled the presence of tropylium cation as shown in **Scheme 3.14**. Loss of 16 mass unit from m/z 107 to m/z 91 indicated the loss of oxygen moiety.

As molecular ion peak was with even number, even number of nitrogen atom may be present. Odd number of nitrogen atom was ruled out. From rule of thirteen, molecular formula came out to be C₁₈H₃₄. By adjusting two oxygen atoms and two nitrogen atoms modified molecular formula became C₁₄H₁₄N₂O₂. Calculated HDI came out to be 9, that were satisfied by 5 double bonds, 2 carbonyl moiety and by two

cyclic rings. So, identified compound was N-(3-acetyl-2-methyl-4-quinolinyl) acetamide as shown in **Fig. 3.5.2**, that were characterized by using combined interpretation of retention time and fragmentation pattern.

Identified Compound

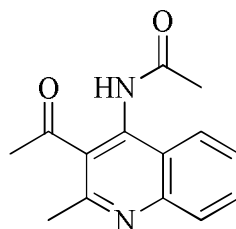
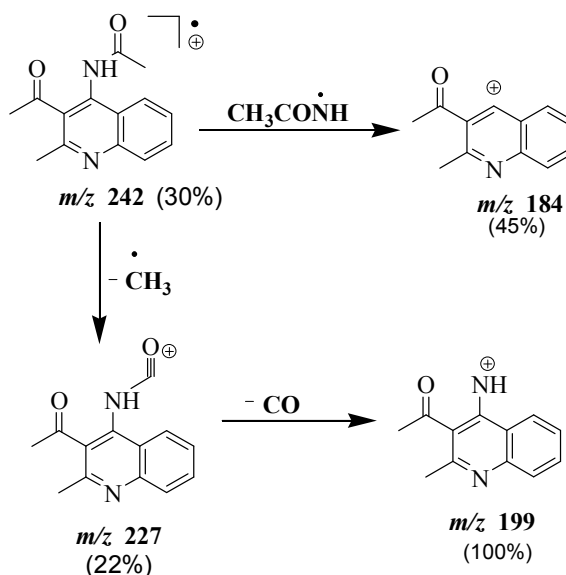


Fig. 3.5.2: N-(3-acetyl-2-methyl-4-quinolinyl) acetamide (CS-H2)

Fragmentation Scheme



Scheme 3.3.2. Fragmentation Scheme of N-(3-acetyl-2-methyl-4-quinolinyl) acetamide

3.5.3 CS-H3

Explanation

The signal at retention time 12.449 min. in the HPLC profile of *n*-hexane extract of *C. sativa* roots was assigned a code CS-H3. Molecular ion peak appeared at *m/z* 294. Molecular ion peak was with an even mass, odd number of nitrogen atoms

were absent as stated by nitrogen rule (Pavia *et al.*, 2011). So, amines, amides, nitro or nitriles containing odd nitrogen were absent. Loss of 32 mass unit from m/z 294 to m/z 262 may be because of methanol loss. From m/z 294 to m/z 240 difference of 54 mass unit may be because of butane. Loss of 41 mass unit from m/z 262 to m/z 221 may inferred loss of allylic radical. 44 mass unit difference from m/z 221 to m/z 177 may be because of McLafferty of aldehydes. 26 mass unit difference from m/z 177 to m/z 151 might be due to loss of ethyne. Cleavage of 28 mass unit from m/z 151 to m/z 123 may be because of ethene or CO loss. 29 mass unit difference from m/z 109 to m/z 138 may be due to loss of ethyl radical. 14 mass unit loss from m/z 109 to m/z 95 may be due to methylene. Again 28 mass unit loss from m/z 95 to m/z 67 might be due to ethene or CO. Loss of 85 mass unit from m/z 262 to m/z 177 may be due to hexyl radical. No M-1 or M-29 peak, aldehydes were also absent. M-15, M-29 or M-43 peak unveiled the presence of alkyl chain. From m/z 294 to m/z 263 difference of 31 mass unit inferred the presence of methoxy. Loss of 98 mass unit from m/z 196 to m/z 294 indicated the presence of heptene. The fragment ion peak at m/z 221 was due to the $C_3H_5O_2$ radical loss. From m/z 221 to m/z 177 propane loss was confirmed. Due to butyne loss from m/z 177 fragment ion peak appeared at m/z 123. Base peak at m/z 81 betrayed the loss of propene from m/z 123 as shown in **Scheme 3.15**. From rule of thirteen, molecular formula came out to be $C_{22}H_{30}$. By insertion of two oxygen moieties, modified molecular formula became $C_{19}H_{34}O_2$. HDI calculated was 3, satisfied by 2 double bonds and 1 carbonyl moiety. So, the identified compound was methyl-9,12-octadecadienoate as shown in **Fig. 3.5.3**.

Identified Compound

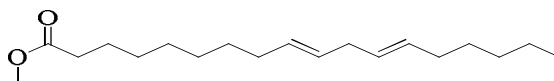
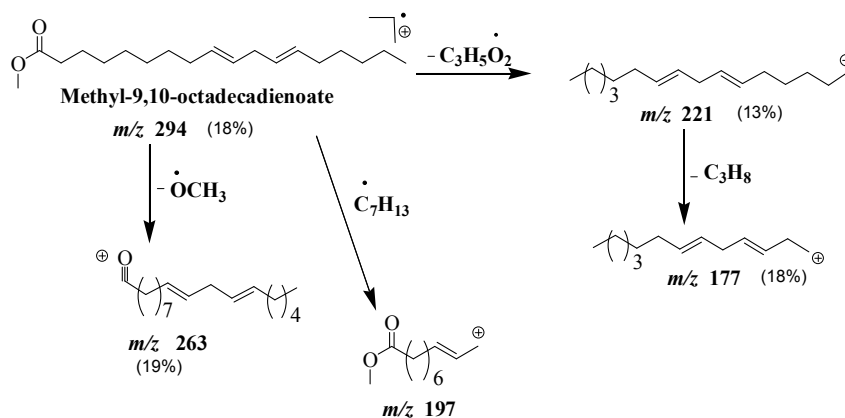


Fig. 3.5.3: Methyl- 9, 12-octadecadienoate (CS-H3)

Fragmentation Scheme



Scheme 3.3.3 Fragmentation Scheme of methyl-9,12-octadecadienoate

3.5.4 CS-H4

Explanation

The signal at retention time 12.701 min. in the HPLC profile of *n*-hexane extract of *C. sativa* roots was assigned a code CS-H4. As the column was heated progressively ramped, less volatile components of a mixture were eluted out (**Greaves and Roboz 2014**). Molecular ion peak appeared at m/z 298. Molecular ion peak was with an even mass, odd number of nitrogen atoms were absent. So, amides, amines, nitro or nitriles containing odd nitrogen atoms were absent. Loss of 43 mass unit from m/z 298 to m/z 255 may be because of propyl radical or $CH_2=CHO$ radical of aldehydes. Difference of 42 mass unit from m/z 255 to m/z 213 might be due to CH_2CHO radical of aldehydes or ketones. 85 mass unit difference from m/z 298 to m/z 213 might be because of hexyl radical. 56 mass unit loss from m/z 255 to m/z 199 may be because of butene. 14 mass unit loss from m/z 199 to m/z 185 may due to methylene loss. 28 loss from m/z 185 to m/z 157 may be due to ethene or CO loss. Again loss of 56 from m/z 185 to m/z 129 may be due to butene loss. Base peak at m/z 74 may be due to McLafferty cleavage of methyl esters. No M-1 or M-29 peak aldehydes were absent. Loss of propyl radical from m/z 298 to m/z 255. The fragment ion peak at m/z 199 was due to loss of butene from m/z 255. Loss of hexyl radical from m/z 298, peak appeared at m/z 213. Loss of decyl radical from m/z 298 to m/z

157 confirmed the presence of alkyl chain. Similarly, loss of 169 from m/z 298 to m/z 129 confirmed the presence of dodecyl radical. Base peak at m/z 74 confirmed the presence of methyl ester as shown in **Scheme 3.3.4**. Loss of propyl, butyl, pentyl or decyl radical confirmed the presence of alkyl chain. From rule of thirteen, molecular formula came out to be $C_{22}H_{34}$. By insertion of two oxygen moiety modified molecular formula became $C_{19}H_{38}O_2$. Calculated HDI was 1, satisfied by 1 carbonyl moiety. So, identified compound was methyl octadecanoate as shown in **Fig. 3.5.4**.

Identified Compound

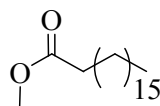
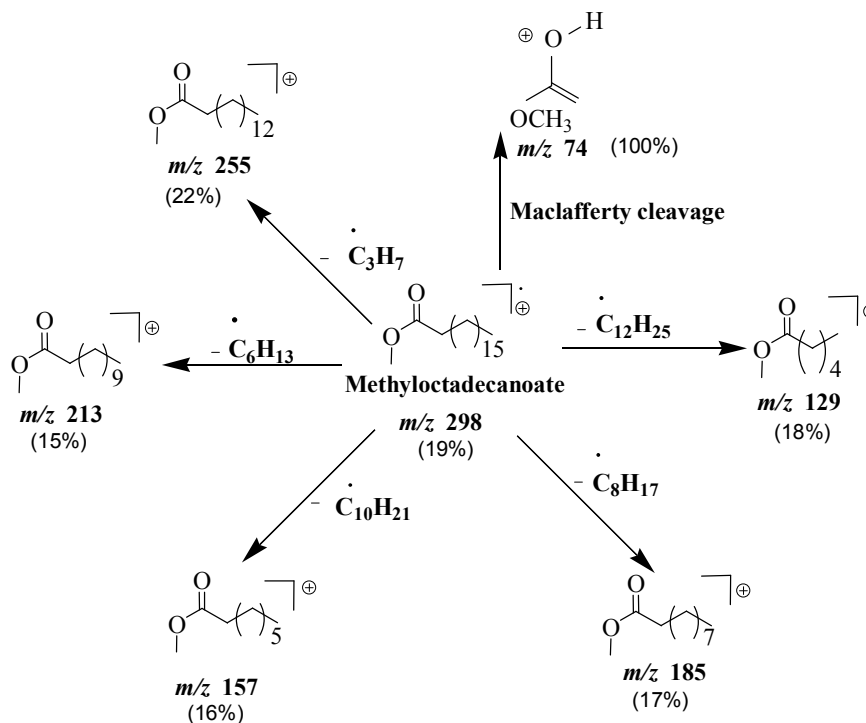


Fig. 3.5.4: Methyl octadecanoate (CS-H4)

Fragmentation Scheme



Scheme 3.3.4 Fragmentation Scheme of Methyl octadecanoate

3.5.5 CS-H5

Explanation

The signal at retention time 16 min. in the HPLC profile of *n*-hexane extract of *C. sativa* roots was assigned a code CS-H5. Molecular ion peak appeared at m/z 354. As column was heated progressively (ramped), less volatile components of mixture were eluted out in a sequence (Greaves and Roboz 2014). As molecular ion peak was with an even mass, odd number of nitrogen atoms were absent. So amides, amines, nitro or nitriles containing odd nitrogen atom were absent. 43 mass unit loss from m/z 354 to m/z 311 may be because of propyl radical or $\text{CH}_2=\text{CHO}$ radical of aldehydes. Difference of 30 mass unit from m/z 311 to m/z 281 might be because of primary amines loss. Cleavage of 56 mass unit from m/z 311 to m/z 256 may infer loss of butene. 27 mass unit loss from m/z 255 to m/z 228 may display loss of ethyne or HCN moiety. Difference of 42 mass unit from m/z 228 to m/z 186 may display loss of $\text{CH}_2=\text{CHO}$ radical of aldehydes or ketones. Again loss of 56 mass unit from m/z 228 to m/z 172 may be because of butene. 14 mass unit cleavage from m/z 186 to m/z 172 might be due to methylene loss. 28 mass unit cleavage from m/z 172 to m/z 144 may be due to cleavage of ethene or CO. Again difference of 43 mass unit from m/z 172 to m/z 129 might be due to propyl radical loss. 41 mass unit difference from m/z 115 to m/z 74 may be because of allylic radical. No M-1 or M-29 peak that inferred absence of aldehydes. As molecular ion peak was with an even mass, displayed absence of HCN. The fragment ion peak at m/z 311 was manifested loss of propyl radical from m/z 354. Loss of pentadecene from m/z 354, peak displayed at m/z 143. From m/z 354 to m/z 228, inferred loss of nonene. Difference of dodecene from m/z 354, peak appeared at m/z 186. Base peak at m/z 74 manifested McLafferty cleavage of methyl esters as shown in Scheme 3.3.5. From rule of thirteen, molecular formula came out to be $\text{C}_{27}\text{H}_{30}$. By insertion of two oxygen moiety, modified molecular formula became $\text{C}_{23}\text{H}_{46}\text{O}_2$. HDI calculated was 1, satisfied by one carbonyl moiety. By consolidating all the information obtained from retention time and fragmentation pattern, identified compound was methyl docosanoate as given in Fig. 3.5.5.

Identified Compound

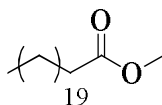
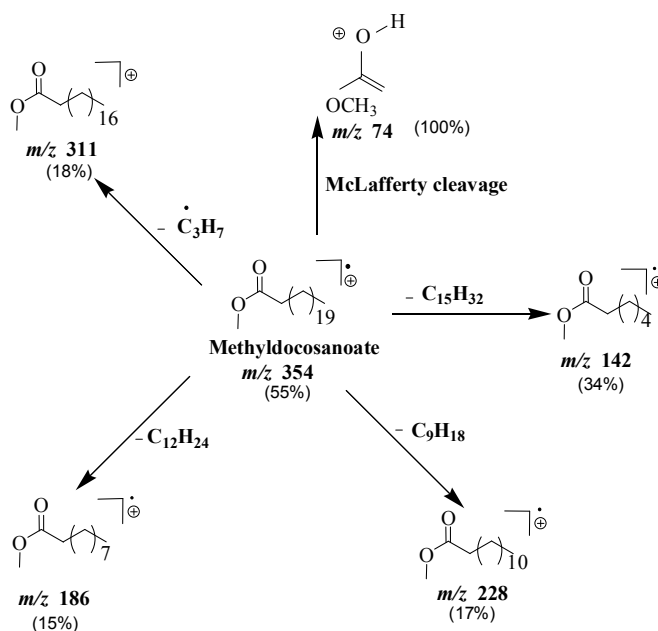


Fig. 3.5.5: Methyl docosanoate (CS-H5)

Fragmentation Scheme



Scheme 3.3.5 Fragmentation Scheme of Methyl docosanoate

3.5.6 CS-H6

The signal at retention time 16.289 min. in the HPLC profile of *n*-hexane extract of *C. sativa* roots was assigned a code CS-H6. Molecular ion peak appeared at m/z 314. As molecular ion peak was with an even mass, odd number of nitrogen atoms were absent. As column was heated progressively (ramped), less volatile component of a mixture were eluted out (Greaves and Roboz 2014). Amines, amides, nitriles or nitro moieties containing odd nitrogen atoms were absent (Pavia *et al.*, 2011). Difference of 15 mass unit from m/z 314 to m/z 299 might be due to loss of methyl radical. From m/z 299 to m/z 281 loss of 18 mass unit may be because of water. Difference of 27 mass unit from m/z 258 to m/z 231 may infer presence of

ethyne or HCN. Cleavage of 16 mass unit from m/z 231 to m/z 215 may be due to oxygen atom. 30 mass unit loss from m/z 231 to m/z 201 might be due to primary amines. Loss of 14 mass unit from m/z 215 to m/z 201 may be due to methylene. 26 mass unit cleavage may be because of ethenyl loss from m/z 189 to m/z 163. Again cleavage of 14 mass unit from m/z 149 to m/z 163 was due to methylene. Loss of 41 mass unit from m/z 149 to m/z 108 may manifest loss of allyl radical. Difference of 14 mass unit from m/z 314 to m/z 299 revealed methyl loss. 56 mass unit loss from m/z 314 to m/z 258 displayed butene. The fragment ion peak at m/z 243 was because of pentyl radical loss from m/z 314. The fragment ion peak at m/z 163, displayed loss of $C_{10}H_7O$ radical. Retro-Diels-Alder reaction accounts for the fragment at m/z 231. Base peak at m/z 299 was also satisfied by the loss of methyl radical as shown in **Scheme 3.3.6**. Base peak didn't corresponded to the molecular ion peak, indicated that these compounds were easily fragmented by GC-MS (**Greaves and Roboz 2014**). From rule of thirteen, molecular formula came out to be $C_{24}H_{26}$. By insertion of two oxygen moiety, modified molecular formula became $C_{21}H_{30}O_2$. Hydrogen deficiency index calculated was 7, satisfied by 4 double bonds and 3 cyclic rings. The fragment ion peak at m/z 314 may be due to $\Delta^{(8)}$ -Tetrahydrocannabinol, $\Delta^{(9)}$ -Tetrahydrocannabinol, Cannabidiol and Cannabichromene. By Retro-Diels-Alder cleavage peak appeared at m/z 231 (**Hazekamp et al., 2007**). This peak was present in $\Delta^{(9)}$ -Tetrahydrocannabinol and absent in $\Delta^{(8)}$ -Tetrahydrocannabinol, Cannabidiol and Cannabichromene. Keeping in view all the information obtained from retention time and fragmentation pattern, identified compound was $\Delta^{(9)}$ -Tetrahydrocannabinol as given in **Fig. 3.5.6**.

Identified Compound

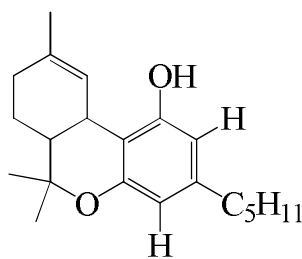
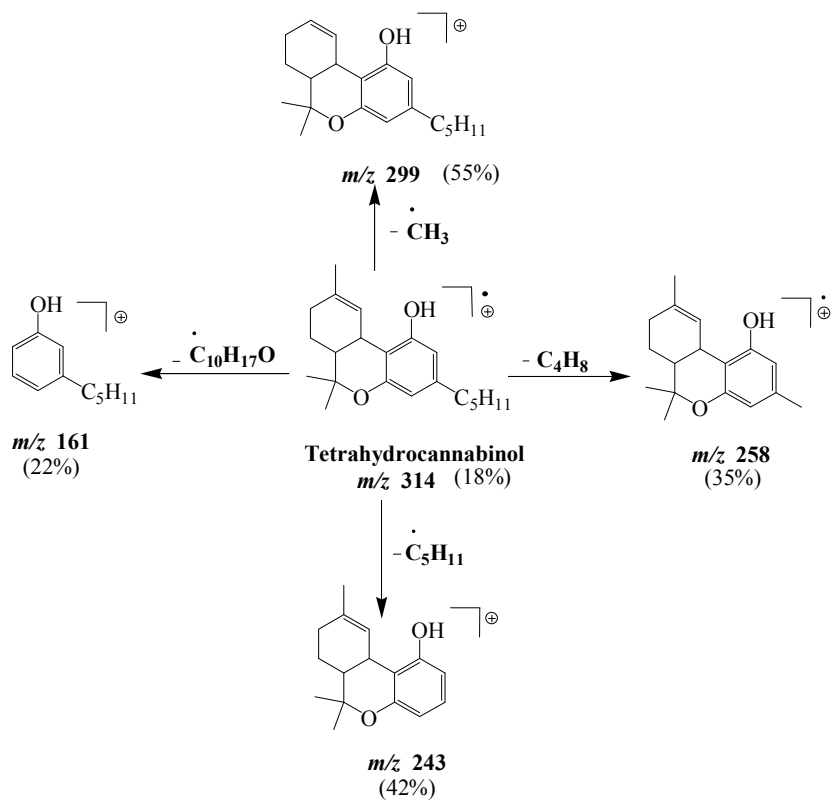


Fig. 3.5.6: Tetrahydrocannabinol (CS-H6)

Fragmentation Scheme



Scheme 3.3.6 Fragmentation Scheme of Tetrahydrocannabinol

3.6 Volatile Compounds of CS-A Extract

Only 1 compound was identified from *C. sativa* acetone extract. TIC profile is given in **Fig. 3.6**.

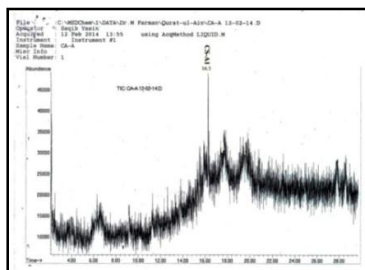


Fig. 3.6 TIC Profile of CS-A Extract

3.6.1 CS-A1

The signal at retention time 16.300 min. in the HPLC profile of acetone extract of *C. sativa* roots was assigned a code CS-A1. As the column was heated progressively (ramped), less volatile component of a mixture was eluted out (**Greaves and Roboz 2014**). Molecular ion peak appeared at m/z 314. As molecular ion peak was with an even mass, odd number of nitrogen atoms were absent indicated by nitrogen rule (**Pavia *et al.*, 2011**). Length of the line in the digital bar graph corresponded to high signal intensity. Amines, amides, nitro or nitriles containing odd nitrogen atoms were absent. From m/z 314 to m/z 299 difference of 15 mass unit may be because of methyl radical loss. Difference of 18 mass unit from m/z 299 to m/z 281 might be due to water loss. 32 mass unit loss from m/z 299 to m/z 267 may infer loss of methanol. Cleavage of 71 mass unit from m/z 243 to m/z 314 may display loss of pentyl radical. From m/z 243 to m/z 288, difference of 45 mass unit may be because of ethoxy or CO_2H loss of carboxylic acid. Loss of 86 mass unit from m/z 228 to m/z 314 may infer pentene. Difference of 14 mass unit from m/z 207 to m/z 193 might be due to methylene cleavage. 16 mass unit loss from m/z 193 to m/z 177 may display oxygen. Fragment ion peak at m/z 91 betrayed the presence of tropilium cation. The fragment ion peak at m/z 299 manifested the loss of methyl radical from m/z 299 to m/z 314 as shown in **Scheme 3.4.1**. Base peak at m/z 207 was justified by the loss of C_8H_{11} radical. As base peak did not corresponded to molecular ion peak, but to a

fragment indicated that these are easily fragmented by GC-MS (**Hazekamp *et al.*, 2007**). Peak at m/z 246 was due to the Retro-Diels-Alder cleavage. Loss of hexyl radical was confirmed from m/z 243 to m/z 314. Fragment ion peak at m/z 176 was due to loss of $C_9H_{14}O$ radical. From above fragmentations no M-1 or M-29 peak that confirmed the absence of aldehydes. Due to loss of 18 mass units, hydroxyl group was confirmed. From rule of thirteen, molecular formula came out to be $C_{24}H_{26}$. By insertion of two oxygen moieties, modified molecular formula became $C_{21}H_{30}O_2$ and HDI was 7, satisfied by 7 double bonds and 2 cyclic rings. Keeping in mind all the information obtained from retention time and fragmentation pattern, identified compound was Cannabidiol as displayed in **Fig. 3.6.1**.

Identified Compound

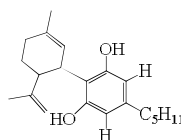
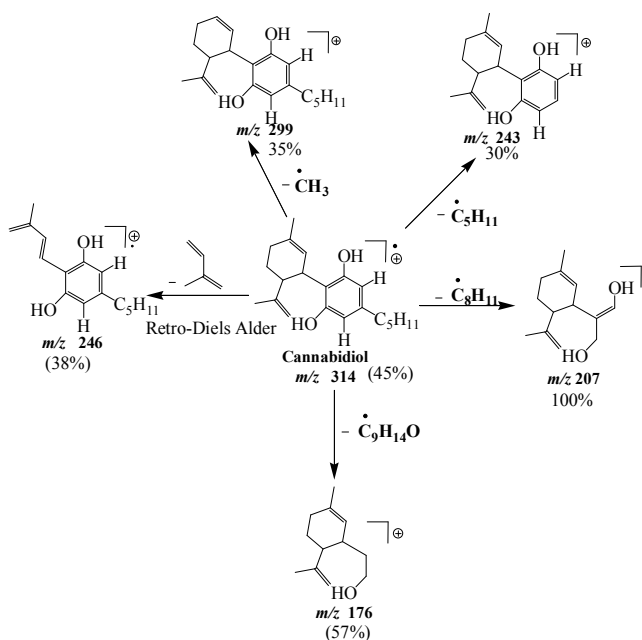


Fig. 3.6.1: Cannabidiol (CS-A1)

Fragmentation Scheme



Scheme 3.4.1 Fragmentation Scheme of Cannabidiol

3.7 Volatile Compounds of CS-PE Extract

7 compounds were identified from *C. sativa* pet-ether extracts. TIC profile is given in Fig. 3.7.

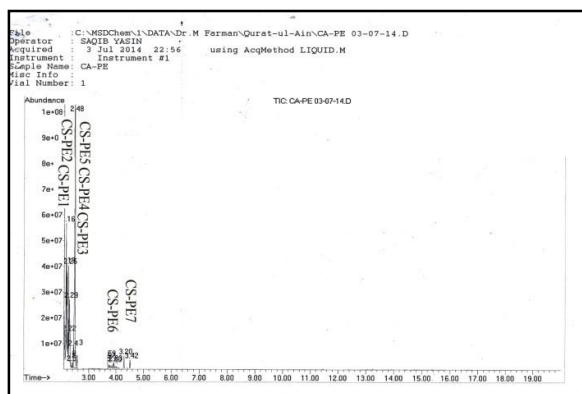


Fig. 3.7 TIC Profile of CS-PE Extract

3.7.1 CS-PE1

Explanation

The signal at retention time 2.021 min. in the HPLC profile of pet ether extract of *C. sativa* roots was assigned a code CS-PE1. Lower retention time inferred the presence of volatile compounds (Greaves and Roboz 2014). Molecular ion peak appeared at m/z 156. As molecular ion peak was with an even mass, odd number of nitrogen atoms were absent (Pavia *et al.*, 2011). Amines, amides, nitro or nitriles containing odd nitrogen atoms were absent. Difference of 57 mass unit from m/z 156 to m/z 99 may be due to loss of butyl radical. Peak at m/z 99 may be because of heptylium cation. 14 mass unit cleavage from m/z 85 to m/z 99 may be due to methylene. Again cleavage of 14 mass unit from m/z 85 to m/z 71 may be because of methylene. Peak at m/z 71 may inferred pentylium cation. Peak at m/z 99, 85, 71, 57 revealed the alkyl chain. From rule of thirteen, molecular formula came out to be $C_{11}H_{24}$. Hydrogen deficiency index was 0, unveiled no unsaturation or cyclic ring. Peak at m/z 57, 71, 85 and 99 displayed the presence of alkyl chain as shown in Scheme 3.5.1. Base peak at m/z 57 indicated the presence of secondary butyl cation. So, identified compound was 3-Methyldecane as shown in Fig. 3.7.1.

Identified Compound

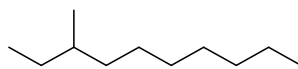
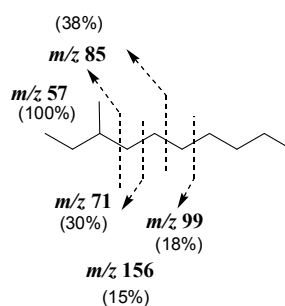


Fig. 3.7.1: 3-Methyldecane (CS-PE1)

Fragmentation Scheme



Scheme 3.5.1 Fragmentation Scheme of 3-Methyldecane

3.7.2 CS-PE2

Explanation

The signal at retention time 2.161 min. in the HPLC profile of pet ether extract of *C. sativa* roots was assigned a code CS-PE2. Molecular ion peak appeared at m/z 120. As molecular ion peak was with an even mass, odd number of nitrogen atoms were absent as stated by nitrogen rule (Pavia *et al.*, 2011). Amines, amides, nitriles or nitro containing odd nitrogen atoms were absent. 15 mass unit loss from m/z 120 to m/z 105 might be due to methyl radical. Peak at m/z 105 may infer benzoylcation or methyl tropilium cation. 14 mass unit loss from m/z 105 to m/z 91 may display methylene loss. Peak at m/z 91 was due to tropilium cation. From m/z 91 to m/z 77 cleavage of 14 mass unit may be due to methylene. Peak at m/z 77 might be due to phenyl radical. Difference of 28 mass unit from m/z 105 to m/z 77 might be because of ethene or CO moiety. From rule of thirteen, molecular formula came out to be C_9H_{12} . Hydrogen deficiency index calculated was 4, satisfied by 3 double bonds and 1 cyclic ring. No loss of M-1 or M-29, which displayed the absence of aldehydes. No loss or appearance of peak at m/z 43 betrayed the absence of ketones. No M-17 or M-45 peak which unveiled the absence of carboxylic acids. Peak at m/z 105, 91, 77

confirmed the presence of benzene ring as shown in **Scheme 3.5.2**. Peak at m/z 77 manifested the substitution of one hydrogen of benzene ring. Two proposed structures were 1,2,3-Trimethylbenzene or propyl benzene. Accepted structure was propyl benzene because of peak at m/z 77 due to loss of propyl radical. So, identified compound was propyl-benzene as shown in **Fig. 3.7.2**.

Identified Compound

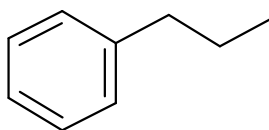
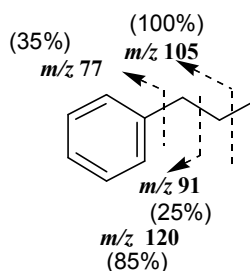


Fig. 3.7.2: Propylbenzene (CS-PE2)

Fragmentation Scheme



Scheme 3.5.2 Fragmentation Scheme of Propylbenzene

3.7.3 CS-PE3

Explanation

The signal at retention time 2.184 min. in the HPLC profile of pet ether extract of *C. sativa* roots was assigned a code CS-PE3. Lower retention time inferred the presence of volatile components. Molecular ion peak appeared at m/z 140. Difference of 29 mass unit from m/z 140 to m/z 111 may infer ethyl radical. 28 mass unit loss from m/z 83 to m/z 111 may be due to ethene. 57 mass unit difference from m/z 83 to m/z 140 might be due to loss of propyl radical. Again loss of 28 mass unit from m/z 55 to m/z 83 represented ethene or CO moiety. As molecular ion peak was with an even mass, odd number of nitrogen atoms were absent (**Pavia et al., 2011**). Amines,

amides, nitriles or nitro containing odd nitrogen atoms were absent. No peak at M-1 or M-29, aldehydes were absent. No M-43 or m/z 43 ketones were also absent. Loss of 28 mass unit may be due to ethene in cycloalkanes. From rule of thirteen, molecular formula came out to be $C_{10}H_{20}$. Hydrogen deficiency index calculated was 1, satisfied by 1 cyclic ring. The fragment ion peak at m/z 111 was due to loss of ethyl radical as shown in **Scheme 3.5.3**. From m/z 140 to m/z 83 difference of 57 mass unit was due to butyl radical loss. The fragment ion peak at m/z 55 was due to loss of ethene from m/z 83. Base peak at m/z 83 was satisfied by loss of ethene from m/z 111. So, identified compound was Butylcyclohexane as shown in **Fig. 3.7.3**.

Identified Compound

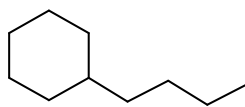
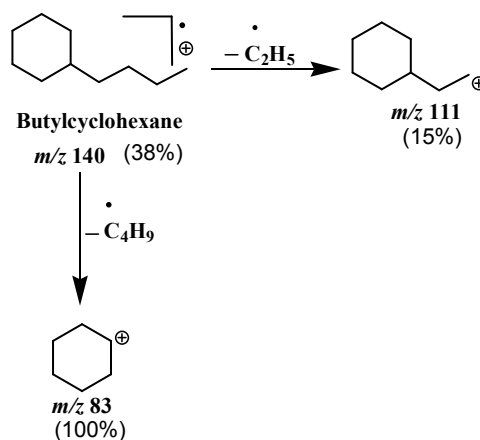


Fig. 3.7.3: Butylcyclohexane (CS-PE3)

Fragmentation Scheme



Scheme 3.5.3 Fragmentation Scheme of Butylcyclohexane

3.7.4 CS-PE4

Explanation

The signal at retention time 2.384 min. in the HPLC profile of pet ether extract of *C. sativa* roots was assigned a code CS-PE4. Lower retention time inferred the presence of volatile components (Greaves and Roboz 2014). Molecular ion peak appeared at m/z 134. As molecular ion peak was with an even mass, odd number of nitrogen atoms were absent as stated by nitrogen rule (Pavia *et al.*, 2011). Amines, amides, nitro and nitriles containing odd nitrogen atoms were absent. 15 mass unit loss from m/z 134 to m/z 119 may be due to loss of methyl radical. Difference of 29 mass unit from m/z 134 to m/z 105 may be because of ethyl radical. 14 mass unit loss inferred methylene radical from m/z 119 to m/z 105. Peak at m/z 105 may be because of benzoyl cation or methyl tropilium cation. Peak at m/z 91 may display tropilium cation. Peak at m/z 77 may be due to presence of phenyl. Loss of 28 mass unit from m/z 105 to m/z 77 may be because of ethene or CO moiety. Again cleavage of 14 mass unit from m/z 91 to m/z 77 may be because of methylene. Difference of 42 mass unit from m/z 119 to m/z 77 may display CH_2CO radical of aldehydes or ketones. M-1 or M-29 peak was absent that inferred the absence of aldehydes. M-43 or m/z 43 was also absent that unveiled the absence of ketones. The fragment ion peak at m/z 105 disclosed the presence of methyl tropilium as shown in Scheme 3.5.4. So, ethyl moiety was unveiled from m/z 134 to m/z 105. From rule of thirteen, molecular formula came out to be $\text{C}_{10}\text{H}_{14}$. Hydrogen deficiency index calculated was 4, satisfied by 3 double bonds and 1 cyclic ring. The fragment ion peak at m/z 119 was due to loss of methyl radical. Fragment ion peak at m/z 105 displayed loss of ethyl radical. Peak at m/z 105 was due to presence of methyl tropilium cation. As the fragment ion peak appeared at m/z 91 was not too much strong. So, *n*-propyl as alkyl chain was taken. By keeping in mind all the information obtained from retention time and fragmentation pattern, identified compound was *n*-propyltoluene as shown in Fig. 3.7.4.

Identified Compound

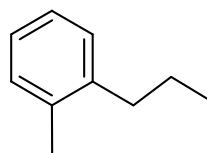
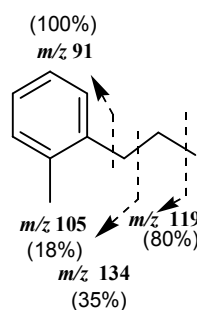


Fig. 3.7.4: *n*-Propyltoluene (CS-PE4)

Fragmentation Scheme



Scheme 3.5.4 Fragmentation Scheme of *n*-Propyltoluene

3.7.5 CS-PE5

Explanation

Molecular ion peak appeared at m/z 154 eluted at retention time 2.825 with code CS-PE5. As molecular ion peak was with an even mass, odd number of nitrogen atoms were absent as stated by nitrogen rule. Amines, amides, nitro or nitriles containing odd nitrogen atoms were absent. From m/z 154 to m/z 119, cleavage of 35 mass unit may be due to loss of chloride ion. Difference of 56 mass unit from m/z 154 to m/z 98 may be due to butene. 15 mass unit loss from m/z 98 to m/z 83 may be due to methyl. Cleavage of 36 mass unit from m/z 119 to m/z 83 may be because of HCl. 28 mass unit loss from m/z 83 to m/z 55 may be due to ethene or CO moiety. Again cleavage of 36 mass unit from m/z 119 to m/z 83 might be due to HCl loss. 71 mass unit difference from m/z 154 to m/z 83 may be because of pentyl radical. As there was no M-1 or M-29 peak, aldehydes were absent. There was no M+2 peak of approximately one third intensity of molecular ion peak, which betrayed the absence of chloride. Ketones were absent, as there was no loss of 43 mass unit. M-17 or M-45

peak was also absent, which manifested the absence of carboxylic acid. Loss of 28 mass unit may display presence of cycloalkanes. From rule of thirteen, molecular formula came out to be C₁₁H₂₂. Hydrogen deficiency index calculated was 1, satisfied by 1 cyclic ring. The fragment ion peak at *m/z* 83 due to loss of pentyl radical from *m/z* 154 as shown in **Scheme 3.5.5**. Loss of 28 mass unit from *m/z* 83 to *m/z* 55 displayed loss of ethene. From *m/z* 55 loss of methylene, peak appeared at *m/z* 41. Pet ether extract of *C. sativa* at retention time 2.825 min. contained alkyl chain and cyclohexane ring. So, identified compound was *n*-amylcyclohexane as shown in **Fig. 3.7.5**.

Identified Compound

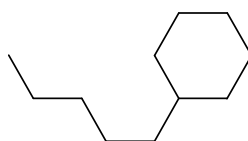
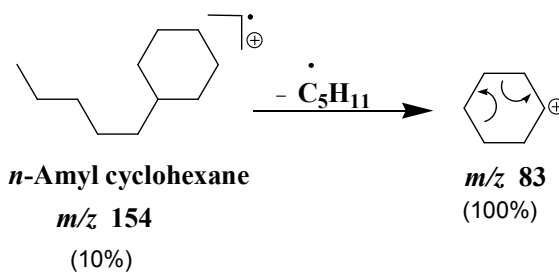


Fig. 3.7.5: *n*-Amylcyclohexane (CS-PE5)

Fragmentation Scheme



Scheme 3.5.5 Fragmentation Scheme of *n*-Amylcyclohexane

3.7.6 CS-PE6

The signal at retention time 3.420 min. in the HPLC profile of pet ether extract of *C. sativa* roots was assigned a code CS-PE6. Molecular ion peak appeared at *m/z* 128. As molecular ion peak was with an even mass, odd number of nitrogen atoms was absent as stated by nitrogen rule (**Pavia et al., 2011**). Amines, amides, nitro or nitriles containing odd nitrogen atoms were absent. Loss of 26 mass unit from *m/z* 128

to m/z 102 may be due to ethyne. The fragment ion peak at m/z 87 may be due to cleavage of methyl radical. Difference of 28 mass unit from m/z 102 to m/z 74 may be due to loss of ethene or CO. Loss of 77 from m/z 128 to m/z 51 might be due to loss of phenyl radical. Peak at m/z 74 may infer McLafferty cleavage of methyl esters as shown in **Scheme 3.5.6**. Peak at m/z 51 may be due to $C_4H_3^+$. As molecular ion peak was also the base peak which indicated the presence of stable molecule. As there was no M-31 or m/z 59 peak, methyl esters were absent. From rule of thirteen, molecular formula came out to be $C_{10}H_8$. HDI calculated was 7, satisfied by 5 double bonds and two cyclic rings. The fragment ion peak at m/z 102 may be due to loss of ethyne from m/z 128. From m/z 102 loss of ethene, peak appeared at m/z 74. Loss of C_4H_3 radical from m/z 102 peak appeared at m/z 51. So, identified compound was naphthalene as shown in **Fig. 3.7.6**.

Identified Compound

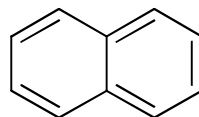
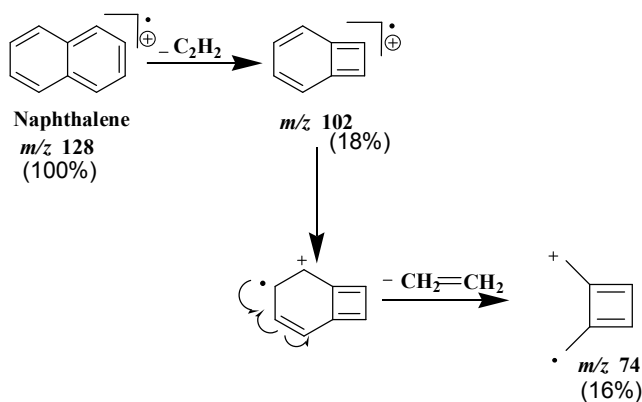


Fig. 3.7.6: Naphthalene (CS-PE6)

Fragmentation Scheme



Scheme 3.5.6 Fragmentation Scheme of Naphthalene

3.7.7 CS-PE7

Molecular ion peak appeared at m/z 240 eluted at retention time 8.427 with code CS-PE7. From m/z 240 to m/z 211 loss of 29 mass unit may be due to ethyl radical. 28 mass unit loss from m/z 211 to m/z 183 may be due to ethene or CO. 45 mass unit loss from m/z 200 to m/z 155 may be due to ethoxy or CO₂H of carboxylic acid. 16 mass unit loss from m/z 155 to m/z 171 may be due to oxygen atom. Difference of 28 mass unit from m/z 155 to m/z 127 may be due to loss of ethene or CO moiety. 42 mass unit loss from m/z 155 to m/z 113 may be due to CH₂CO radical. Again cleavage of 28 mass unit from m/z 141 to m/z 113 may be due to ethene or CO moiety. Peak at m/z 127 may infer iodine. Again loss of 28 mass unit from m/z 127 to m/z 99 may be due to ethene or CO. Successive loss of 14 mass unit from m/z 99 to m/z 85, from m/z 85 to m/z 71, from m/z 71 to m/z 57 displayed the loss of methylene as shown in **Scheme 3.5.7**. Similarly, peak at m/z 99, 85, 71 and 57 manifested the presence of alkyl chain. As there was no loss of 17 mass unit due to hydroxyl group of carboxylic acids. So, carboxylic acids were absent. No M-1 or M-29 peak aldehydes were also absent. M-43 or m/z 43 peak was also absent which confirmed the absence of ketones. As molecular ion peak was with an even mass, odd number of nitrogen atoms were absent as stated by nitrogen rule (**Pavia et al., 2011**). Amines, amides, nitro or nitriles containing odd nitrogen atoms were absent. From rule of thirteen, molecular formula came out to be C₁₈H₂₄. By insertion of iodine, modified molecular formula became C₈H₁₇I. Hydrogen deficiency index calculated was 0. Pet-ether extract of *C. sativa* at retention time 8.427 min. contained iodoctane as shown in **Fig. 3.7.7**.

Identified Compound

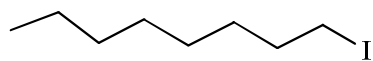
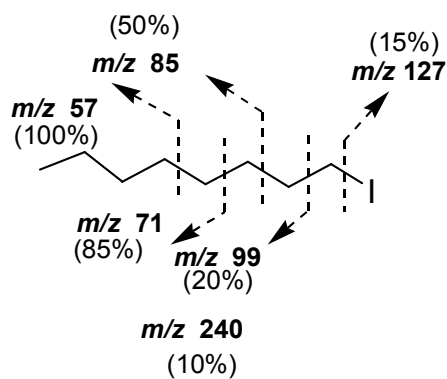


Fig. 3.7.7: Iodoctane (CS-PE7)

Fragmentation Scheme



Scheme 3.5.7 Fragmentation Scheme of Iodoctane

Table 3.4 List of Compounds Identified by HPLC-DAD-ESI-MS

CA-E1	3.115	Band I 265	596.6	<i>p</i> -Hydroxybenzoic acid-1- <i>O</i> -[glucopyranosyl-(1→4)- β -D-xylopyranosyl-(1→4)- β -D-xylopyranoside]
CA-E2	3.296	Band II 228	702	$\Delta^{(8)}$ -THC-1- <i>O</i> -(6-acetylglucose-[1→4]- β -D-rhamnoside)
CA-E3	3.4	Band I 260 Band II 198	508	Syringic Acid-1- <i>O</i> -[β -D-glucopyranosyl-(1→4)- α -L-rhamnopyranoside]
CA-E4	4.262	Band I 265	453	Gallic acid-1- <i>O</i> -[β -D-xylopyranosyl-(1→4)- β -D-xylopyranoside]
CA-E5	14.845	Band I 225	786	Tetrahydrocannabinol-1- <i>O</i> -[α -L-rhamnopyranosyl-(1→4)- α -L-rhamnopyranosyl-(1→4)- α -L-rhamnopyranoside]
CA-E6	29.442	Band I 218 Band II 242	947	THVA-1- <i>O</i> -[α -L-rhamnopyranosyl-(1→4)- β -D-glucopyranosyl-(1→4)- α -L-rhamnopyranosyl-(1→4)- β -D-glucopyranoside]
CA-E7	30.702	Band I 240	818	THCA-C4-1- <i>O</i> -[β -D-glucopyranosyl-(1→4)- α -L-rhamnopyranosyl-(1→4)- β -D-xylopyranoside]
CS-A1	5.2	Band I 227	935	$\Delta^{(8)}$ -Tetrahydrocannabinol-1- <i>O</i> -[β -D-xylopyranosyl-(1→4)- β -D-glucopyranosyl-(1→4)- β -D-glucopyranosyl-(1→4)- β -D-rhamnopyranoside]

CS-A2	35.287	Band I 295 Band II 230	589	Luteolin-4- <i>O</i> -[β -D-xylopyranosyl-(1 \rightarrow 4)- β -D-rhamnopyranoside]
CS-A3	49.9	Band I 230 Band II 280	842	THCA-C4-1- <i>O</i> -[β -D-glucopyranosyl-(1 \rightarrow 4)- β -D-glucopyranosyl-(1 \rightarrow 4)- β -D-xylopyranoside]
CA-Ex1	24.6	Band I 228 Band II 276	905	Cannabinol-1- <i>O</i> -[β -D-xylopyranosyl-(1 \rightarrow 4)- β -D-xylopyranosyl-(1 \rightarrow 4)- β -D-glucopyranosyl-(1 \rightarrow 4)- α -L-rhamnopyranoside]
CA-EX2	35.191	Band I 300-350 Band II 230-240	927	Luteolin-1- <i>O</i> -[β -D-xylopyranosyl-(1 \rightarrow 4)- β -D-xylopyranosyl-(1 \rightarrow 4)- β -D-xylopyranosyl-(1 \rightarrow 4)- β -D-glucopyranoside]
CA-EX3	48.984	Band I 300-350 Band II 230-240	800	6-Hydroxytricetin-7- <i>O</i> -[β -D-xylopyranosyl-(1 \rightarrow 4)- α -L-rhamnopyranosyl-(1 \rightarrow 4)- β -D-glucopyranosyl]
CA-EX4	49.411	Band I 215 Band II 280	755	Cannabinol-1- <i>O</i> -[β -D-glucopyranosyl-(1 \rightarrow 4)- β -D-xylopyranosyl-(1 \rightarrow 4)- β -D-xylopyranoside]
Ca-AH1	3.538	Band I 230	529	Syringic acid-1- <i>O</i> -[β -D-glucopyranosyl-(1 \rightarrow 4)- β -D-xylopyranoside]
Ca-AH2	4.04	Band I 195-400	751	Cannabinol-1- <i>O</i> -[α -L-rhamnopyranosyl-(1 \rightarrow 4)- β -D-xylopyranosyl-(1 \rightarrow 4)- β -D-[glucopyranoside]

Ca-AH3	9.198	Band I 300-550 Band II 240-285	505	Cannabichromene-1- <i>O</i> - β -D-glucoside
Ca-AH4	13.291	Band I 220 Band II 265	625	Tetrahydrocannabivarinic acid-1- <i>O</i> - [β -D-glucopyranosyl-(1 \rightarrow 4)- β -D- xylopyranoside]
Ca-AH5	14.544	Band I 210 Band II 280	736	Cannabinol-1- <i>O</i> -[β -D- xylopyranosyl-(1 \rightarrow 4)- α -L- rhamnopyranosyl-(1 \rightarrow 4)- β -D- rhamnopyranoside]
Ca-AH6	17.991	Band I 280-340 Band II 220-240	455	Luteolin-7- <i>O</i> - α -L-rhamnopyranoside
Ca-AH7	18.924	Band I 250	817	Cannabichromenic acid-1- <i>O</i> -[β -D- xylopyranosyl-(1 \rightarrow 4)- β -D- glucopyranosyl-(1 \rightarrow 4)- α -L- rhamnopyranoside]
CA-AH8	23.838	Band I 230 Band II 260	826	Tetrahydrocannabinolic acid (C4)- 1- <i>O</i> -[α -L-rhamnopyranosyl-(1 \rightarrow 4)- β -D-glucopyranosyl-(1 \rightarrow 4)- β -D- xylopyranoside]
CA-AH9	26.124	Band I 265- 350 Band II 220- 240	860	Quercetin-4'-methylether-3- <i>O</i> -[β -D- rhamnopyranosyl-(1 \rightarrow 4)- β -D- xylopyranosyl-(1 \rightarrow 4)- α -L- rhamnopyranosyl-(1 \rightarrow 4)- β -D- glucopyranoside]

Phytochemical study of *C. sativa* roots were successfully carried out by using HPLC-DAD-ESI-MS analyses.

3.8 Results of HPLC-DAD-ESI-MS analysis

High-performance Liquid Chromatography (HPLC) coupled to Electrospray Ionization Mass Spectrometry (ESI-MS) detection in the positive mode was used to identify phenolic compounds and Cannabinoids in extracts from *C. sativa* roots. Diode-array detection (DAD) was used for the screening of different classes of phenolic compounds and Cannabinoids, whereas MS fragmentation data were employed for their structural characterization. In contrast to GC, no decomposition of the Cannabinoids occurs during HPLC analysis and hence the cannabinoid acidic form was also analyzed (**Hazekamp *et al.*, 2007**).

3.9 HPLC

HPLC was the most widely used instrumental technique for analytical purposes in natural product studies and also in pharmaceutical, cosmetics and food industries, surpassing the use of Gas chromatography (GC). The reason for this was versatility and relatively simple sample treatment required for analysis. GC required the analytes of interest to be stable at high temperature required to reach volatility, while HPLC was most frequently carried out at room temperature or at temperature no higher than 45°C. HPLC required only the analyte to be soluble in the mobile phase, while GC required all analytes to be volatile. All these characteristics were suitable for the analyses of natural samples, with two major exceptions, the study of volatile fractions such as lipids and essential oils.

Most frequently used analytical technique for the separation of phenolic compounds and Cannabinoids were Reversed-Phase High-Performance Liquid Chromatography (RP-HPLC). Gradient-elution mode was successfully used for phenolics and Cannabinoids identification, yielding fully exploitable DAD spectra.

3.10 Diode Array Detector (DAD)

DAD was valuable for a preliminary identification and for quantification using characteristic absorption maxima. The chief characteristic of DAD was light provided

by a continuum source was focused on the sample cell and transmitted light impacts an array of photodiodes which was then translated the information of the energy transmitted into absorption information. UV spectra were measured online by DAD in the range of 195-400nm. DAD of Cannabinoids were lying in the range of 195-300nm. The chromophore of Cannabinoids corresponded to its substituted phenolic ring. Alkyl side chain of cannabinoid didn't influence the UV-absorbance, as there was no difference between THCA (C₅-side chain) and THVA (C₃-side chain). Similarly, Cyclization of the non-phenolic part of Cannabinoids also has no influence on the absorbance, except when another aromatic ring (CBN, CBNA) or a conjugated double bond was introduced (Hazekamp *et al.*, 2007).

UV spectra of Cannabinoids in the range 195-300nm was given below in **Fig. 3.8**.

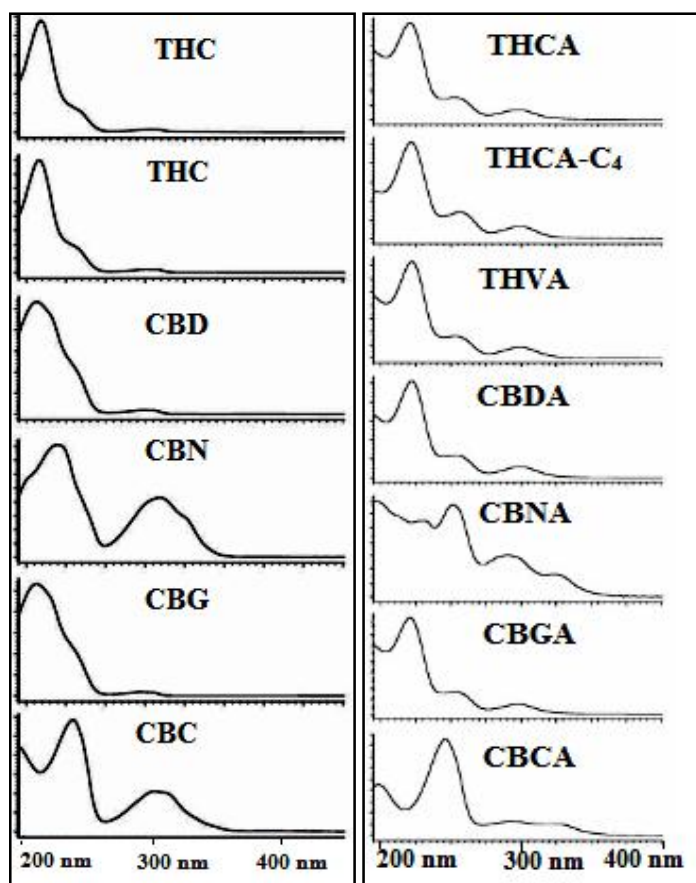


Fig. 3.8 DAD spectra in the range of 190-300nm obtained by HPLC

DAD spectrum of flavonoids consisted of two absorption maxima in the ranges 240-285 nm (band II) and 300-550 (band I). Relative intensities and the precise position of these maxima gave valuable information on the nature of flavonoid and its oxygenation pattern. Additional oxygenation causes shift of band to longer wavelengths (**Markham 1982**). Similarly, glycosylation or methylation causes band shift to shorter wavelength. Band I due to cinnamoyl moiety and band II as a result of benzoyl moiety was responsible in flavonoids for UV absorbance as shown in **Fig. 3.8.1**.

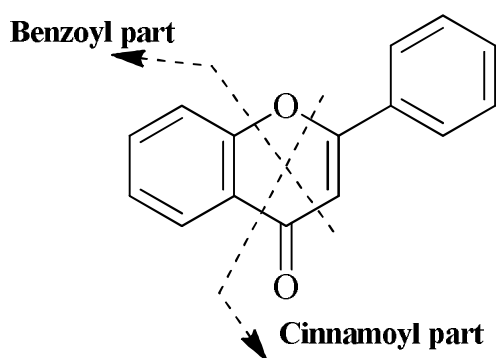


Fig. 3.8.1 Absorbing Portion of Flavonoid Skelton

UV absorption maxima and intensities of both bands gave an idea about the family of flavonoids. Typical spectra of major flavonoid types with oxygenation patterns were given below as given in **Table 3.5**.

Flavonoids class	Band I (nm)	BandII (nm)
Flavones	310-350	250-280
Flavonols(3-OH substituted)	330-360	250-280
Flavonols (3-OH free)	350-385	250-280
Isoflavones	310-330 shoulder	245-275
Isoflavones-5-deoxy-6,7-dioxygenated	c. 320 peak	
Flavanones and dihydrofavonols	300-330 shoulder	275-295

Chalcones	340-390	230-270 (low intensity)
Aurones	380-430	230-270 (low intensity)
Anthocyanidins	465-560	270-280

Table 3.5 UV Absorption Ranges for Flavonoids

In the DAD spectrum of phenolic acids, benzoic acid frame work having chromophoric part was responsible for UV absorbance in the range of 150-290 nm. λ_{\max} of some of phenolic acids (Lin *et al.*, 2007) was mentioned in Table 3.6.

Phenolic acids	λ_{\max} (nm)	Molecular mass (<i>a.m.u.</i>)
Chlorogenic acid	240, 298s, 326	354
<i>p</i> -Coumaric acid	224, 310	164
<i>m</i> -coumaric acid	192, 213, 278	164
Ferulic acid	236 sh, 324	194
Caffeic acid	220, 240, 294, 326	180
Cinnamic acid	265	148
Gallic acid	217, 272	170
Vanillic acid	219, 261, 294, 320	168
Syringic acid	218, 276, 328	198
Salicylic acid	205, 236, 302	138
Sinapic acid	224, 310	224
Gentistic acid	213, 239 sh, 332, 370	154
Ellagic acid	253, 367	302

Table.3.6 Absorption Maxima and Molecular Masses of Phenolic Acids

3.11 ESI-MS

Electrospray Ionization (ESI) was used for analysis of the polyphenolic compounds and cannabinoids involving detection of the pseudomolecular ion. Mass

spectra contributed greatly to structural characterization. MS data provided structural information about flavonoids and Cannabinoids in term of their molecular masses and distribution of substitution at A and B ring. Mass spectra obtained under electrospray ionization were widely used for the structural investigations of flavonoids. In flavonoid aglycone fragmentation, the most useful fragmentation was the cleavage of two C-C bonds of the C ring resulting in the structurally informative $^{ij}A^+$ and $^{ij}B^+$. This ionization technique was applied for all classes of flavonoid aglycones. Retro-Diels-Alder (RDA) reactions were found to be the most diagnostic fragments for the flavonoid identification, also provide information on the number and type of substituents in the A and B rings. $^{ij}A^+$ and $^{ij}B^+$ labels inferred the fragments containing intact A and B rings, superscripts i and j indicated the C-ring bond that was broken as shown in **Fig. 3.8.2**.

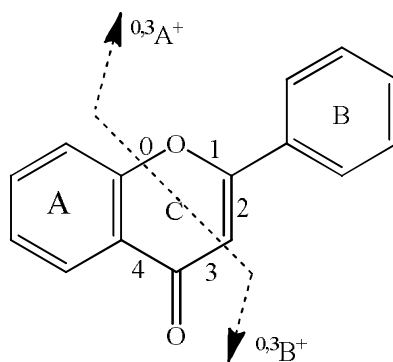


Fig. 3.8.2 Ion Nomenclature for Flavonoids.

Glycosidic-*O*-linkage cleavage with the concomitant H-rearrangement led to the elimination of monosaccharide residue, loss of hexose 162 *amu.*, 146 *amu.* loss manifested rhamnose and 132 *amu.* inferred the xylose as shown in **Fig. 3.8.3**.

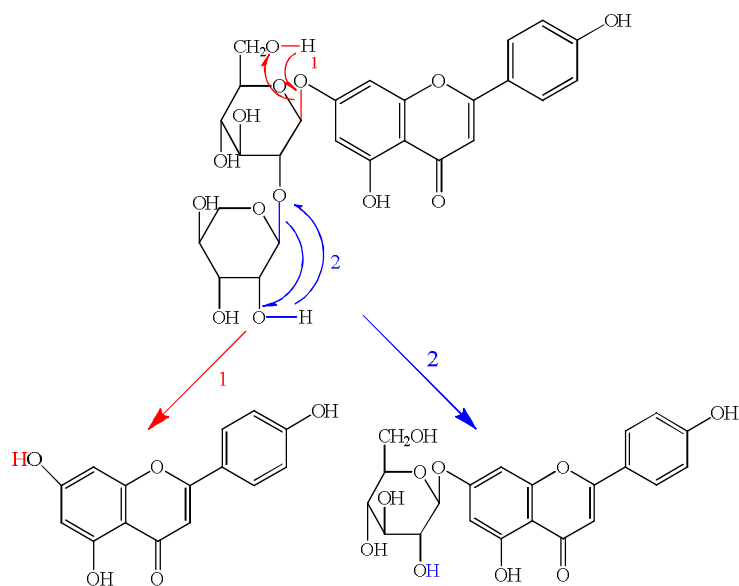


Fig 3.8.3. Cleavages at the glycosidic-O-linkage

MS gave information about the cross linked cleavages of saccharides residue. They also gave information about the sequence, glycosylation and interglycosidic linkage of saccharides moieties attached to flavonoid skelton. In the systematic nomenclature of saccharide moiety X stands for cleavage while the superscript represented the number of bonds of molecule that was cleaved as shown in **Fig. 3.8.4.**

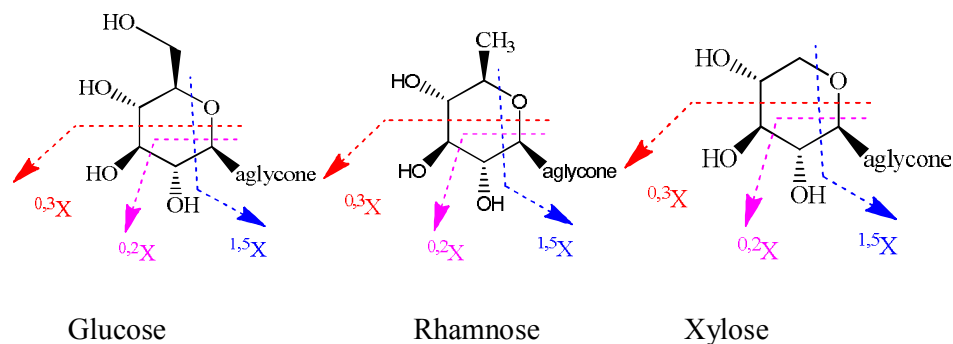


Fig. 3.8.4 Products ions formed by cross ring cleavage of Monosaccharides

Following are the common ion adducts in the positive ion mode as shown in **Table 3.7.**

Adducts	Mass units	References
$[M+H]^+$	1	Huang Y. <i>et al.</i> , (2013)
$[M+H_2O]^+$	18	Atoui A. K. <i>et al.</i> , (2005)
$[M+H_2O+H]^+$	19	Steiner W. E. <i>et al.</i> , (2003)
$[M+MeOH+H]^+$	33	Huang Y. <i>et al.</i> , (2013)
$[M+2H_2O+H]^+$	37	Watson J. T. and Sparkman O. D. (2009)
$[M+K]^+$	39	Huang Y. <i>et al.</i> , (2013)
$[M+CH_3CN+H]^+$	42	Huang Y. <i>et al.</i> , (2013)
$[M+3H_2O+H]^+$	55	Watson J. T. and Sparkman O. D. (2009)
$[M+2MeOH+H]^+$	65	Watson J. T. and Sparkman O. D. (2009)
$[M+2CH_3CN+H]$	83	Huang Y. <i>et al.</i> , (2013)

Table 3.7 Common Ion Adducts in Positive Ion Mode

3.12 Compounds Identified from CA-E extracts

3.12.1 Chromatographic Profiling of CA-E extracts

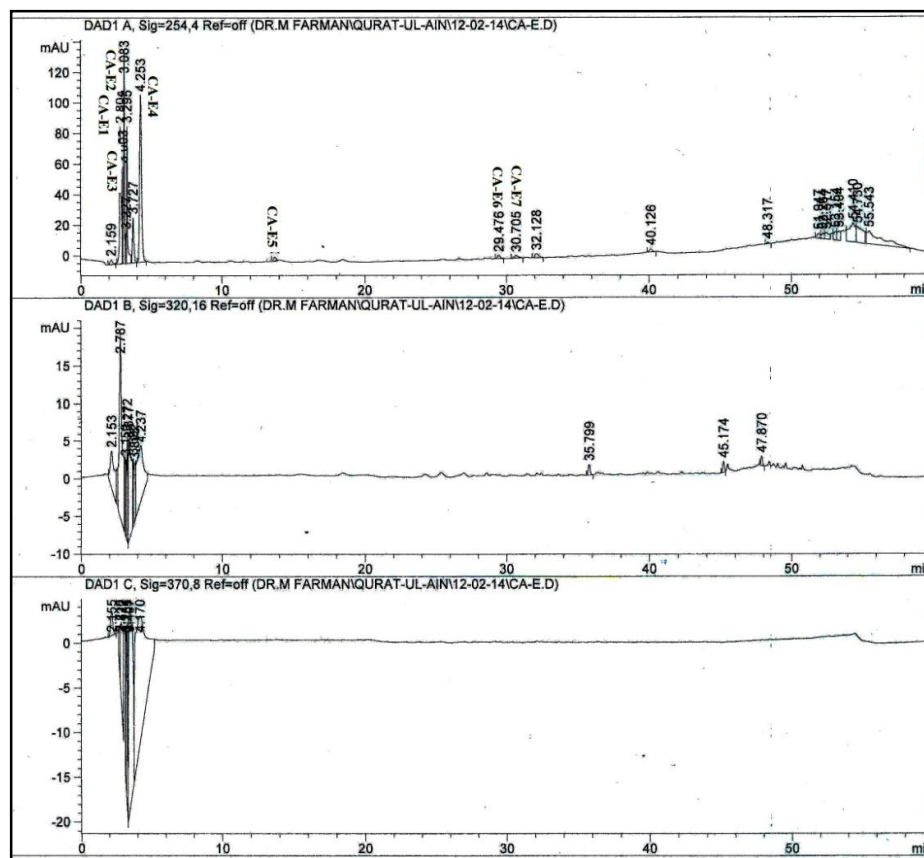


Fig.3.9 Chromatographic Profiling of Compound with code CA-E

Chromatographic profiling of CA-E extracts was recorded online by DAD at wavelength 254nm, 320nm, 370nm as shown in **Fig. 3.9**. For a given mobile phase composition, there was differential retention of sample components according to their hydrophobicity in a manner such that more hydrophilic compounds were retained less in the stationary phase and eluted first, while the more hydrophobic compounds were more retained and eluted last. This was the basic principle to develop, optimize or customize methods. In Reverse phase chromatography (RPC), gradient elution was carried out using mobile phase composition programmed in which water proportion was reduced as the run progresses, while the organic solvent was increased. So, the

polar acids having large molecular weight were eluted out first followed by phenolic acids, flavonoid and cannabinoid glycosides and lastly the flavonol aglycones.

Chromatographic profiling recorded under wavelength 254nm showed maximum absorption at this wavelength. Maximum absorption indicated the large number of compounds that were eluted out in first five minutes. Few of compounds were also identified in middle and at end of retention time. Chromatographic profiling recorded under wavelength 320nm showed minimum absorption. Very less absorption occurred at wavelength 370nm.

3.12.1.1 CA-E1

Compound with code CA-E1 eluted at retention time 3.4 min. having mobile phase composition 10% acetonitrile in deionized water. Lower retention time manifested the presence of highly hydrophilic compounds like phenolic acid. DAD and ESI-MS spectrum of compound with code CA-E1 is shown in **Fig. 3.9.1**.

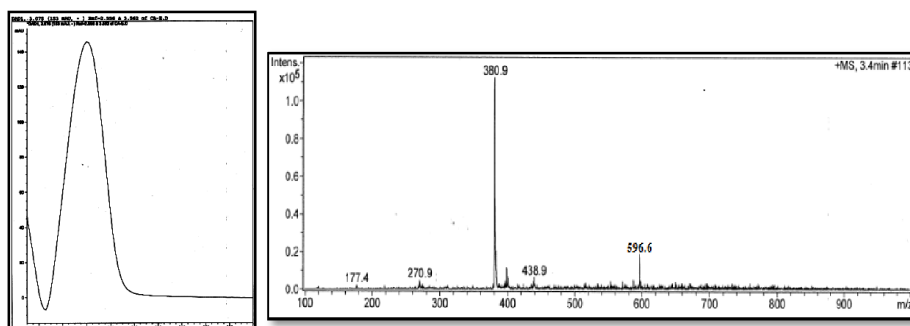


Fig.3.9.1 DAD and ESI-MS Spectrum of Compound with Code CA-E1

DAD Spectrum

Single band with broad peak was observed by the compound with code CA-E1. Band I appeared at 265nm. Shape, intensity and λ_{\max} resembled to that of phenolic acids. When the substitution was symmetrical in phenolic acids, spectrum exhibited only one absorption band. Hydroxylation of benzoic acid at the para position exhibited 9nm hypsochromic shift of major absorption band from 272nm to 265nm. As this hydroxylation was symmetrical on benzoic acid, only one absorption band

was observed (Campos and Markham 2007). So, from above interpretations of DAD spectrum *p*-Hydroxybenzoic acid was identified.

ESI-MS Spectrum

Mass spectrum exhibited pseudomolecular ion peak at m/z 596.6 in positive ion mode with calculated molecular weight was 564 *amu*. Pseudomolecular ion peak was justified with adduct as $[M+MeOH+H]^+$. Fragment ion peak at m/z 439 inferred the cleavage of glucose with adduct $2H_2O+H$ *i.e.*, $[M+2H_2O+H-glc]^+$. Base ion peak at m/z 381 manifested the cleavage of terminal glucose along with $^{1,5}X_{xyl}$ with adduct $2CH_3CN+H$ as $[M+2CH_3CN+H-glc-^{1,5}X_{xyl}]^+$ (Huang *et al.*, 1999). As a result of cleavage of terminal glucose with xylose, peak appeared at m/z 271 as $[M+H-glc-xyl]^+$. Another loss of xylose from m/z 271, peak appeared at m/z 177 with adduct K *i.e.*, $[M+K-glc-xyl-xyl]^+$. Pseudomolecular ion peak was justified with adduct *i.e.*, $[M+MeOH+H]^+$. By consolidating all the information obtained from retention time, DAD and ESI-MS spectrum, identified compound is 1-*O*-[β -D-glucopyranosyl-(1 \rightarrow 4)- β -D-xylopyranosyl-(1 \rightarrow 4)- β -D-xylopyranosyl]-*p*-hydroxybenzoate as shown in Fig. 3.7.2.

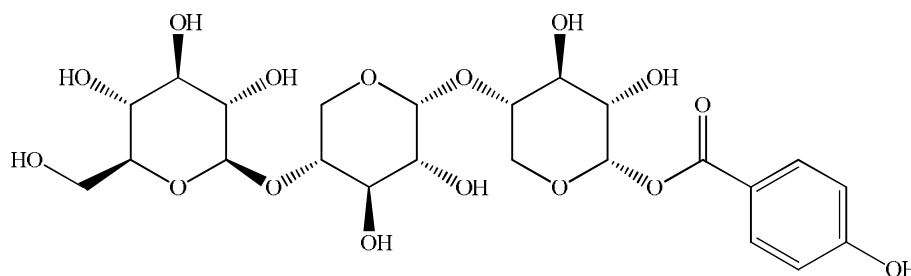
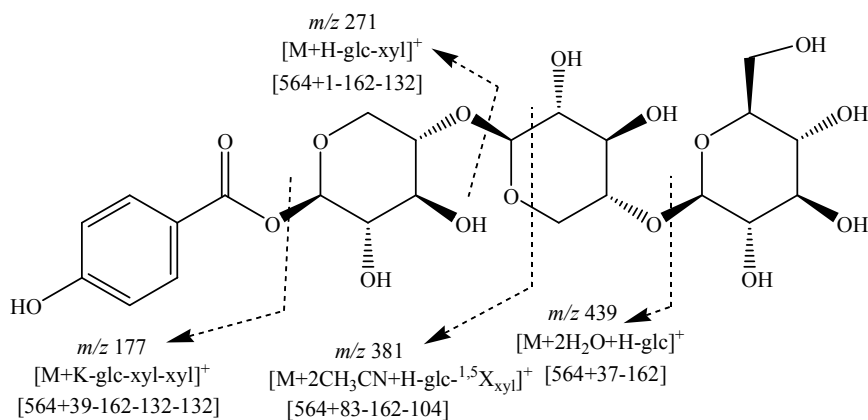


Fig. 3.9.2.1-*O*-[β -D-glucopyranosyl-(1 \rightarrow 4)- β -D-xylopyranosyl-(1 \rightarrow 4)- β -D-xylopyranosyl]-*p*-hydroxybenzoate (CA-E1)

Fragmentation scheme of compound with code CA-E1 was shown in **Scheme 3.6.1**.



Scheme 3.6.1 Fragmentation Scheme of 1-*O*-[β -D-glucopyranosyl-(1 \rightarrow 4)- β -D-xylopyranosyl-(1 \rightarrow 4)- β -D-xylopyranosyl]-*p*-hydroxybenzoate

3.12.1.2 CA-E2

The compound CA-E2 eluted at t_R 3.296 min. with the mobile phase composition was 10% acetonitrile in deionized water. This composition suggested the presence of hydrophilic moiety. DAD and ESI-MS spectrum of this compound was shown in **Fig. 3.9.3**.

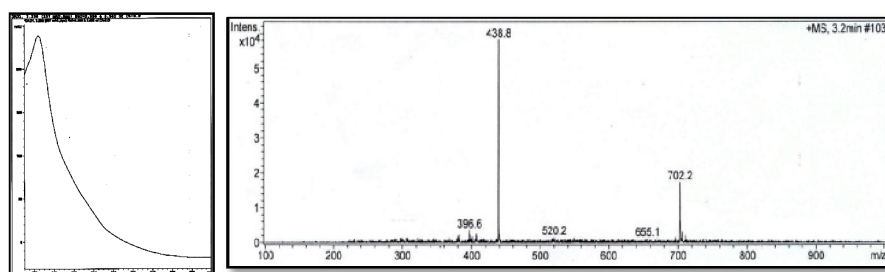


Fig. 3.9.3. DAD and ESI-MS Spectrum of Compound with Code CA-E2

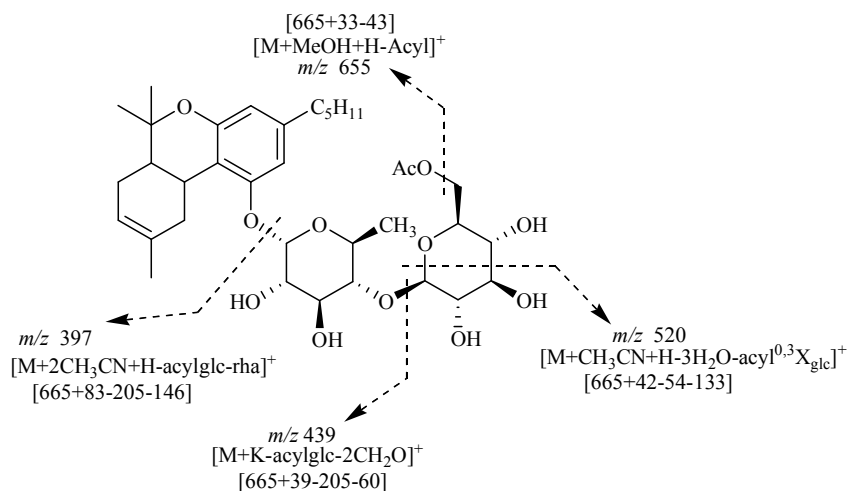
DAD Spectrum

DAD spectrum of compound displayed one band pattern at 228nm. DAD spectrum of flavonoids showed two absorption maxima in the range 240-285nm (band II) and 300-550nm (band I). In this spectrum, there was no peak above 300nm which confirmed the absence of flavonoids. One sharp peak at 228 nm was due to

Tetrahydrocannabinol. Position of double bond and alkyl side chain doesn't influence the UV absorbance (**Hazekamp *et al.*, 2007**). So, the DAD spectrum of Δ^9 -THC and Δ^8 -THC was similar. Shape, intensity and λ_{max} values were closely related to tetrahydrocannabinol. DAD spectrum of compound is shown in **Fig. 3.9.3**.

ESI-MS

ESI-MS spectrum of compound corresponded to t_R 3.296min. in positive ion mode was given in **Fig. 3.9.3**. Pseudomolecular ion peak appeared at m/z 702, from where the molecular mass of the compound calculated was 665 *amu*. The pseudomolecular ion peak was justified by adduct $2\text{H}_2\text{O}+\text{H}$. From m/z 655 to m/z 702 indicated the loss of acyl moiety, that was justified by adduct $[\text{M}+\text{MeOH}+\text{H}-\text{acyl}]^+$. Peak at m/z 520 inferred the cleavage of $^{0,3}\text{X}_{\text{glc}}$ from m/z 655 that was justified by adduct $[\text{M}+\text{CH}_3\text{CN}+\text{H}-3\text{H}_2\text{O}-\text{acyl}^{0,3}\text{X}_{\text{glc}}]^+$. Appearance of peak at m/z 439 was due to the loss of acylglucose along with 2 formaldehydes with potassium adduct as $[\text{M}+\text{K}-\text{acylglc}-2\text{CH}_2\text{O}]^+$. Peak at m/z 439 was also act as base peak. Peak at m/z 397 was due to adduct $2\text{CH}_3\text{CN}+\text{H}$ by the loss of acylglucose and rhamnose as $[\text{M}+2\text{CH}_3\text{CN}+\text{H}-\text{acylglucose}-\text{rha}]^+$ as shown in **Scheme 3.6.2**.



Scheme 3.6.2 Fragmentation Scheme of Tetrahydrocannabinol-1-*O*-[6- β -D-acetylglucopyranosyl-(1 \rightarrow 4)- α -L-rhamnoside]

All the information from t_R time, DAD and ESI-MS spectrum the identified compound was Tetrahydrocannabinol-1-*O*-[6- β -D-acetylglucopyranosyl-(1 \rightarrow 4)- α -L-rhamnopyranoside] as shown in **Fig. 3.9.4**.

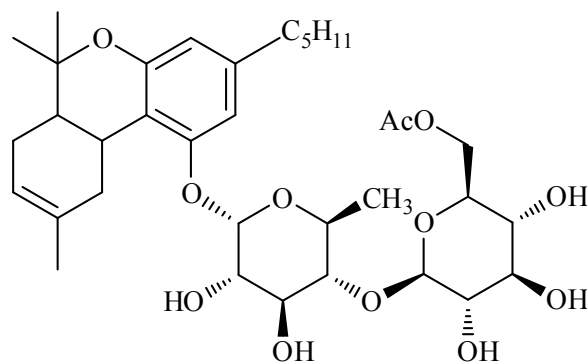


Fig. 3.9.4 Tetrahydrocannabinol-1-*O*-[6- β -D-acetylglucopyranosyl-(1 \rightarrow 4)- α -L-rhamnopyranoside] (CA-E2)

3.12.1.3 CA-E3

Compound with code CA-E3 eluted at t_R 3.4 min. with the mobile phase composition was 10% acetonitrile in deionized water. Mobile phase composition indicated the presence of hydrophilic compounds. The proportion of water in a mobile phase was directly related to retention time of compound. Lowered retention time inferred the presence of phenolic acid glycosides. DAD and ESI-MS Spectrum of compound were shown in **Fig. 3.9.5**.

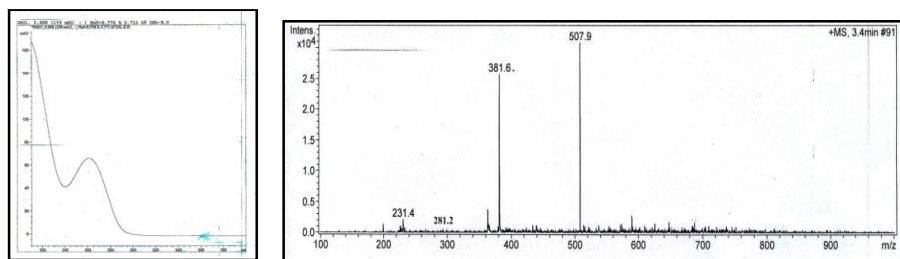


Fig. 3.9.5. DAD and ESI-MS Spectrum of compound with code CA-E1

DAD Spectrum

CA-E3 compound displayed two band pattern, band I appeared at 260nm while band II at 198nm. As there were no band above 280nm that confirmed the

absence of flavonoids. Shape, intensity and λ_{\max} of this compound resembled Syringic acid (Long *et al.*, 2007). Usually, phenolic acid spectrum displayed a single band spectrum. But when methoxylation and hydroxylation of compound was unsymmetrical, a double absorption band appeared (Campos and Markham 2007). Reported absorption band value of syringic acid was 276nm in band I and 218 nm in band II. This hypsochromic shift of major absorption band from 276nm to 260nm and 218nm to 198nm may be due to methylation and glycosylation (Markham 1982). From all above information asymmetric syringic acid was unveiled.

ESI-MS Spectrum

ESI-MS of compound with pseudomolecular ion peak at m/z 508 in positive ion mode was given in Fig. 3.9.5. Calculated molecular weight was 506 *amu*. Fragment ion peak at m/z 381 was due to the cleavage of glucose *i.e.*, $[M+2H_2O+H-glc]^+$. Due to loss of glucose and rhamnose, peak appeared at m/z 281 as $[M+2CH_3CN+H-glc-rha]^+$. Base peak at m/z 231 was due to the loss of terminal glucose, rhamnose with another adduct *i.e.*, $[M+MeOH+H-glc-rha]^+$ as shown in Scheme 3.6.3. From above cleavages two sugars were identified *i.e.*, rhamnose and glucose and aglycone part was syringic acid.

By consolidating all the above information obtained from retention time, DAD and ESI-MS spectrum, it was inferred that given compound is Syringate-1-*O*-[β -D-glucopyranosyl-[1 \rightarrow 4]- α -L-rhamnopyranoside] as shown in Fig. 3.9.6.

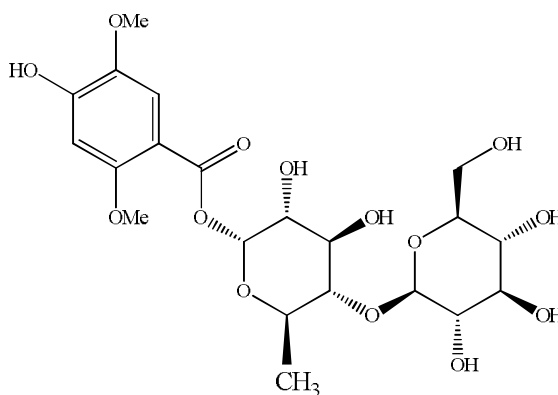
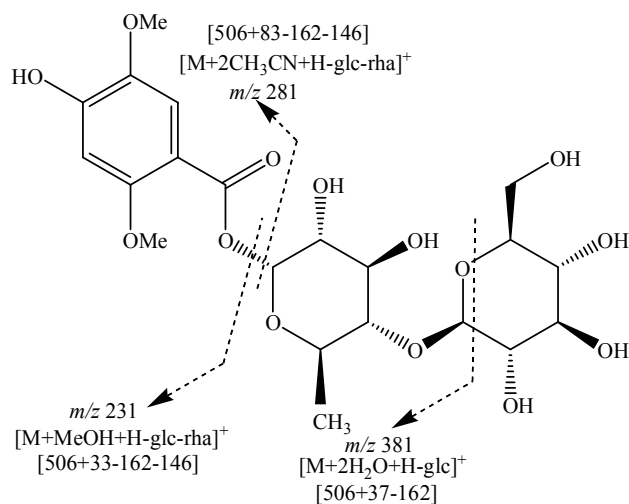


Fig. 3.9.6 Syringate-1-*O*-[β -D-glucopyranosyl-[1 \rightarrow 4]- α -L-rhamnopyranoside] (CA-E3)

Suggested cleavages of compound with code CA-E3 was given below:



Scheme.3.6.3 Fragmentation Scheme of Syringate-1-*O*-[β -D-glucopyranosyl]-[1 \rightarrow 4]- α -L-rhamnopyranoside]

3.12.1.4 CA-E4

Compound with code CA-E4 eluted at retention time 4.262 min. having mobile phase composition 10% acetonitrile in deionized water. DAD and ESI-MS spectrum was shown in **Fig. 3.9.7**. Retention time of compound was directly proportional to the concentration of water in a mobile phase. Lower retention time inferred the presence of phenolic acids.

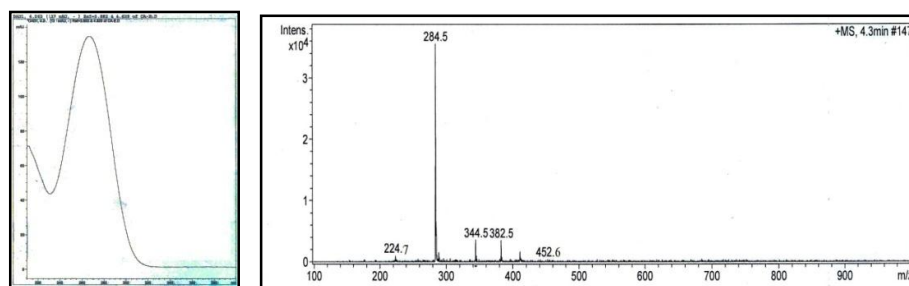


Fig. 3.9.7 DAD and ESI-MS Profiling of Compound with code CA-E4

DAD Spectrum

One band pattern was exhibited by compound with code CA-E4 when the substitution was symmetric in case of phenolic acids, the spectrum comprised of only one absorption band (**Campos and Markham 2007**). Shape, intensity and λ_{\max} resembled to that of gallic acids. Band I appeared at 265nm. In original spectrum of gallic acid, band I appeared at 272nm. This hypsochromic shift of band from 272nm to 265nm was due to glycosylation or methylation (**Markham 1982**).

ESI-MS Spectrum

Pseudomolecular ion peak appeared on mass spectrum at m/z 453 in positive ion mode, having calculated molecular weight 434 *amu*. Pseudomolecular ion peak was justified with adduct as $[M+H_2O+H]^+$. Fragment ion peak at m/z 344 manifested the cleavage of terminal xylose with adduct CH_3CN+H *i.e.*, $[M+CH_3CN+H-xy]^+$. As a result of cleavage of terminal xylose along with $^{0,3}X_{xy}$ with adduct CH_3CN+H , peak appeared at m/z 284 as $[M+CH_3CN+H-xy-^{0,3}X_{xy}]^+$. Peak at m/z 284 was also the base peak. Loss of terminal xylose along with second molecule of xylose cleavage, peak appeared at m/z 225 *i.e.*, $[M+3H_2O+H-xy-xy]^+$ as shown in **Scheme 3.6.4**. From above fragmentation patterns two xylose sugars were identified. By keeping in view all the information obtained from retention time, DAD and ESI-MS spectrum, identified compound is 1-*O*-[β -D-xylopyranosyl-(1 \rightarrow 4)- β -D-xylopyranosyl]gallate as shown in **Fig. 3.9.8**.

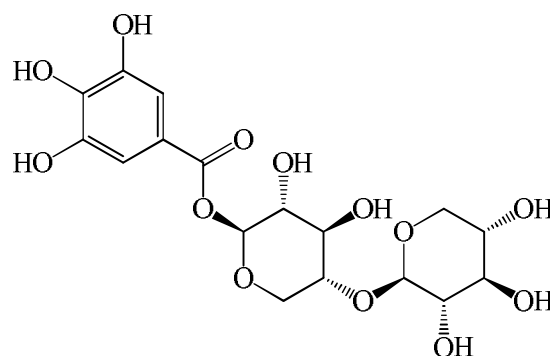
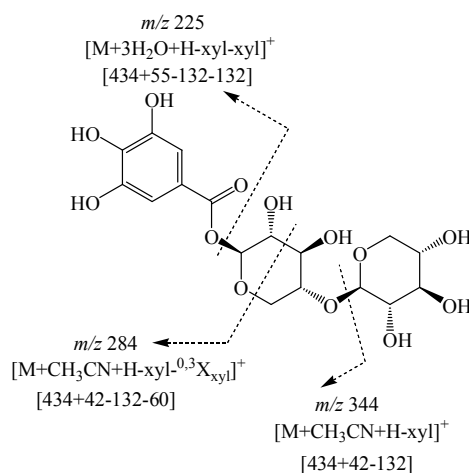


Fig. 3.9.8 1-*O*-[β -D-xylopyranosyl-(1 \rightarrow 4)- β -D-xylopyranosyl]gallate (CA-E4)



Scheme 3.6.4 Fragmentation Scheme of 1-*O*-[β -D-xylopyranosyl-(1 \rightarrow 4)- β -D-xylopyranosyl]gallate

3.12.1.5 CA-E5

Compound with code CA-E5 eluted at retention time 14.845 min. having mobile phase composition 10% acetonitrile in deionized water. Concentration of water in a mobile phase was directly related to the retention time of compound. This retention time corresponded to presence of cannabinoid glycosides. DAD and ESI-MS spectrum was shown in **Fig. 3.9.9**.

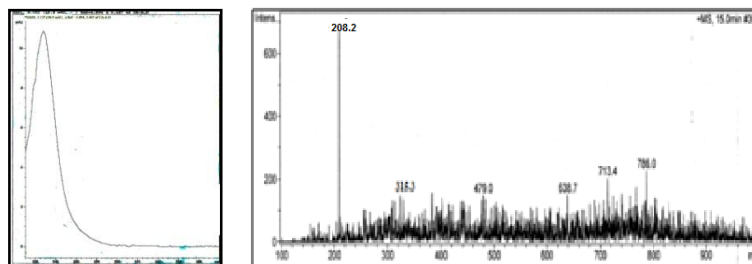


Fig. 3.9.9 DAD and ESI-MS Spectrum of Compound with Code CA-E5

DAD Spectrum

DAD spectrum of compound with code CA-E5 exhibited one band pattern. Band I appeared at 225nm. One band pattern was also exhibited by symmetric phenolic acids, but they usually appeared at lower retention time. Shape, intensity and λ_{max} of this compound resembled to that of Tetrahydrocannabinol. Alkyl side chain of

cannabinoid did not influence the UV absorbance (Hazekamp *et al.*, 2007). Hypsochromic shift of band from 225nm to 220nm (original spectrum) was due to glycosylation or methylation. So, from above spectrum glycosylated or methylated THC was identified (Markham 1982).

ESI-MS Spectrum

ESI-MS spectrum exhibited pseudomolecular molecular ion peak at m/z 786 in positive ion mode and the molecular weight of the compound calculated was 752 *amu*. Fragment ion peak at m/z 713 was due to the cleavage of $^{0,2}X_{\text{rha}}$ as $[M+2\text{MeOH}+\text{H}-^{0,2}X_{\text{rha}}]^+$. As a result of cleavage of terminal rhamnose, peak appeared at m/z 639 *i.e.*, $[M+\text{MeOH}+\text{H}-\text{rha}]$. Cleavage of rhamnose along with another molecule of rhamnose, peak appeared at m/z 479 as $[M+\text{H}_2\text{O}+\text{H}-\text{rha}-\text{rha}]^+$. Successive loss of three rhamnose, peak appeared at m/z 315 with proton adduct *i.e.*, $[M+\text{H}-\text{rha}-\text{rha}-\text{rha}]^+$ as shown in **Scheme 3.6.5**. Aglycone peak was justified with proton adduct. From above fragmentation pattern, three rhamnoses were identified. By consolidating all the information obtained from retention time, DAD and ESI-MS spectrum, identified compound is Tetrahydrocannabinol-1-*O*-[α -L-rhamnopyranosyl-(1 \rightarrow 4)- α -L-rhamnopyranosyl-(1 \rightarrow 4)- α -L-rhamnopyranoside] as given in **Fig. 3.9.10**.

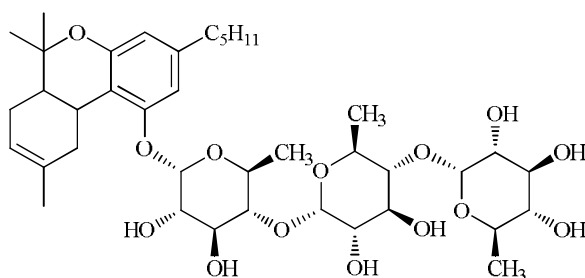
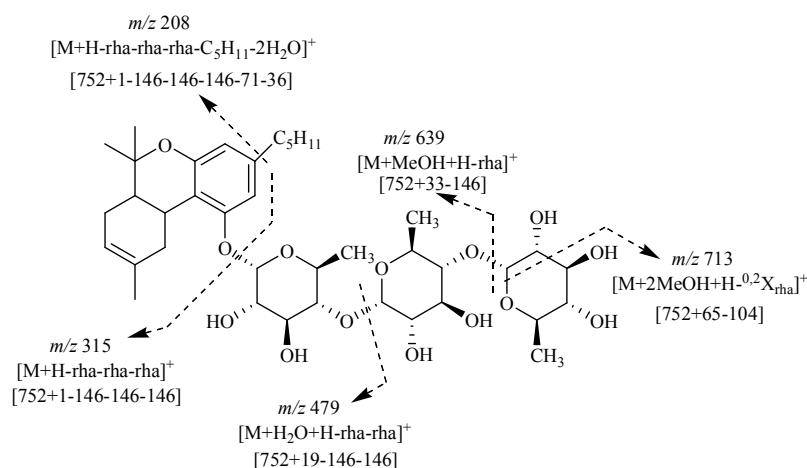


Fig. 3.9.10 Tetrahydrocannabinol-1-*O*-[α -L-rhamnopyranosyl-(1 \rightarrow 4)- α -L-rhamnopyranosyl-(1 \rightarrow 4)- α -L-rhamnopyranoside]



Scheme 3.6.5 Fragmentation Scheme of Tetrahydrocannabinol-1-*O*-[α -L-rhamnopyranosyl-(1 \rightarrow 4)- α -L-rhamnopyranosyl-(1 \rightarrow 4)- α -L-rhamnopyranoside]

3.12.1.6 CA-E6

The compound eluted at t_R 29.442min. with the mobile phase composition 40% acetonitrile in deionized water. This compound suggested the presence of hydrophilic moiety. DAD and ESI-MS spectrum was shown in **Fig. 3.9.11**.

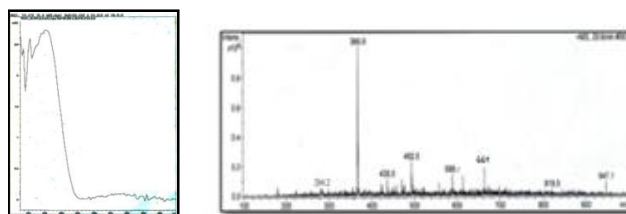


Fig. 3.9.11 DAD and ESI-MS Spectrum of Compound with Code CA-E6

DAD Spectrum

DAD spectrum of compound displayed two band pattern, one band appeared at 218nm while other band appeared at 242nm. DAD spectrum of flavonoid also showed two band pattern, one band appeared at 240-285nm (band I) while other band appeared at 300-550nm. In this spectrum there was no band above 280nm, which confirmed the absence of flavonoids. Shape and intensity of DAD closely resembled to Cannabinoids. Band I of THCA, THCA-C₄ and THVA appeared at 215nm, while band II appeared at 232nm. Methylation and glycosylation causes band shift to shorter

wavelength. This spectrum resembled to THCA, THCA-C4 and THVA. Alkyl side chain did not influence the UV absorbance (Hazekamp *et al.*, 2007).

ESI-MS Spectrum

ESI-MS spectrum of compound corresponded to t_R 29.6 min. in positive ion mode was given in **Fig. 3.9.11**. Molecular mass of the compound calculated was 946 *amu*. Pseudomolecular ion peak appeared at m/z 947, that was justified by $[M+H]^+$. From m/z 947 to m/z 819 loss of 146 mass unit indicated the loss of rhamnose that was justified by adduct H_2O+H as $[M+H_2O+H-rha]^+$. Fragment ion peak at m/z 661 was justified by the loss of glucose. Peak at m/z 661 appeared as adduct $[M+Na-rha-glc]^+$. Fragment ion peak at m/z 589 indicated the loss of 146 mass unit due to rhamnose, that was justified by adduct $3MeOH+H$ as $[M+3MeOH+H-rha-glc-rha]^+$. Peak at m/z 493 was also justified by the proton as $[M+H-rha-glc-rha]^+$. Base peak at m/z 367 was due to loss of 162 mass unit indicated the cleavage of another glucose moiety from aglycone part *i.e.*, $[M+2H_2O+H-rha-glc-rha-glc]^+$. Peak at m/z 284 manifesting the loss of propyl from aglycone part along with the loss of two water molecules with adduct $MeOH+H$ *i.e.*, $[M+MeOH+H-rha-glc-rha-glc-C_3H_7-2H_2O]^+$. So, from ESI-MS spectrum THVA was confirmed.

By consolidating all the above information obtained from retention time, DAD and ESI-MS spectrum, it was concluded that CA-E6 is Tetrahydrocannabivarinic acid-1-*O*-[α -L-rhamnopyranosyl-(1 \rightarrow 4)- β -D-glucopyranosyl-(1 \rightarrow 4)- α -L-rhamnopyranosyl-(1 \rightarrow 4)- β -D-glucopyranoside] as shown in **Fig. 3.9.12**.

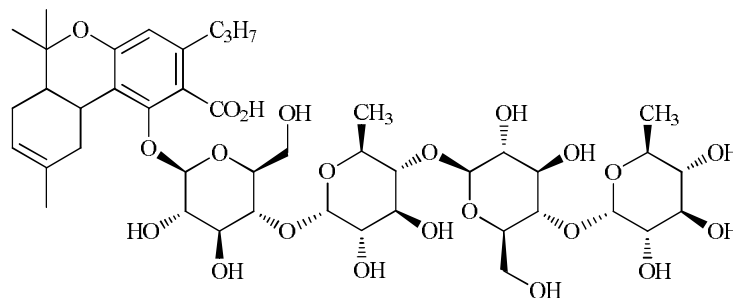
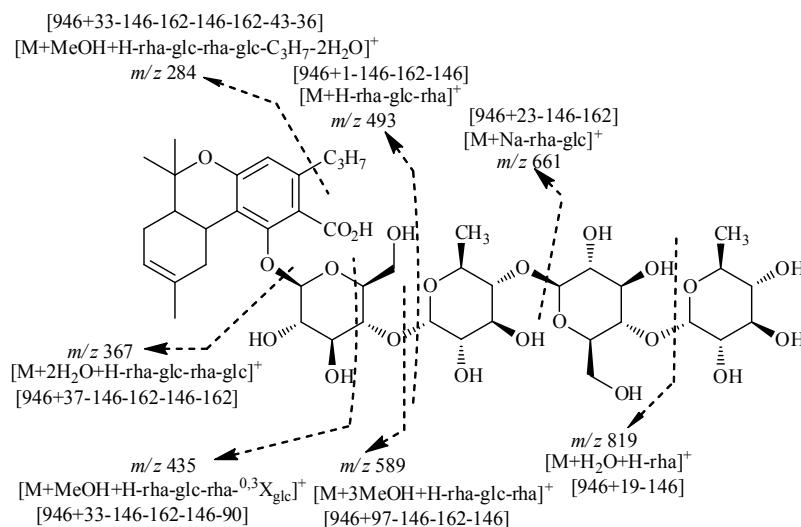


Fig. 3.9.12 Tetrahydrocannabivarinic acid-1-*O*-[α -L-rhamnopyranosyl-(1 \rightarrow 4)- β -D-glucopyranosyl-(1 \rightarrow 4)- α -L-rhamnopyranosyl-(1 \rightarrow 4)- β -D-glucopyranoside] (CA-E6)

Fragmentation Scheme of compound CA-E6 was given below in **Scheme 3.6.6**.



Scheme 3.6.6 Fragmentation Scheme of Tetrahydrocannabivarinic acid-1-O-[\alpha-L-rhamnopyranosyl-(1→4)-β-D-glucopyranosyl-(1→4)-α-L-rhamnopyranosyl-(1→4)-β-D-glucopyranoside]

3.12.1.7 CA-E7

Compound with code CA-E7 eluted at retention time 30.702 min. having mobile phase composition 10% acetonitrile in deionized water. Concentration of water in a mobile phase was directly proportional to retention time of compound as shown in **Fig. 3.9.13**. Higher retention time inferred the presence of cannabinoid glycosides.

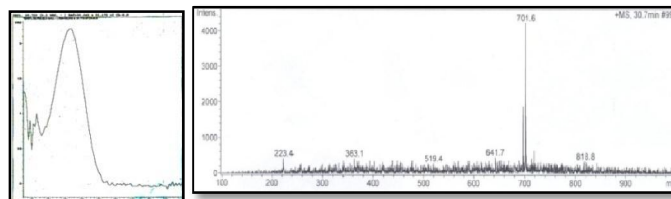


Fig. 3.9.13 DAD and ESI-MS Spectrum of Compound with Code CA-E7

DAD Spectrum

One major band with distorted shoulders was inferred by compound with code CA-E7. Shape, intensity and λ_{max} resembled to that of Cannabinoids. This UV

spectrum resembled to that of THCA-C4 and THVA. Alkyl side chain did not influence the UV absorbance, as there was no difference between THCA-C4 and THVA (Hazekamp *et al.*, 2007).

ESI-MS Spectrum

Mass spectrum exhibited pseudomolecular ion peak at m/z 818 in positive ion mode and calculated molecular weight was 784 *amu*. Pseudomolecular ion peak was justified with adduct as $[M+MeOH+2H]^+$. Base peak at m/z 701 was due to the cleavage of fragment $^{0,2}X_{glc}$ with adduct $2H_2O+H$ as $[M+2H_2O+H-^{0,2}X_{glc}]^+$. Fragment ion peak at m/z 641 was due to the cleavage of terminal glucose *i.e.*, $[M+H_2O+H-glc]^+$. As a result of loss of terminal glucose along with rhamnose, peak appeared at m/z 518 *i.e.*, $[M+CH_3CN+H-glc-rha]^+$. Cleavage of terminal glucose, rhamnose along with xylose, peak appeared at m/z 363 *i.e.*, $[M+H_2O+H-glc-rha-xyl]^+$ as shown in **Scheme 3.6.7**. From above fragmentation scheme identified sugars are glucose, rhamnose and xylose. The aglycone part was justified with adduct H_2O+H . From DAD spectrum, two Cannabinoids THCA-C4 and THVA were not distinguished. But on the basis of retention time, they were easily identified. THCA-C4 was eluted at higher retention time as compared to THVA (Hazekamp *et al.*, 2007). So, identified aglycone is Tetrahydrocannabivarinic acid-C4-1-*O*-[β -D-glucopyranosyl-(1 \rightarrow 4)- α -L-rhamnopyranosyl-(1 \rightarrow 4)- β -D-xylopyranoside] as shown in **Fig. 3.9.14**.

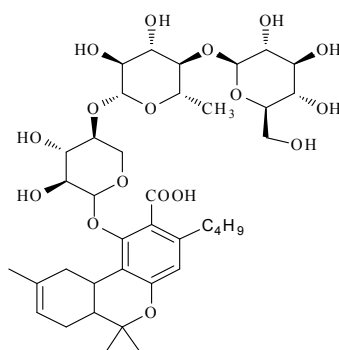
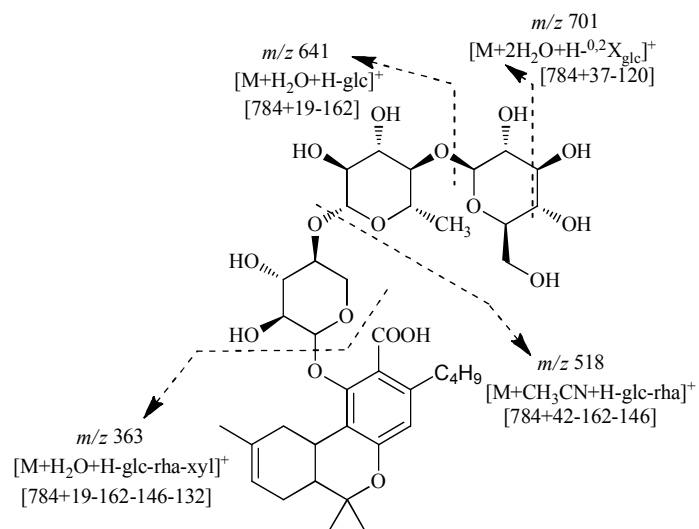


Fig. 3.9.14 Tetrahydrocannabivarinic acid-C4-1-*O*-[β -D-glucopyranosyl-(1 \rightarrow 4)- α -L-rhamnopyranosyl-(1 \rightarrow 4)- β -D-xylopyranoside] (CA-E7)



Scheme 3.6.7 Fragmentation Scheme of Tetrahydrocannabivarinic acid-C4-1-*O*-[β -D-glucopyranosyl-(1 \rightarrow 4)- α -L-rhamnopyranosyl-(1 \rightarrow 4)- β -D-xylopyranoside]

3.12.2 Chromatographic Profiling of CS-A Extracts

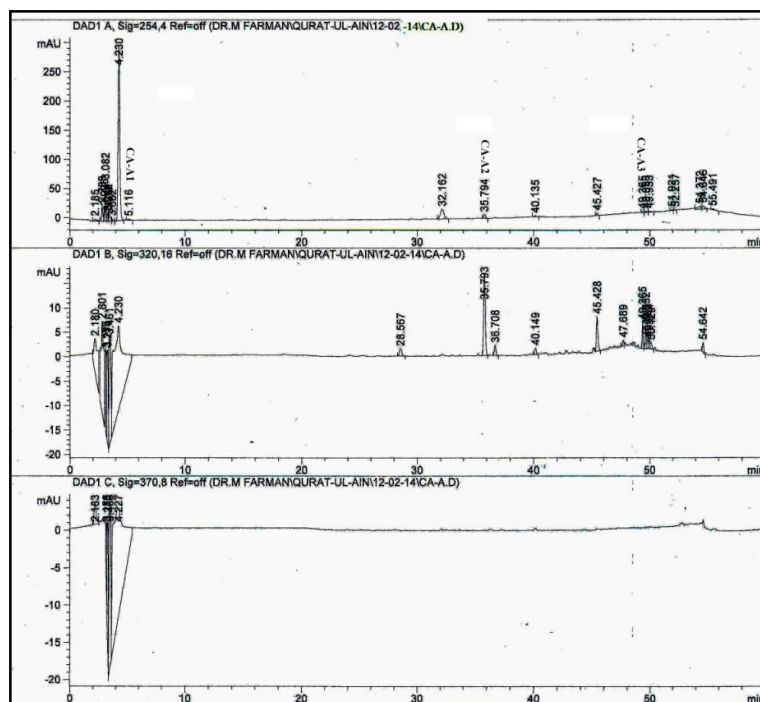


Fig.3.10 Chromatographic Profiling of Compound with Code CS-A

Chromatographic profiling of compound with code CS-A was recorded online by DAD at wavelength 254nm, 320nm and 370nm as shown in **Fig. 3.10**. There was a differential retention of sample components according to their hydrophobicity such that more hydrophilic compounds were retained less in the stationary phase and eluted out first. Chromatographic profiling under wavelength 254nm unveiled maximum absorption. Maximum absorption inferred that large numbers of compounds were eluted out in first five minutes. Significant numbers of compounds were also present after 30 min. From 5 to 30 min., no compounds were eluted out. Profile obtained under 320nm and 370nm manifested that very few of compounds were eluted out.

3.12.2.1 CS-A1

Compound CS-A1 eluted at retention time 5.2 min. showed hydrophilic nature of compound with the mobile phase composition 10% acetonitrile in deionized water. The proportion of water in a mobile phase was directly proportional to the retention

time of compound as shown in **Fig. 3.10.1**. A lower retention time corresponded to cannabinoid glycosides.

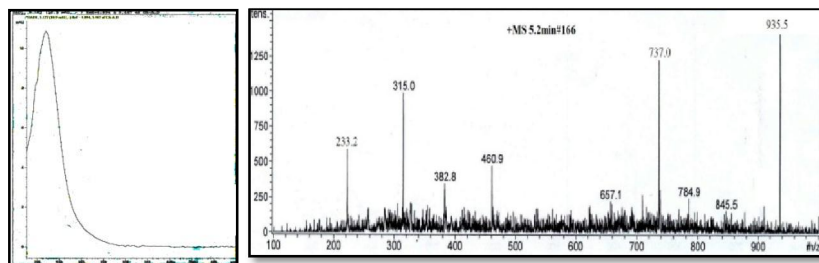


Fig. 3.10.1 DAD and ESI-MS Spectrum of Compound with code CS-A1

DAD Spectrum

DAD spectrum displayed one band pattern at 227nm with maximum absorbance. This spectrum showed no band above 280nm that suggested the absence of flavonoids. The shape, intensity and λ_{\max} of this compound were found in agreement with the Cannabinoids. λ_{\max} of this compound was 227nm that resembled with λ_{\max} of Tetrahydrocannabinol having value 230nm. Band shift toward shorter wavelength was due to glycosylation or methylation. So, from DAD spectrum THC glycosides were detected (**Markham 1982**).

ESI-MS Spectrum

Pseudomolecular ion peak of compound eluted at retention time 5.2min. with positive ion mode was with m/z 935. The molecular weight suggested was 916 *amu*. Pseudomolecular ion peak was justified with adduct as $[M+H_2O+H]^+$. Fragment ion peak at m/z 845 manifesting the loss of $^{0,3}X_{\text{xyI}}$ as $[M+H_2O+H-^{0,3}X_{\text{xyI}}]^+$. The peak at m/z 785 suggested the cleavage of xylose as $[M+H-\text{xyI}]^+$. Base peak at m/z 737 was justified by the loss of terminal xylose and formaldehyde *i.e.*, $[M+H-\text{xyI}-H_2O-CH_2O]^+$. The fragment ion peak at m/z 657 inferred the loss of terminal xylose and glucose along with the formaldehyde as $[M+2MeOH+H-\text{xyI}-\text{glc}-CH_2O]^+$. As a result of cleavage of terminal xylose, glucose and again glucose peak appeared at m/z 461 as $[M+H-\text{xyI}-\text{glc}-\text{glc}]^+$. By the loss of xylose, glucose, again glucose and $^{1,5}X_{\text{rha}}$ peak appeared at m/z 382. Peak at m/z 315 suggested the cleavage of xylose, glucose, glucose and rhamnose *i.e.*, $[M+H-\text{xyI}-\text{glc}-\text{glc}-\text{rha}]^+$. By keeping in view all above

information xylose, glucose, glucose and rhamnose was confirmed. And the aglycone part was Tetrahydrocannabinol that was justified by proton. From aglycone part loss of C_5H_{11} along with xylose, glucose, glucose and rhamnose suggested the peak at m/z 233.

With the view of all this content including retention time. DAD and ESI-MS spectrum the suggested CA-A compound was $\Delta^{(8)}$ -Tetrahydrocannabinol-1-*O*-[β -D-xylopyranosyl-(1 \rightarrow 4)- β -D-glucopyranosyl-(1 \rightarrow 4)- β -D-glucopyranosyl-(1 \rightarrow 4)- α -L-rhamnopyranoside] as shown in **Fig. 3.10.2**.

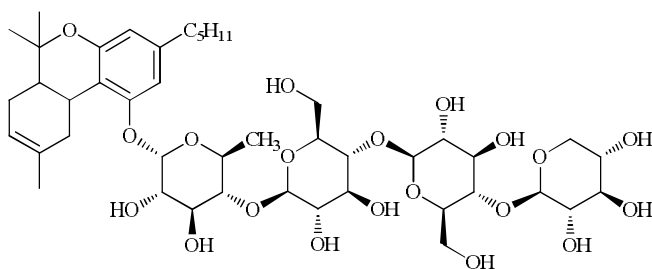
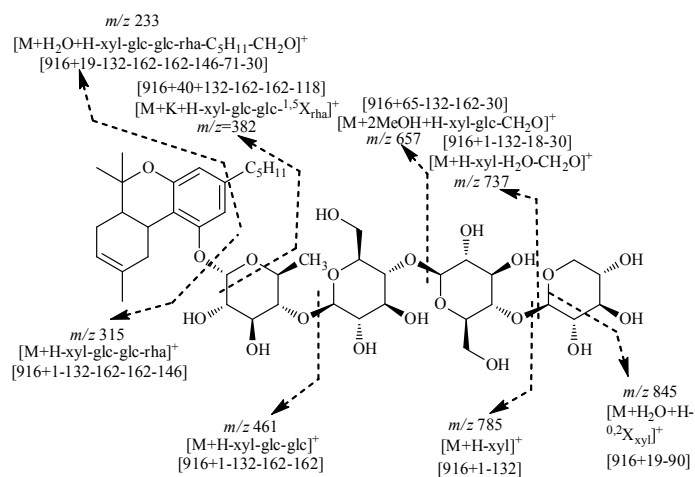


Fig. 3.10.2 $\Delta^{(8)}$ -Tetrahydrocannabinol-1-*O*-[β -D-xylopyranosyl-(1 \rightarrow 4)- β -D-glucopyranosyl-(1 \rightarrow 4)- β -D-glucopyranosyl-(1 \rightarrow 4)- α -L-rhamnopyranoside]
(CS-A1)

Suggested cleavages of CA-A1 were given in **Scheme 3.7.1** below:



Scheme 3.7.1 Fragmentation Scheme of Δ^8 -Tetrahydrocannabinol-1-*O*-[β -D-xylopyranosyl-(1 \rightarrow 4)- β -D-glucopyranosyl-(1 \rightarrow 4)- β -D-glucopyranosyl-(1 \rightarrow 4)- α -L-rhamnopyranoside]

3.12.2.2 CA-A2

Compound with code CA-2 eluted at retention time 35.287 min. having mobile phase composition 40% acetonitrile in deionized water. By changing the composition of mobile phase, variety of compounds were eluted out. In this composition, hydrophilic compounds eluted first and hydrophobic compounds were eluted later as shown in **Fig. 3.10.3**.

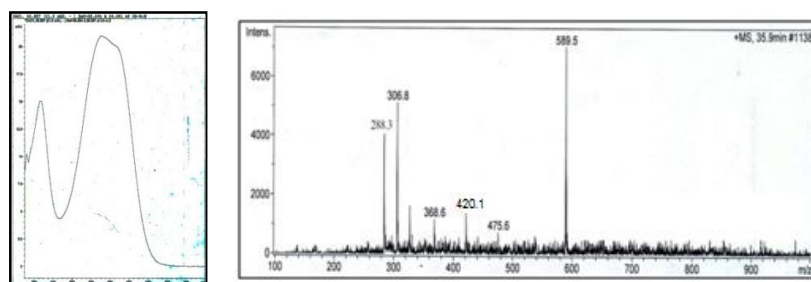


Fig. 3.10.3 DAD and ESI-MS of compound with code CA-A2

DAD Spectrum

DAD spectrum of this compound showed characteristics two band pattern, band(I) appeared at 295nm while band(II) appeared at 230nm. The two band pattern was characteristic for flavonoids. The UV absorbance value of this compound suggested the presence of flavones having band I appeared in range of 310-350nm and band II in range of 250-280nm. Band shift towards shorter wavelength was due to glycosylation or methylation. The λ_{\max} , intensities and shape were in agreement with that of Luteolin.

ESI-MS Spectrum

Pseudomolecular ion peak appeared in mass spectrum was at m/z 589 and the molecular weight of compound calculated was 546 *amu*. Fragment ion peak at m/z 420 suggested the loss of xylose along with two water molecules *i.e.*, $[M+CH_3CN+H\text{-xyl}-2H_2O]^+$. As a result of cleavage of terminal xylose and $^{0,3}X_{rha}$ with the loss of two water molecules, peak appeared at m/z 369 *i.e.*, $[M+2MeOH+H\text{-xyl}-^{0,3}X_{rha}-2H_2O]^+$. Base peak at m/z 307 inferred the cleavage of terminal xylose and rhamnose as $[M+K\text{-xyl-rha}]^+$. From all above information, the sugars identified were xylose and rhamnose with the aglycone part Luteolin.

Keeping in mind all the above information obtained from retention time, DAD and ESI spectrum suggested compound is Luteolin-4-*O*-[β -D-xylopyranosyl-(1 \rightarrow 4)- α -L-rhamnopyranoside] as shown in **Fig. 3.10.4**.

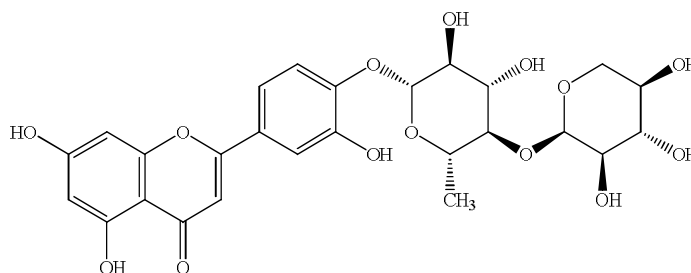
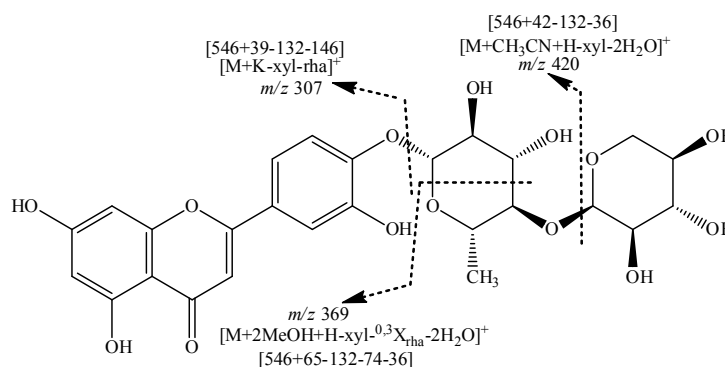


Fig. 3.10.4 Luteolin-4-*O*-[β -D-xylopyranosyl-(1 \rightarrow 4)- α -L-rhamnopyranoside] (CA-A2)

Fragmentation Scheme of compound CA-A2 was given below in **Scheme 3.7.2**.



Scheme 3.7.2 Fragmentation Scheme of Luteolin-4-O-[β -D-xylopyranosyl-(1 \rightarrow 4)- α -L-rhamnopyranoside]

3.12.2.3 CA-A3

CA-A3 compound eluted at retention time 49.9 min. showed hydrophobic nature of compound with mobile phase composition of 49% acetonitrile in deionized water. Proportion of water in a mobile phase was directly proportional to retention time of compounds. DAD along with ESI-MS spectrum was given below in **Fig. 3.10.5**.

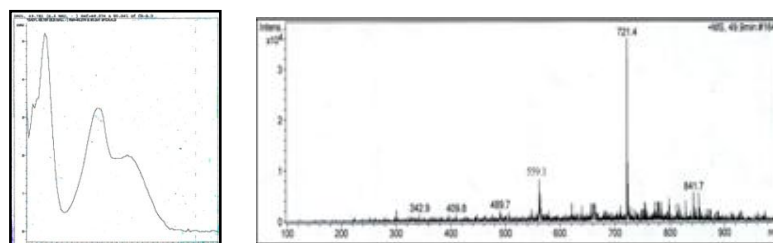


Fig. 3.10.5 DAD and ESI-MS Spectrum of compound with code CA-A3

DAD Spectrum

DAD of this compound showed two band patterns, one band appeared at 230nm while other band appeared at 280nm. Flavonoids also showed two band patterns, band I appeared in the range of 300-550nm while band II appeared at 240-285nm. In this spectrum, there was no band above 300nm that confirmed the absence of flavonoids. Shape, intensity and λ_{max} resembled to that of Cannabinoids. DAD spectrum showed resemblance with Tetrahydrocannabinolic acid and its derivatives.

As the alkyl part chains don't influenced the DAD, so the identified compound may be the C5, C4 and C3 isomer of THC (**Hazekamp *et al.*, 2007**). Standard DAD of these acids appeared at 232nm band I and band II appeared at 290nm. Shift of bands toward shorter wavelength was due to glycosylation and methylation.

ESI-MS Spectrum

Pseudomolecular ion peak on mass spectrum appeared at m/z 842 with calculated molecular mass was 800amu. Pseudomolecular ion peak was justified with adduct as $[M+CH_3CN+H]^+$. Fragment ion peak at m/z 721 inferred the loss of glucose as $[M+2CH_3CN+H-glc]^+$. As a result of two terminal glucose cleavage, peak appeared at m/z 559 *i.e.*, $[M+2CH_3CN+H-glc-glc]^+$. Peak at m/z 409 was due to loss of two terminal glucose and one xylose moiety *i.e.*, $[M+2MeOH+H-glc-glc-xyl]^+$ as shown in **Scheme 3.7.3**. From above cleavages, two terminal glucoses and one xylose was confirmed. Identified aglycone part was C4 isomer of Tetrahydrocannabinoic acid. So, C4 isomer of Tetrahydrocannabinolic acid was confirmed from above cleavages.

By consolidating all the above information obtained from retention time, DAD and ESI-MS spectrum, it was inferred that CA-A3 compound is Tetrahydrocannabivarinic acid-C4-1-*O*-[β -D-glucopyranosyl-(1 \rightarrow 4)- β -D-glucopyranosyl-(1 \rightarrow 4)- β -D-xylopyranoside]. Structure of compound with code CA-A3 was given below in **Fig. 3.10.6**.

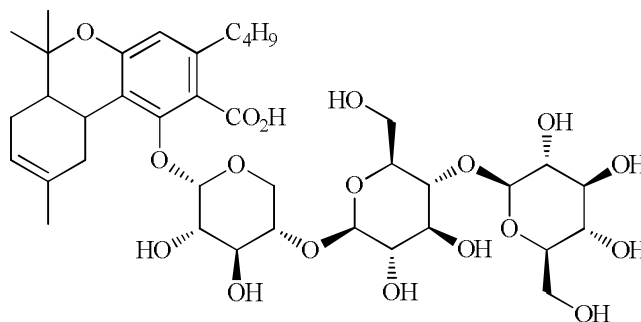
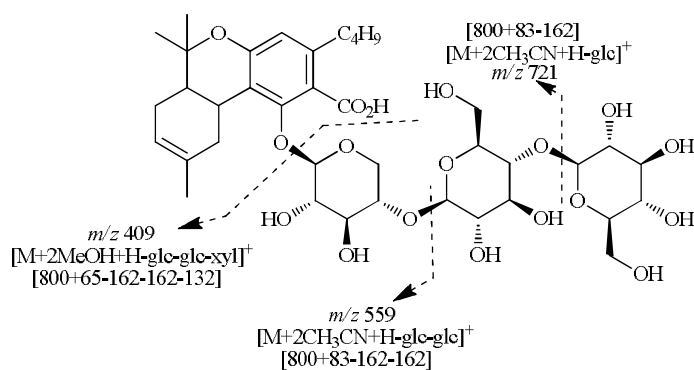


Fig.3.10.6 Tetrahydrocannabivarinic acid-C4-1-*O*-[β -D-glucopyranosyl-(1 \rightarrow 4)- β -D-glucopyranosyl-(1 \rightarrow 4)- β -D-xylopyranoside] (CA-A3)

Suggested cleavages of compound with code CA-A3 is given below:



Scheme 3.7.3 Fragmentation Scheme of Tetrahydrocannabivarinic acid-C4-1-
O-[β -D-glucopyranosyl-(1 \rightarrow 4)- β -D-glucopyranosyl-(1 \rightarrow 4)- β -D-
xylopyranoside]

3.12.3 Chromatographic Profiling of CA-Ex-Sox

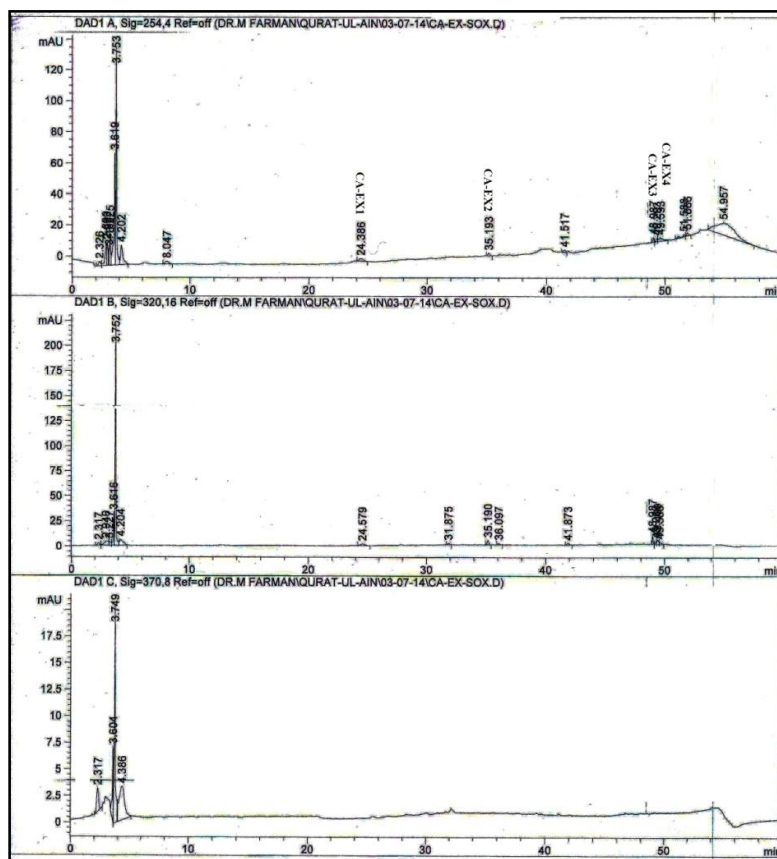


Fig.3.11 Chromatographic Profiling of CA-Ex-Sox

Chromatographic profiling of compound with code CA-Ex-Sox was recorded online by DAD obtained at wavelength 254nm, 320nm and 370nm as shown in **Fig. 3.11**. For a given mobile phase, there was a differential retention of sample components such that hydrophilic compounds were eluted out first and hydrophobic compounds were eluted at end. Profile obtained under 254nm showed maximum absorption that inferred large numbers of compounds were eluted out in first eight minutes. By increasing the concentration of acetonitrile, one compound was eluted at about 24.386 min. At the end few of the hydrophobic compounds were eluted out. While the chromatographic profiling obtained under 320nm and 370nm displayed the presence of few compounds.

3.12.3.1 CA-Ex1

Compound with code CA-EX1 eluted at retention time 24.6 min. having mobile phase composition of 40% acetonitrile in deionized water. In given mobile phase composition, there was differential retention of sample components according to their hydrophobicity in a manner such that more hydrophilic compounds was retained less in the stationary phase and eluted first, while the more hydrophobic compounds will be more retained and eluted last. DAD and ESI-MS spectrum of compound is given in **Fig. 3.11.1**.

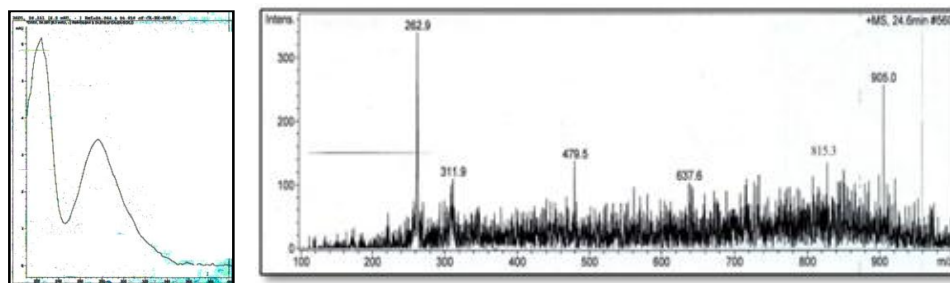


Fig. 3.11.1 DAD and ESI-MS Spectrum of compound with code CA-EX1

DAD Spectrum

Double band pattern was manifested by compound with code CA-EX1. Band I appeared at 228nm while band II appeared at 276nm. Flavonoids also showed two band patterns with band I in range of 300-550nm, while band II in range 240-285nm. In this spectrum, there was no band above 300 nm that confirmed the absence of flavonoids. Shape, intensity and λ_{\max} of this spectrum closely resembled to that of Cannabinoids. In Cannabinol (standard) band I appeared at 230nm while band II appeared at 290nm. Shift of band towards shorter wavelength was due to glycosylation or methylation (**Markham 1982**).

ESI-MS Spectrum

Pseudomolecular molecular ion peak appeared as $[M+Na]^+$ on mass spectrum with positive ion mode. Molecular weight calculated was 882 *amu*. Peak at *m/z* 815 manifested the loss of terminal xylose as $[M+2MeOH+H-xy]^+$. As a result of cleavage of two xylose moiety, peak appeared at *m/z* 637 as $[M+H_2O+H-xy-xy]^+$.

Peak appeared at m/z 479 was due to loss of two xylose moiety along with one glucose i.e., $[M+Na-xyl-xyl-glc]^+$. Aglycone part was cannabinol with C5 alkyl chain. Peak appeared at m/z 262 corresponding to the loss of two terminal xylose moiety, one glucose, one rhamnose along with C_5H_{11} unit as $[M+2H-xyl-xyl-glc-rha]^+$.

Keeping in mind all the information obtained from retention time, DAD and ESI-MS spectrum, it was inferred that given compound with code CA-EX1 is Cannabinol-1-*O*-[β -D-xylopyranosyl-(1 \rightarrow 4)- β -D-xylopyranosyl-(1 \rightarrow 4)- β -D-glucopyranosyl-(1 \rightarrow 4)- α -L-rhamnopyranoside]. Structure of this compound is given below as shown in **Fig. 3.11.2**.

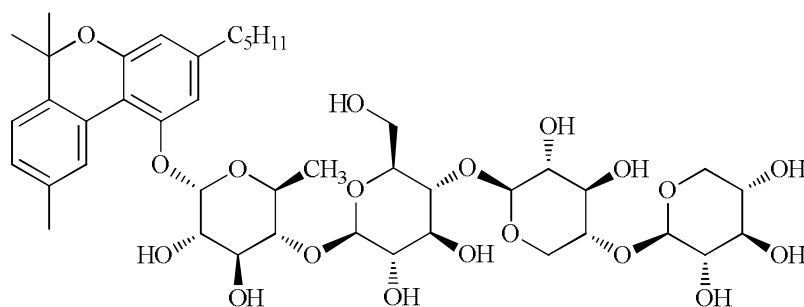
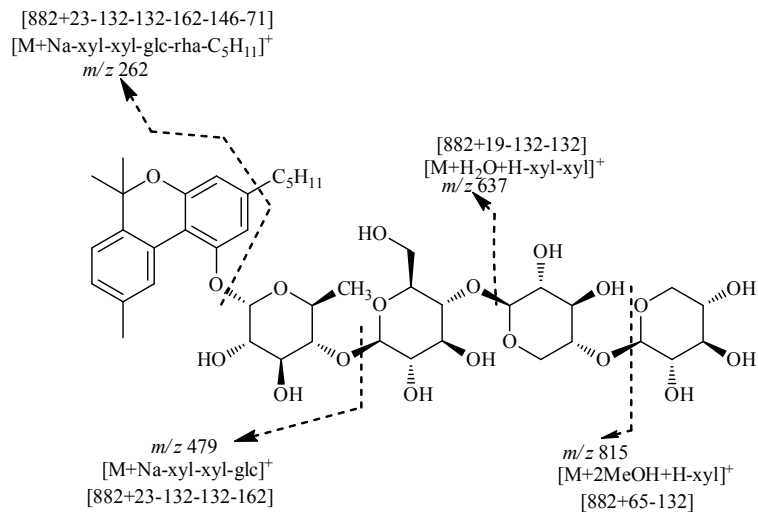


Fig. 3.11.2 Cannabinol-1-*O*-[β -D-xylopyranosyl-(1 \rightarrow 4)- β -D-xylopyranosyl-(1 \rightarrow 4)- β -D-glucopyranosyl-(1 \rightarrow 4)- α -L-rhamnopyranoside] (CA-EX1)

Suggested cleavages of compound with code CA-EX1 was shown here in **Scheme 3.8.1**.



Scheme 3.8.1 Fragmentation Scheme of Cannabinol-1-*O*-[β -D-xylopyranosyl-(1 \rightarrow 4)- β -D-xylopyranosyl-(1 \rightarrow 4)- β -D-glucopyranosyl-(1 \rightarrow 4)- α -L-rhamnopyranoside]

3.12.3.2 CA-EX2

Compound eluted at retention time 35.191 min. having mobile phase composition 10% acetonitrile in deionized water. Higher retention time inferred the presence of flavonoid glycosides as shown in **Fig. 3.11.3**. Higher retention time also inferred the presence of hydroxyl group in position 3 and 5 because of the formation of an intramolecular hydrogen bonding with the carbonyl group on C-4 that was considered as the strongest hydrogen bond acceptor in the flavones.

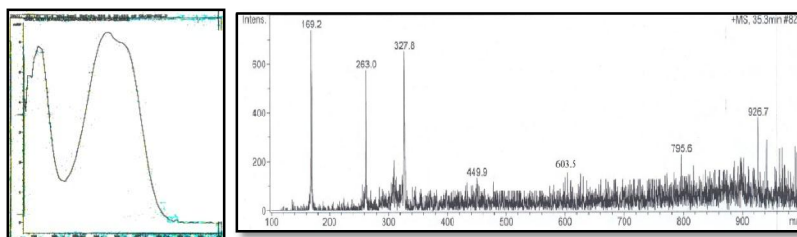


Fig. 3.11.3 DAD and ESI-MS Spectrum of compound with code CA-EX2

DAD Spectrum

Two band patterns were exhibited by the compound with code CA-EX2. Band I in the range 300-350nm and band II in the range 230nm to 250nm. Shape, intensity and λ_{max} resembled to that of flavones. If the flavones lack B-ring substitution or possess a 4'-oxygenation B ring, band II of spectrum appeared as only one peak. The introduction of additional B ring oxygenation commonly produced a double band II (band IIa and band IIb). When oxygenation was only in A ring and included 5 hydroxyl, spectrum was dominated by band II. Introduction of B ring oxygenation enhanced the intensity of band I. Enhancement of band I was greater, when the substitution was at C-4'. Band II of compound with code CA-EX2 was further splitted in to band IIa and band IIb. Splitting of band II into band IIa and band IIb was the characteristic of DAD spectrum of Luteolin. Band II splitting also unveil the presence of 3', 4'-dioxygenation pattern. Shoulder at 290nm was evident in the spectrum of luteolin. But 7-O-glycosylated luteolin caused this shoulder to disappear. Due to the presence of shoulder at 290nm, 7-O-glycosylated luteolin was absent. 5-O-glycosylation produced spectrum similar to that of Luteolin, with a shoulder at 290nm. If 3'-4'-hydroxyls were glycosylated in luteolin, enhancement of band IIa was accompanied by a marked drop in the intensity of band I as well as hypsochromic shift. As band I was highly intense, that inferred 3'-4'-hydroxyls were not glycosylated in luteolin. 3'-O-glycosylation displayed a dramatic effect on the spectrum of luteolin (**Campos and Markham 2007**). Hypsochromic shift of band I from 345nm to 310nm, band IIa from 260nm to 237nm and band IIb from 250nm to 230nm was because of glycosylation or methylation (**Markham 1982**). 3'-O-glycosylated Luteolin was unveiled from DAD spectrum of compound with code CA-EX2.

ESI-MS Spectrum

Mass spectrum exhibited pseudomolecular ion peak at m/z 927 in positive ion mode molecular weight calculated was 844 *amu*. Pseudomolecular ion peak was justified with adduct as $[M+2\text{CH}_3\text{CN}+\text{H}]^+$. Fragment ion peak at m/z 795 inferred the cleavage of terminal xylose *i.e.*, $[M+2\text{CH}_3\text{CN}+\text{H-xyl}]^+$. As a result of cleavage of terminal xylose along with second molecule of xylose, peak appeared at m/z 603 *i.e.*, $[M+\text{Na-xyl-xyl}]^+$. Third molecule of xylose was lost from m/z 603, peak appeared at

m/z 449 as $[M+H\text{-xyl-xyl-xyl}]^+$. Peak at m/z 328 was due to cleavage of glucose along with three molecule of xylose *i.e.*, $[M+\text{CH}_3\text{CN}+H\text{-xyl-xyl-xyl-glc}]^+$. From above fragmentation pattern, three xylose along with one glucose sugars were identified. Aglycone luteolin was justified by the cleavage of C-ring at m/z 169 as $^{0,3}X$ *i.e.*, $[M+\text{MeOH}+H\text{-xyl-xyl-xyl-glc-}^{0,3}X_{\text{lute}}]^+$ as shown in **Scheme 3.8.2**.

By keeping in mind all the information obtained from retention time, DAD and ESI-MS spectrum, it was inferred that identified compound is Luteolin-3'-*O*-[β -D-xylopyranosyl-(1 \rightarrow 4)- β -D-xylopyranosyl-(1 \rightarrow 4)- β -D-xylopyranosyl-(1 \rightarrow 4)- β -D-glucopyranoside] as shown in **Fig. 3.11.4**.

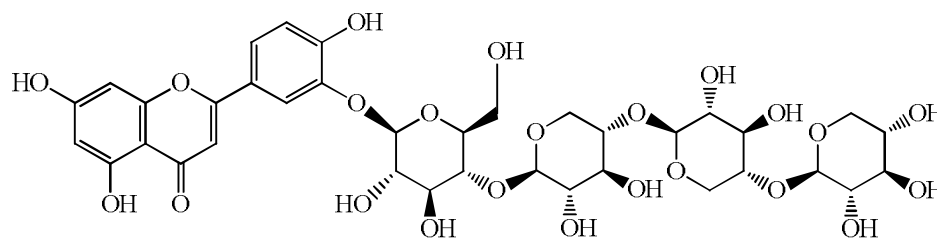
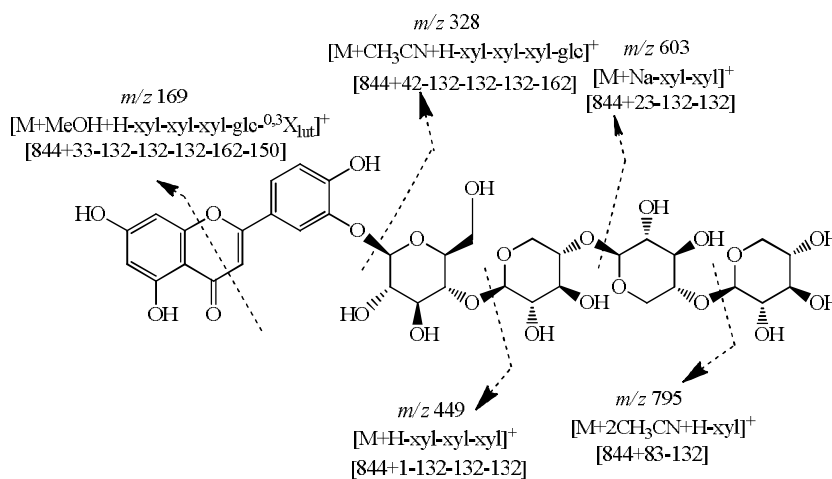


Fig. 3.11.4 Luteolin-3'-*O*-[β -D-xylopyranosyl-(1 \rightarrow 4)- β -D-xylopyranosyl-(1 \rightarrow 4)- β -D-xylopyranosyl-(1 \rightarrow 4)- β -D-glucopyranoside] (CA-EX2)



Scheme.3.8.2 Fragmentation Scheme of Luteolin-3'-*O*-[β -D-xylopyranosyl-(1 \rightarrow 4)- β -D-xylopyranosyl-(1 \rightarrow 4)- β -D-xylopyranosyl-(1 \rightarrow 4)- β -D-glucopyranoside]

3.12.3.3 CA-EX3

Compound with CA-EX3 eluted at retention time 48.984 min. having mobile phase composition 40% acetonitrile in deionized water. Higher retention time inferred the presence of flavonoid glycosides. Higher retention time revealed the presence of hydroxyl group in position 3 and 5 because of the formation of an intramolecular hydrogen bond with the carbonyl group on C-4. While the introduction of methoxy group did not affect the retention time. DAD and ESI-MS spectrum of compound was shown in **Fig. 3.11.5**.

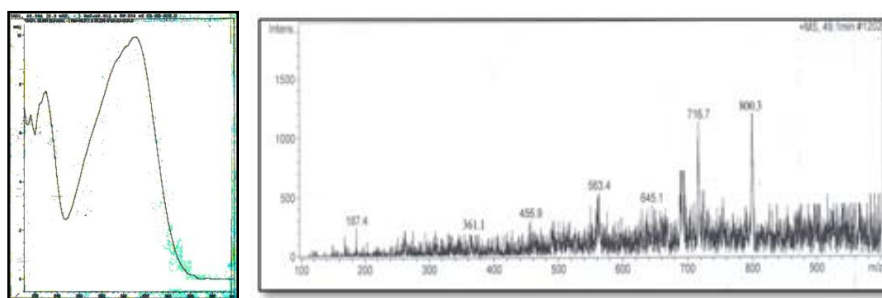


Fig. 3.11.5 DAD and ESI-MS Spectrum of compound with code CA-EX3

DAD Spectrum

Compound with code CA-EX3 displayed two band pattern, band I in the range 300-350nm while band II in the range of 230-240nm. Band II was further splitted into band IIa and band IIb. These band ranges betrayed the presence of flavones. Band II of spectrum appeared as only one peak, if flavones lack B ring substitution or posses a 4'-oxygenation of B ring. But the introduction of additional B ring oxygenation produced a double band II (band IIa and band IIb). Spectrum contained broad band II that displayed oxygenation was on A ring included 5 hydroxyl position. Enhanced intensity of band I manifested the presence of B ring oxygenation pattern. Shape, intensity and λ_{\max} resembled to that of Tricetin. Spectrum of Tricetin differ from luteolin with major band IIa absorption at 240 nm and also with relative increase in the intensity of band I. Hypsochromic shift of band I from 370nm to 330nm and band II from 250nm to 230nm displayed the presence of 11-Hydroxy Tricetin. As there was no shoulder at 290nm that manifest the presence of glycosylation at 7 hydroxyl group.

Form above information it was inferred that DAD spectrum resembled to that of 7-*O*-glycosylated-6-Hydroxytricetin.

ESI-MS Spectrum

Pseudomolecular ion peak appeared on mass spectrum at m/z 800 in positive ion mode and molecular weight calculated was 758 *amu*. Pseudomolecular ion peak was justified with adduct as $[M+CH_3CN+H]^+$. Fragment ion peak at m/z 717 manifested the cleavage of $^{0,3}X_{xyl}$ with adduct H_2O+H *i.e.*, $[M+H_2O+H-^{0,3}X_{xyl}]^+$. Complete loss of terminal xylose was inferred from m/z 645 *i.e.*, $[M+H_2O+H-xyl]^+$. As a result of cleavage of rhamnose along with terminal xylose, peak appeared at m/z 563 *i.e.*, $[M+2CH_3CN+H-xyl-rha]^+$ as shown in **Scheme 3.8.3**. Fragment ion peak at m/z 360 manifested the cleavage of glucose, rhamnose and xylose as $[M+CH_3CN+H-xyl-rha-glc]^+$. By keeping in consideration all the information obtained from retention time, DAD and ESI-MS spectrum, identified compound is 6-Hydroxytricetin-7-*O*-[β -D-xylopyranosyl-(1 \rightarrow 4)- α -L-rhamnopyranosyl-(1 \rightarrow 4)- β -D-glucopyranoside] as shown in **Fig. 3.11.6**.

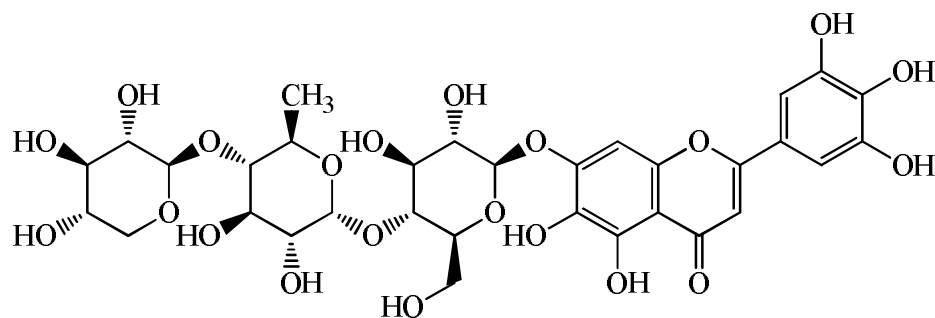
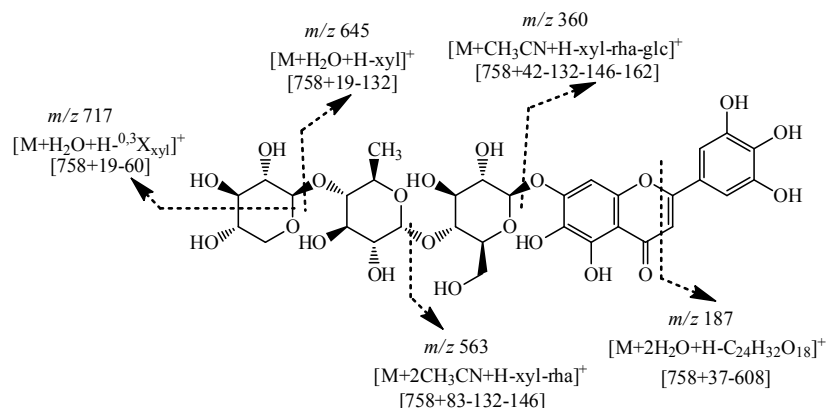


Fig. 3.11.6 6-Hydroxytricetin-7-*O*-[β -D-xylopyranosyl-(1 \rightarrow 4)- α -L-rhamnopyranosyl-(1 \rightarrow 4)- β -D-glucopyranoside] (CA-EX3)



Scheme 3.8.3 Fragmentation Scheme of 6-Hydroxytricetin-7-*O*-[β -D-xylopyranosyl-(1 \rightarrow 4)- α -L-rhamnopyranosyl-(1 \rightarrow 4)- β -D-glucopyranoside]

3.12.3.4 CA-EX4

Compound with code CA-EX4 eluted at retention time 49.411 min. having 40% acetonitrile in deionized water. Concentration of water in a mobile phase was directly proportional to the retention time of compound. Higher retention time inferred the presence of flavonoid or cannabinoid glycosides. DAD and ESI-MS spectrum was given in **Fig. 3.11.7**.

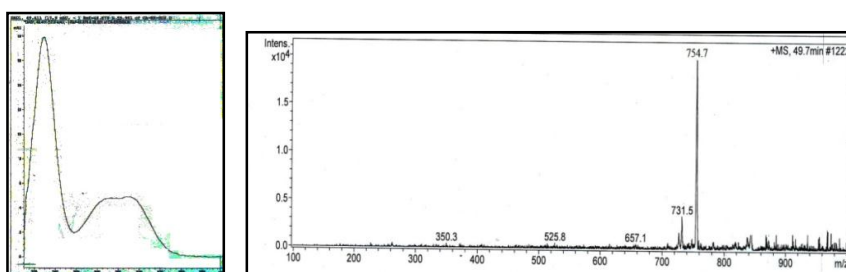


Fig. 3.11.7 DAD and ESI-MS Spectrum of compound with code CA-EX4

DAD Spectrum

Two band patterns were exhibited by compound with code CA-EX4. Band I at 215nm, while band II appeared at 280nm. Two band patterns were also observed by phenolic acids, but they usually appeared at lower retention time. Shape, intensity and λ_{max} resembled to that of cannabinol. Shift of band II from 290nm to 280nm, was due to glycosylation or methylation (**Markham 1982**).

ESI-MS Spectrum

Mass spectrum exhibited Pseudomolecular ion peak at m/z 755 in positive ion mode. Calculated molecular weight of compound was 736 *amu*. Pseudomolecular ion peak was justified with adduct H_2O+H *i.e.*, $[M+H_2O+H]^+$. As a result of cleavage of terminal glucose, peak appeared at m/z 657 as $[M+2CH_3CN+H-glc]^+$. Fragment ion peak at m/z 525 manifested the cleavage of xylose along with terminal glucose *i.e.*, $[M+2CH_3CN+H-glc-xyl]^+$. Peak at m/z 349 was justified by the cleavage of second xylose along with the loss of terminal glucose and xylose as $[M+K-glc-xyl-xyl]^+$ as shown in **Scheme 3.8.4**. By keeping in mind all the information obtained from retention time, DAD and ESI-MS spectrum, identified compound is Cannabinol-1-*O*-[β -D-glucopyranosyl-(1 \rightarrow 4)- β -D-xylopyranosyl-(1 \rightarrow 4)- β -D-xylopyranoside] as shown in **Fig. 3.11.8**.

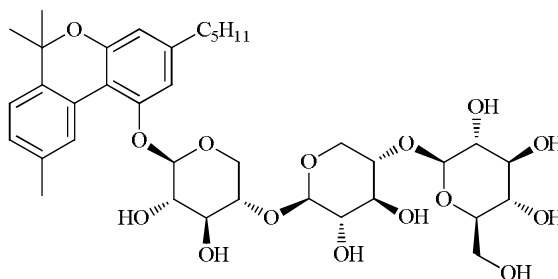
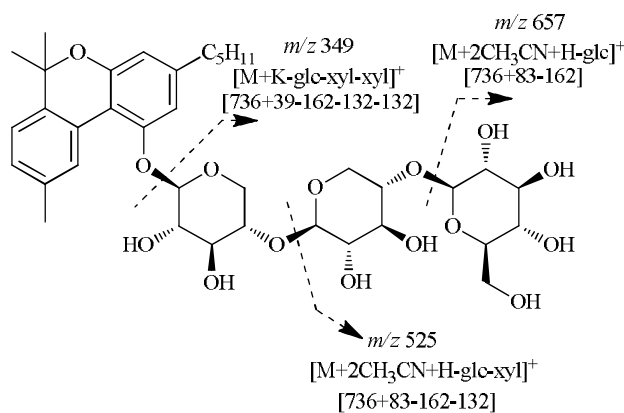


Fig. 3.11.8. Cannabinol-1-*O*-[β -D-glucopyranosyl-(1 \rightarrow 4)- β -D-xylopyranosyl-(1 \rightarrow 4)- β -D-xylopyranoside] (CA-EX4)



Scheme 3.8.4 Fragmentation Scheme of Cannabinol-1-*O*-[β -D-glucopyranosyl-(1 \rightarrow 4)- β -D-xylopyranosyl-(1 \rightarrow 4)- β -D-xylopyranoside]

3.12.4 Chromatographic profiling of Ca-AH

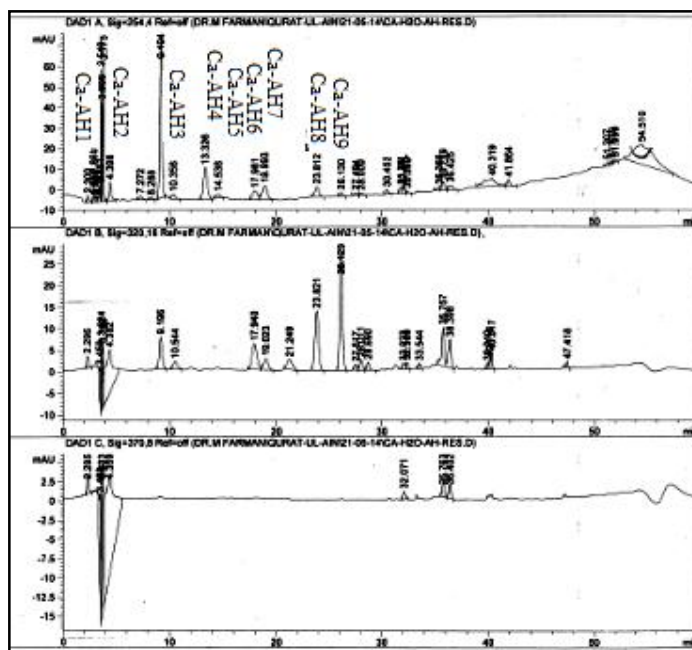


Fig. 3.12 Chromatographic Profiling of Compound with Code Ca-AH

Chromatographic profiling of compound with code Ca-AH was recorded online by DAD at wavelength 254nm, 320nm and 370nm as shown in **Fig. 3.12**. In a given mobile phase composition, there was a differential retention of sample components in such a way that hydrophilic compound were retained less in the stationary phase and eluted out first while the hydrophobic compounds were eluted out at the end. Profile obtained under 254nm manifested the ample compounds. In first few minutes abundant compounds with high peak intensity was eluted out. While from 10min. to onwards continuous elution of compounds were displayed. Similarly chromatographic profiling obtained under 320nm also revealed wealthy compounds. But very few of compounds were unveiled under wavelength 370nm.

3.12.4.1 Ca-AH1

Compound with code Ca-AH1 eluted at retention time 3.538 min. having mobile phase composition 10% acetonitrile in deionized water. The proportion of water in a mobile phase was directly related to the retention time of compound. For a given mobile phase composition, more hydrophilic compound was retained less in the

stationary phase and eluted out first. Lower the retention time indicated the presence of phenolic acids. DAD and ESI-MS spectrum was shown in **Fig. 3.12.1**.

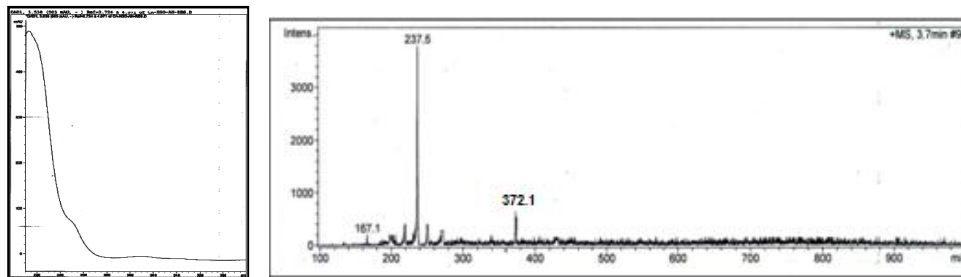


Fig. 3.12.1. DAD and ESI-MS Spectrum of Compound with Code Ca-AH1

DAD Spectrum

Single band pattern at 230 nm was observed under code Ca-AH1. Lower retention time as well as single band ruled out the presence of flavonoids. Band intensity, retention time and shape were found in agreement with phenolic acids. Single band pattern inferred the presence of symmetric phenolic acids (**Campos and Markham 2007**). Shape, intensity and λ_{max} inferred the presence of syringic acid. Standard DAD of syringic acid appeared at 260 nm. Hypsochromic shift towards shorter wavelength from 260nm to 230nm was due to glycosylation or methylation (**Markham 1982**).

ESI-MS Spectrum

Pseudomolecular ion peak appeared on mass spectrum at m/z 529 and molecular weight of compound calculated was 492 *amu* with positive ion mode. Pseudomolecular ion peak was justified with adduct as $[M+2H_2O+H]^+$. Fragment ion peak at m/z 372 was due to loss of terminal glucose *i.e.*, $[M+CH_3CN+H-glc]^+$. As a result of cleavage of terminal glucose and xylose, peak appeared at m/z 237 with potassium adduct as $[M+K-glc-xy]^+$ as shown in **Scheme 3.9.1**. Loss of terminal glucose and xylose with H adduct, peak appeared at m/z 199 as $[M+H-glc-xy]^+$. Keeping in view all the above information from fragmentation pattern, DAD spectrum and retention time, it was inferred that identified compound contained two sugar moieties *i.e.*, glucose and xylose along with aglycone part syringic acid.

So, the identified compound was 1-*O*-[β -D-glucopyranosyl-(1 \rightarrow 4)- β -D-xylopyranosyl]syringate as shown in **Fig. 3.12.2**.

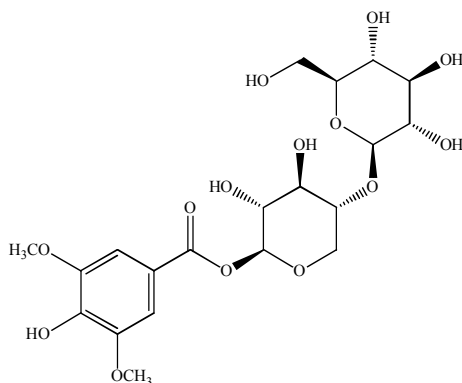
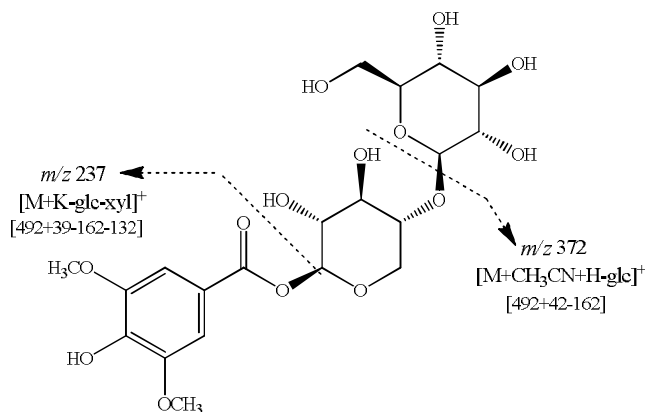


Fig. 3.12.2 1-*O*-[β -D-glucopyranosyl-(1 \rightarrow 4)- β -D-xylopyranosyl]syringate (Ca-AH1)

Suggested cleavages of identified compound were given below in **Scheme 3.9.1**.



Scheme 3.9.1 Fragmentation pattern of 1-*O*-[β -D-glucopyranosyl-(1 \rightarrow 4)- β -D-xylopyranosyl]syringate

3.12.4.2 Ca-AH2

Compound with code Ca-AH2 eluted at retention time 4.04 min. having mobile phase composition 10% acetonitrile in deionized water. For a given mobile phase composition, there was a differential retention of sample components according to their hydrophobicity in a manner such that more hydrophilic compounds retained less in the stationary phase and eluted out first. DAD and ESI-MS spectrum of compound with code Ca-AH2 was given in **Fig. 3.12.3**.

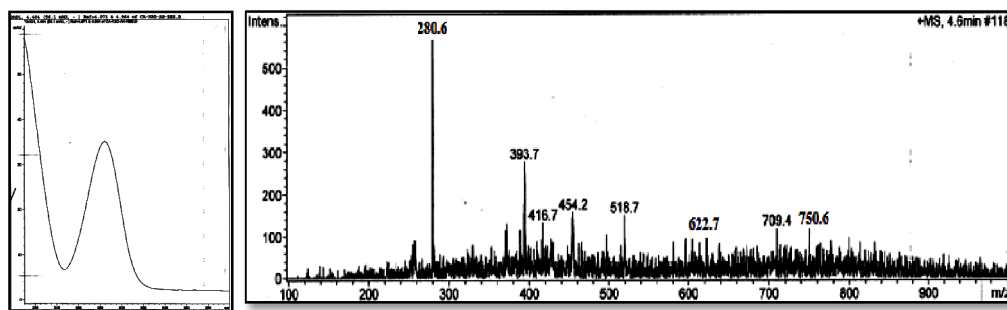


Fig. 3.12.3 DAD and ESI-MS Spectrum of Compound with code Ca-AH2

DAD Spectrum

Double band pattern was exhibited by compound with code Ca-AH2. UV spectrum was in the range of 195-400nm. This range corresponded to the Cannabinoids. Flavonoids also consisted of two band pattern, band I in the range 300-550nm and band II in range of 240-285nm. In given spectrum, there was no band above 300nm that inferred the absence of flavonoids. Band I appeared at 205nm, while band II at 280nm. Shape, intensity and λ_{\max} were found in agreement with Cannabinol. In original spectrum of CBN, band I appeared at 210nm, while band II at 290nm. This decrease of shift from 290nm to 280nm in band II and 210nm to 205nm in band I was due to glycosylation or methylation (**Markham 1982**). Alkyl side chain did not influence the UV absorbance. So, there was no difference of DAD having C₅ and C₄ side chain of CBN (**Hazekamp et. al., 2007**). Similarly, there was no influence of cyclization of non-phenolic part of the Cannabinoids on absorbance. In view of all this, compound identified from DAD spectrum was Cannabinol.

ESI-MS Spectrum

ESI-MS of compound with code Ca-AH2 obtained with a computerized data system showed a molecular ion peak at m/z 751 in positive ion mode. Calculated molecular weight of compound was 750 *amu*. Dominant fragment ion peak at m/z 623 corresponded to loss of terminal rhamnose as $[M+H_2O+H-rha]^+$. Loss of rhamnose along with ^{1,5}X_{xy1} corresponded to peak at m/z 519 *i.e.*, $[M+H_2O+H-rha-^{1,5}X_{xy1}]^+$. As a result of cleavage of terminal rhamnose and xylose along with 2H adduct peak appeared at m/z 473 as $[M+H-rha-xy1]^+$. Peak with significant intensity appeared at

m/z 393 as a result of loss of terminal rhamnose, xylose and glucose *i.e.*, $[M+2CH_3CN+H-rha-xyl-glc]^+$ as shown in **Scheme 3.9.2**. Base peak at m/z 281 was justified by the loss of alkyl chain of aglycone part. Loss of C_5H_{11} along with terminal rhamnose, xylose and glucose peak appeared at m/z 281 with significant intensity as $[M+CH_3CN+H-rha-xyl-glc-C_5H_{11}]^+$. So, pentyl alkyl chain was confirmed with aglycone part. Aglycone part was cannabinol justified with adduct $2CH_3CN+H$. From above fragmentations, three sugars were identified along with cannabinol having C_5 side chain.

By consolidating all the above information obtained from retention time, DAD and ESI-MS spectrum, it was inferred that given compound is Cannabinol-1-*O*-[α -L-rhamnopyranosyl-(1 \rightarrow 4)- β -D-xylopyranosyl-(1 \rightarrow 4)- β -D-glucopyranoside] as shown in **Fig. 3.12.4**.

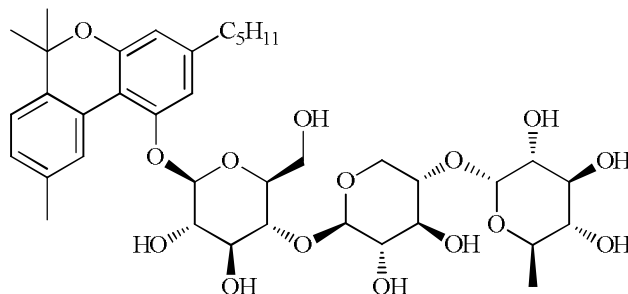
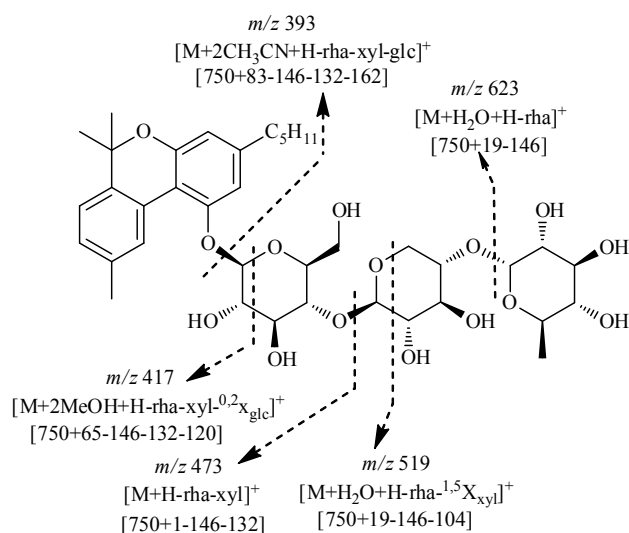


Fig. 3.12.4 Cannabinol-1-*O*-[α -L-rhamnopyranosyl-(1 \rightarrow 4)- β -D-xylopyranosyl-(1 \rightarrow 4)- β -D-glucopyranoside] (Ca-AH2)

Suggested cleavages of given compound was given below in **Scheme 3.9.2**.



Scheme 3.9.2 Fragmentation pattern of Cannabinol-1-*O*-[α -L-rhamnopyranosyl-(1 \rightarrow 4)- β -D-xylopyranosyl-(1 \rightarrow 4)- β -D-glucopyranoside]

3.12.4.3 Ca-AH3

Compound with code Ca-AH3 eluted at retention time 9.198 min. having mobile phase composition 10% acetonitrile in deionized water. Proportion of water in a mobile phase was directly proportional to the retention time of compound. Hydrophilic compound was retained less in the stationary phase and eluted out first. Retention time inferred the presence of Cannabinoid glycosides.

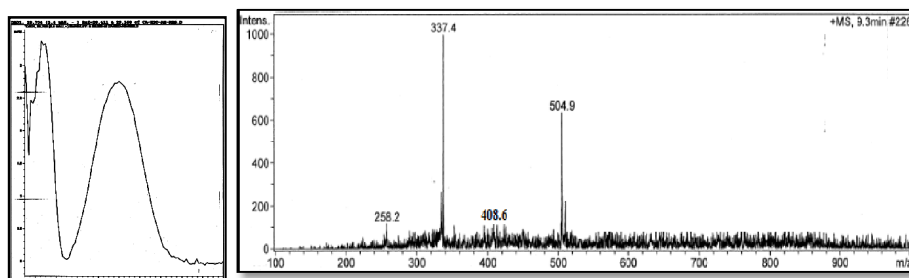


Fig. 3.12.5 DAD and ESI-MS Spectrum of compound with code Ca-AH3

DAD Spectrum

Two band patterns were observed by the compound under code Ca-AH3 as shown in **Fig. 3.12.5**. Flavonoids also exhibited two band pattern band I in the range 300-550nm while band II in the range of 240-285nm (**Markham 1982**). As there was no band above 300nm, that confirmed the absence of flavonoids. Band I appeared at 225nm, while band II at 268nm. Two band pattern was also observed by Cannabinoids in the range 195-400nm (**Hazekamp et. al., 2007**). Shape and intensity of spectrum showed resemblance with THC, CBD and CBC. But in spectrum of THC, there was just one band at 210nm with high intensity that ruled out the THC. Similarly, CBD also showed one band with high intensity at 210nm along with small shoulder. While two band pattern was observed by CBC band I appeared at 227nm while band II at 280nm. Hypsochromic shift from 227nm to 225nm in band I and from 280nm to 268nm in band II was due to glycosylation or methylation. Cyclization of non-phenolic part of the Cannabinoids did not influence the UV absorbance except when another conjugated double bond (CBC, CBCA) was introduced (**Hazekamp et. al., 2007**). So, CBC was confirmed from DAD spectrum.

ESI-MS Spectrum

ESI-MS spectrum of compound under code Ca-AH3 obtained with a computerized data system showed a molecular ion peak at m/z 505 in positive ion mode. Molecular weight calculated was 476 *amu*. Fragment ion peak at m/z 409 from m/z 505 manifested the loss of $^{0,3}X_{\text{glc}}$ along with adduct sodium as $[M+\text{Na}-^{0,3}X_{\text{glc}}]^+$. Base peak at m/z 337 inferred the cleavage of terminal glucose along with sodium adduct i.e., $[M+\text{Na}-\text{glc}]^+$ as given in **Scheme 3.9.3**. This is the high intensity peak that confirmed the presence of glucose.

Keeping in mind all the information obtained from retention time, DAD and ESI-MS spectrum, it was inferred that suggested compound is Cannabichromene-1- O - β -D-glucopyranoside as shown in **Fig. 3.12.6**.

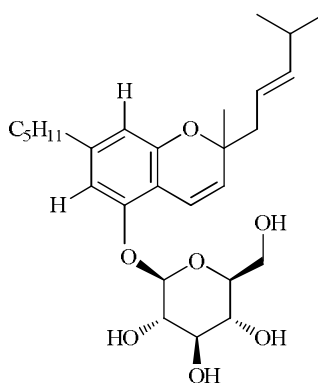
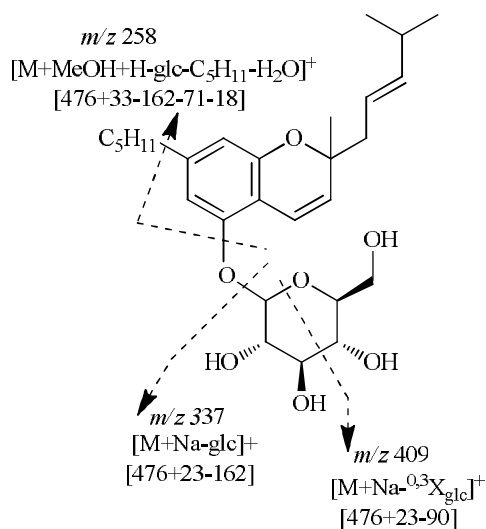


Fig. 3.12.6 Cannabichromene-1-*O*- β -D-glucopyranoside (Ca-AH3)

Suggested fragmentation given below was in accordance with proposed structure.



Scheme 3.9.3 Fragmentation scheme of Cannabichromene-1-*O*- β -D-glucopyranoside

3.12.4.4 Ca-AH4

Compound with code Ca-AH4 eluted at retention time 13.291 min. having mobile phase composition 10% acetonitrile in deionized water. Retention time of compound was directly related to the proportion of water in a mobile phase. This retention time inferred the presence of Cannabinoids glycosides. For a given mobile phase, hydrophilic compound was retained less in the stationary phase and eluted out first.

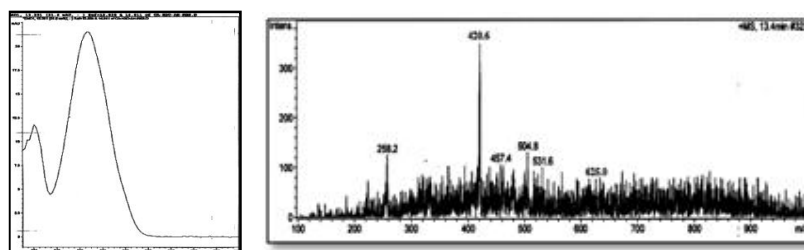


Fig. 3.12.7 DAD and ESI-MS Spectrum of Compound with Code Ca-AH4

DAD Spectrum

Two band patterns were displayed by compound with code Ca-AH4 as shown in **Fig. 3.10.7**. Band I appeared at 220nm having distorted peaks and band II appeared at 265nm with sharp bell shape peak. Flavonoids also exhibited two band pattern band I in the range 300-550nm while band II in the range of 240-285nm (**Markham 1982**). As there was no band above 300nm, that confirmed the absence of flavonoids. Cannabinoids appeared in the range of 195-400nm, also displayed two band pattern. This distorted type of peak was observed by THCA, THVA and CBDA Cannabinoids. Shape, intensity and λ_{\max} were found in agreement with THVA with decrease in wavelength from 270nm to 265nm due to glycosylation or metylation. Alkyl side chain of Cannabinoids also did not influence the UV absorbance (**Hazekamp et al., 2007**).

ESI-MS Spectrum

Pseudomolecular ion peak appeared on mass spectrum at m/z 625 with positive ion mode and molecular weight of compound calculated was 624 *amu*. Pseudomolecular ion peak was justified with adduct as $[M+H]^+$. Fragment ion peak at m/z 504 unveiled the loss of terminal glucose from m/z 625 as $[M+CH_3CN+H-glc]^+$. Loss of terminal glucose and $^{0,3}X_{xy1}$ with adduct H_2O+H , peak appeared at m/z 421 as $[M+H_2O+H-glc-^{0,3}X_{xy1}]^+$. Peak at m/z 421 also act as base peak. From above fragmentation, two sugars were identified *i.e.*, glucose and xylose.

Keeping in mind all the above information obtained from retention time, DAD and ESI-MS spectrum, it was revealed that identified compound is

Tetrahydrocannabivarinic acid-1-*O*-[β -D-glucopyranosyl-(1 \rightarrow 4)- β -D-xylopyranoside] as shown in **Fig. 3.12.8**.

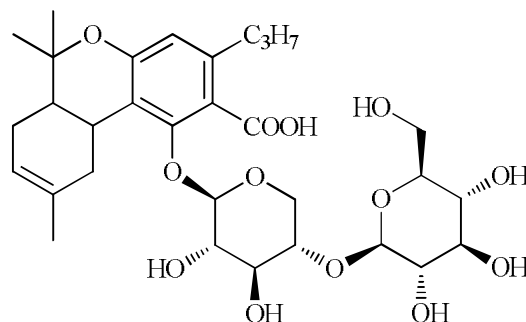
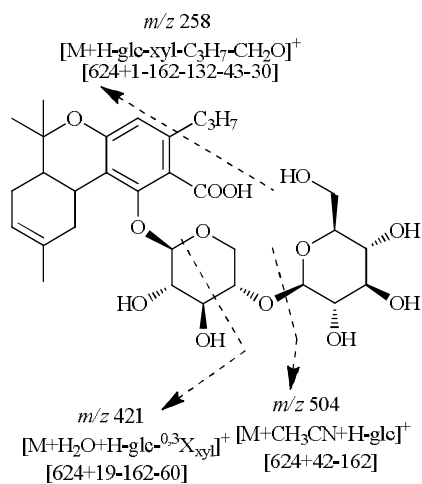


Fig. 3.12.8 Tetrahydrocannabivarinic acids-1-*O*-[β -D-glucopyranosyl-(1 \rightarrow 4)- β -D-xylopyranoside] (Ca-AH4)

Suggested cleavages of above compound are given below as given in **Scheme 3.9.4**.



Scheme 3.9.4 Fragmentation pattern of Tetrahydrocannabivarinic acid-1-*O*-[β -D-glucopyranosyl-(1 \rightarrow 4)- β -D-xylopyranoside]

3.12.4.5 Ca-AH5

Compound with code CA-AH7 eluted at retention time 14.544min. with mobile phase composition 10% acetonitrile in deionized water. Concentration of water in a mobile phase was directly proportional to retention time of compound. DAD and ESI-MS spectrum was given in **Fig. 3.12.9**.

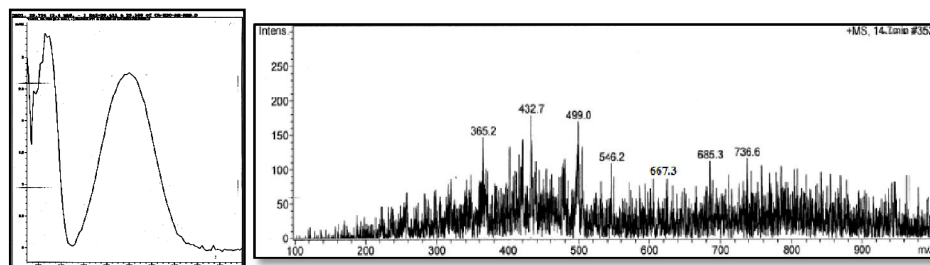


Fig. 3.12.9 DAD and ESI-MS Spectrum of Compound with Code Ca-AH5

DAD Spectrum

Two band pattern was exhibited by the compound with code CA-AH7, band I in the range 210nm while band II at 280nm. Two band patterns were also exhibited by the phenolic acids, but they appeared at lower retention time. Shape, intensity and λ_{max} resembled to Cannabinoids. Shift of band towards shorter wavelength in band II from 290nm to 280nm was due to glycosylation or methylation (**Markham 1982**). Alkyl side chain did not influence the UV absorbance of Cannabinoids. Cyclization of non-phenolic part of the Cannabinoids also did not influence the UV absorbance (**Hazekamp *et al.*, 2007**). This spectrum closely resembled to that of Cannabinol.

ESI-MS Spectrum

Compound with code CA-AH7 exhibited pseudomolecular ion peak at m/z 736 in positive ion mode. 734 *amu.* was the calculated molecular weight. Fragment ion peak at m/z 667 was due to the loss of terminal xylose with adduct as $[M+2\text{MeOH}+\text{H-xyl}]^+$. As a result of cleavage of rhamnose along with terminal xylose, peak appeared at m/z 498 as $[M+\text{CH}_3\text{CN}+\text{H-xyl-rha}]^+$. Peak at m/z 365 inferred the cleavage of second molecule of rhamnose along with rhamnose and xylose as $[M+3\text{H}_2\text{O}+\text{H-xyl-rha-rha}]^+$ as shown in **Scheme.3.9.5**. From above fragmentation pattern three sugars was identified, terminal xylose along with two rhamnose moiety. By keeping in view all the information obtained from retention time, DAD and ESI-MS spectrum, identified compound is Cannabinol-1-*O*- $[\beta\text{-D-xylopyranosyl-(1}\rightarrow\text{4)-}\alpha\text{-L-rhamnopyranosyl-(1}\rightarrow\text{4)-}\alpha\text{-L-rhamnopyranoside}]$ as given in **Fig. 3.12.10**.

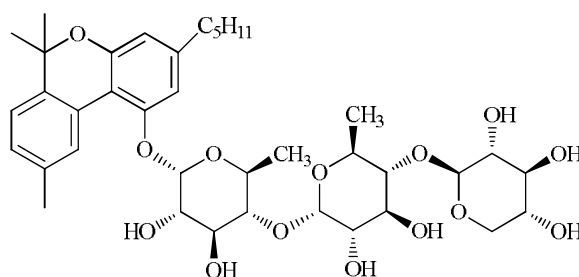
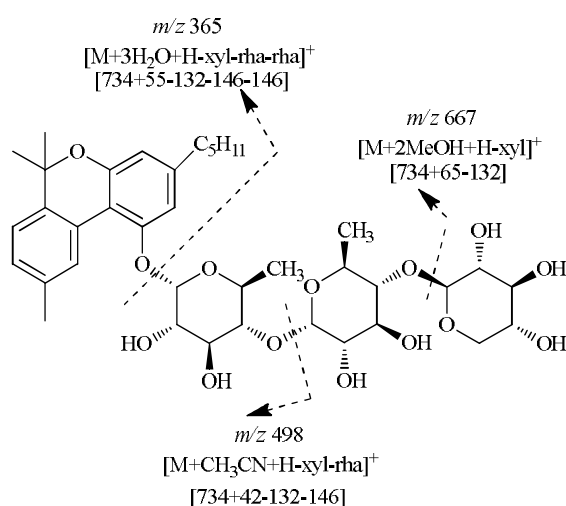


Fig. 3.12.10. Cannabinol-1-*O*-[β -D-xylopyranosyl-(1 \rightarrow 4)- α -L-rhamnopyranosyl-(1 \rightarrow 4)- α -L-rhamnopyranoside] (Ca-AH5)



Scheme.3.9.5 Fragmentation Scheme of Cannabinol-1-*O*-[β -D-xylopyranosyl-(1 \rightarrow 4)- α -L-rhamnopyranosyl-(1 \rightarrow 4)- α -L-rhamnopyranoside]

3.12.4.6 CA-AH6

Compound eluted at retention time 17.991min. having mobile phase composition 10% acetonitrile in deionized water. Concentration of water in a mobile phase was directly proportional to retention time of compound. DAD and ESI-MS spectrum was shown in **Fig. 3.12.11**.

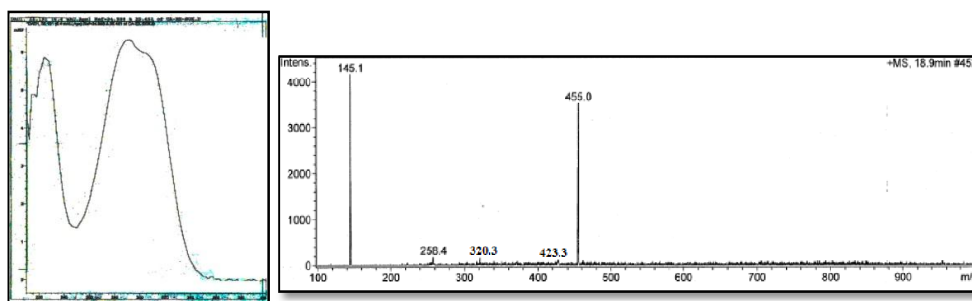


Fig. 3.12.11 DAD and ESI-MS Spectrum of Compound with Code CA-AH6

DAD Spectrum

Two band pattern was exhibited by the compound with code CA-AH6 with band I in the range 280-345nm while band II in range of 220nm-240nm. These band ranges was exhibited by flavones. Band II of the spectrum appeared as only one peak, if the flavones lack B ring substitution or possess a 4'-oxygenation B ring. By the introduction of additional B ring oxygenation produced a double band II (band IIa and band IIb) was observed. Spectrum was dominated by band II, that unveiled oxygenation was on A ring especially 5-hydroxyl position. Introducing the B ring oxygenation, enhanced the intensity of band I. Enhanced intensity of band I inferred the substitution at C-4'. Shape, intensity and λ_{max} resembled to that of luteolin. Hypsochromic shift of band I from 345-380nm to 280-345nm and band I from 254nm to 220-240nm displayed the glycosylation or methylation (**Markham 1982**). Shoulder at around 290nm was evident in spectrum of 3' and 5-O-luteolin. This shoulder disappeared in spectrum that manifested the presence of 7-O-glycosylated luteolin (**Campos and Markham 2007**). So, from above evidences it was inferred that given compound is 7-O-glycosylated luteolin.

ESI-MS Spectrum

Pseudomolecular ion peak appeared on mass spectrum at m/z 455 in positive ion mode. 432 *amu.* was the calculated molecular weight. Pseudomolecular ion peak justified as $[M+Na]^+$ was also the base peak that inferred these compounds were easily fragmented by LC-DAD-ESI-MS. Base peak was justified by the adduct as $[M+Na]^+$. Fragment ion peak at m/z 319 manifested the loss of terminal rhamnose *i.e.*, $[M+MeOH+H-rha]^+$. As a result of cleavage of $^{0,3}X_{\text{rha}}$ along with loss of water, peak

appeared at m/z 423 as $[M+2CH_3CN+H-^{0.3}X_{rha}-H_2O]^+$ as given in **Scheme.3.9.6**. By keeping in mind all the information obtained from retention time, DAD and ESI-MS spectrum, identified compound is Luteolin-7-*O*- α -L-rhamnopyranoside as shown in **Fig. 3.12.12**.

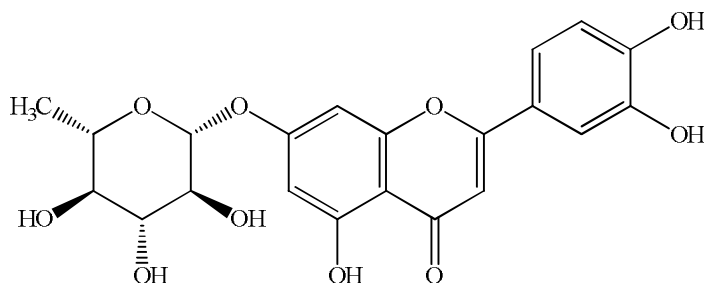
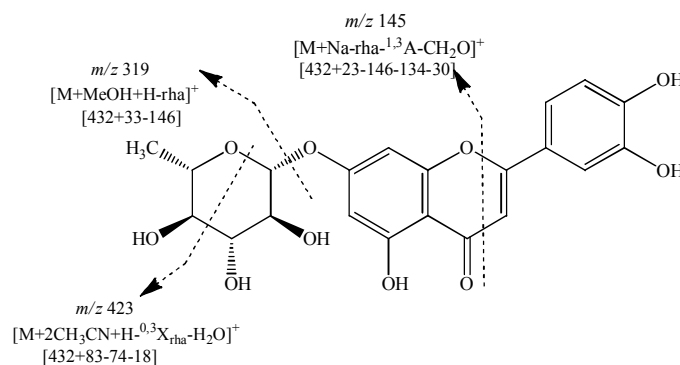


Fig. 3.12.12. Luteolin-7-*O*- α -L-rhamnopyranoside (CA-AH6)



Scheme.3.9.6 Fragmentation Scheme of Luteolin-7-*O*-rhamnopyranoside

3.12.4.7 Ca-AH7

Compound with code Ca-AH7 eluted at retention time 18.924 min having mobile phase composition 40% acetonitrile in deionized water. Proportion of water in a mobile phase was directly proportional to the retention time of compound. Low retention time indicated the presence of acidic Cannabinoids. In a given mobile phase, hydrophilic compound was retained less in the stationary phase and eluted out first.

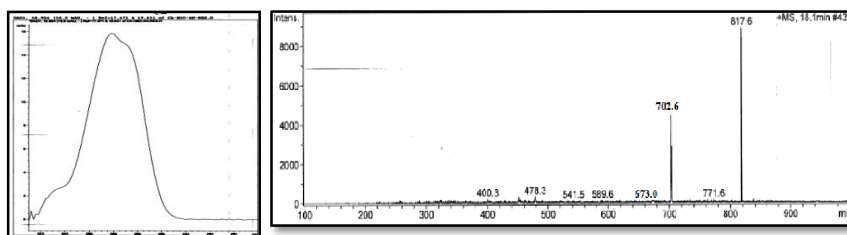


Fig. 3.12.13 DAD and ESI-MS Spectrum of compound with Code (Ca-AH7)

DAD Spectrum

DAD spectrum of given compound manifested one band pattern as given in **Fig. 3.12.13**. One band pattern was also observed by phenolic acids and Cannabinoids. Phenolic acid appeared at lower retention time, so these acids were ruled out. Flavonoids were also absent, as they showed two band pattern. Shape and intensity of given spectrum resembled to Cannabinoids. Band I appeared at 250 nm. Shape of spectrum matched with Cannabichromenic acid. In original spectrum of CBCA band appeared at 253 nm. Shift of band towards shorter wavelength was due to glycosylation or methylation. Acidic Cannabinoids were easily detected by LC-DAD-ESI-MS, while these are decarboxylated in GC-MS. Cyclization of non-phenolic part of Cannabinoids also did not influenced the UV absorbance except when another conjugated double bond (CBC or CBCA) was introduced (**Hazekamp et. al., 2007**).

ESI-MS Spectrum

Pseudomolecular ion peak appeared on mass spectrum appeared at m/z 817 in positive ion mode. Calculated molecular weight of compound was 798 *amu*. Pseudomolecular molecular ion peak was also the base peak and justified as $[M+H_2O+H]^+$. Fragment ion peak at m/z 703 inferred the loss of xylose moiety *i.e.*, $[M+2H_2O+H-xyl]^+$. Peak at m/z 541 manifested the loss of xylose along with glucose *i.e.*, $[M+2H_2O+H-xyl-glc]^+$. Fragment ion peak at m/z 400 inferred the cleavage of xylose, glucose and rhamnose as $[M+CH_3CN+H-xyl-glc-rha]^+$ as given in **Scheme 3.9.7**. By keeping in mind all the information obtained from retention time, DAD and ESI-MS spectrum, identified compound is Cannabichromenic acid-1-*O*-[β -D-xylopyranosyl-(1 \rightarrow 4)- β -D-glucopyranosyl-(1 \rightarrow 4)- α -L-rhamnopyranoside] as shown in **Fig. 3.12.14**.

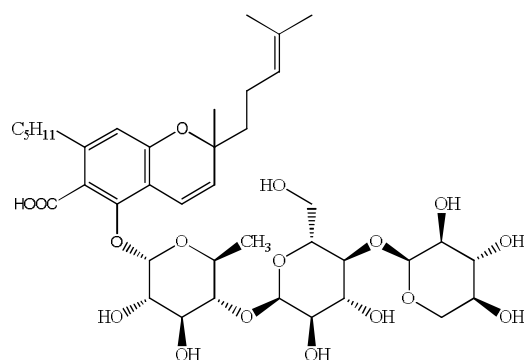
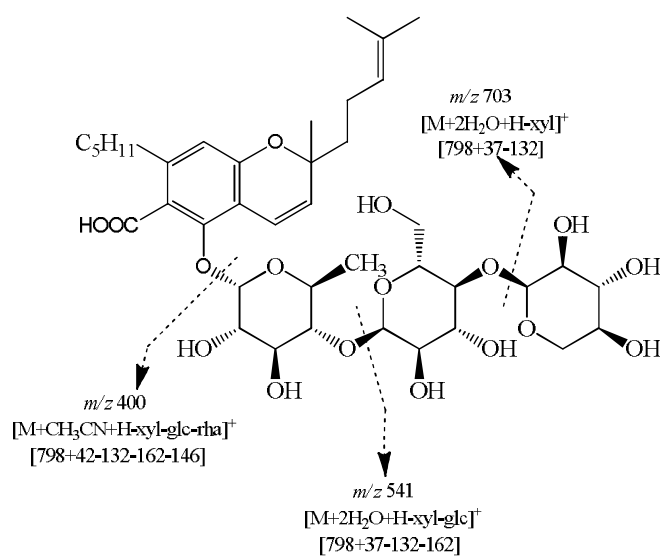


Fig. 3.12.14 Cannabichromenic acid-1-*O*- β -D[xylopyranosyl(1 \rightarrow 4)glucopyranosyl(1 \rightarrow 4)rhamnopyranoside] (Ca-AH7)



Scheme 3.9.7 Fragmentation Scheme of Cannabichromenic acid-1-*O*-[β -D-xylopyranosyl-(1 \rightarrow 4)- β -D-glucopyranosyl-(1 \rightarrow 4)- α -L-rhamnopyranoside]

3.12.4.8 CA-AH8

Compound with code CA-AH8 eluted at retention time 23.838 min. having mobile phase composition 10% acetonitrile in deionized water. Water concentration in a mobile phase was directly proportional to retention time of compound. DAD and ESI-MS Spectrum of compound were given in **Fig. 3.12.15**.

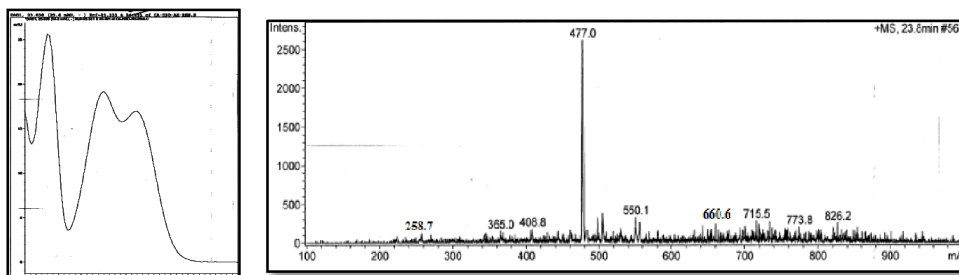


Fig. 3.12.15 DAD and ESI-MS Spectrum of Compound with Code CA-AH8

DAD Spectrum

Two band was observed by compound with code CA-AH8, band I at 230nm while band II at 260nm with decreasing intensity. Lower retention time ruled out the presence of phenolic acids. Shape, intensity and λ_{max} resembled to Tetrahydrocannabinolic acid as well as with Tetrahydrocannabivarinic acid (Cannabinoids). Acidic Cannabinoids were not identified by GC, but they were easily detected by LC-MS. Alkyl side chain did not affect the UV absorbance of Cannabinoids (**Hazekamp *et al.*, 2007**). So, by focusing on DAD spectrum these two acidic Cannabinoids were not distinguished. Shift of band II towards shorter wavelength was due to glycosylation or methylation (**Markham 1982**).

ESI-MS Spectrum

Pseudomolecular ion peak appeared on mass spectrum at m/z 826 in positive ion mode and calculated molecular weight was 784 *amu*. Pseudomolecular ion peak appeared with adduct as $[M+CH_3CN+H]^+$. Fragment ion peak at m/z 661 was due to the cleavage of terminal rhamnose *i.e.*, $[M+Na-rha$. As a result of cleavage of glucose along with terminal rhamnose, peak appeared at m/z 477 as $[M+H-rha-glc]^+$. Loss of xylose along with glucose and terminal rhamnose peak appeared at m/z 409 as $[M+2MeOH+H-rha-glc-xyl]^+$. Peak at m/z 258 unveiled the presence of alkyl chain of aglycone part that inferred the loss of butyl chain, rhamnose, glucose, xylose with the removal of CH_2O as $[M+H-C_4H_9-rha-glc-xyl-CH_2O]^+$ as given in **Scheme 3.9.8**. So, from above fragmentation identified aglycone is Tetrahydrocannabinolic acid with butyl chain. (THCA-C4).

With the view of this content, identified compound is Tetrahydrocannabinolic acid (C4)-1-*O*-[α -L-rhamnopyranosyl-(1 \rightarrow 4)- β -D-glucopyranosyl-(1 \rightarrow 4)- β -D-xylopyranoside] as shown in **Fig. 3.12.16**.

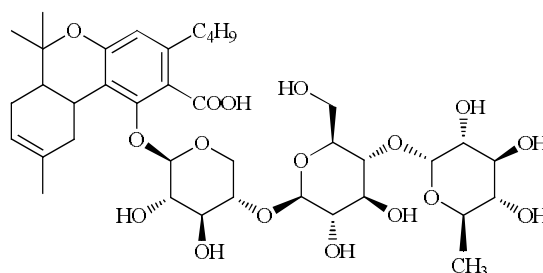
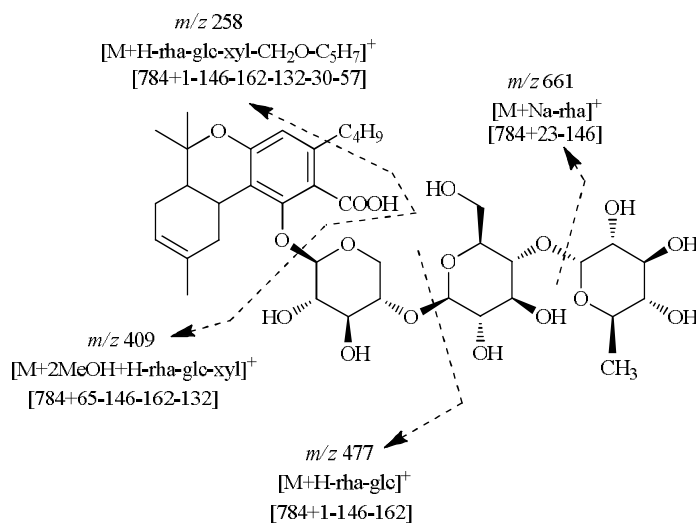


Fig. 3.12.16 Tetrahydrocannabinolic acid (C4)-1-*O*-[α -L-rhamnopyranosyl-(1 \rightarrow 4)- β -D-glucopyranosyl-(1 \rightarrow 4)- β -D-xylopyranoside] (CA-AH8)



Scheme 3.9.8 Fragmentation Scheme of Tetrahydrocannabinolic acid (C4)-1-*O*-[α -L-rhamnopyranosyl-(1 \rightarrow 4)- β -D-glucopyranosyl-(1 \rightarrow 4)- β -D-xylopyranoside]

3.12.4.9 CA-AH9

Compound eluted at retention time 26.124 min. having mobile phase composition 10% acetonitrile in deionized water. DAD and ESI-MS spectrum of compound was given in **Fig. 3.12.17**.

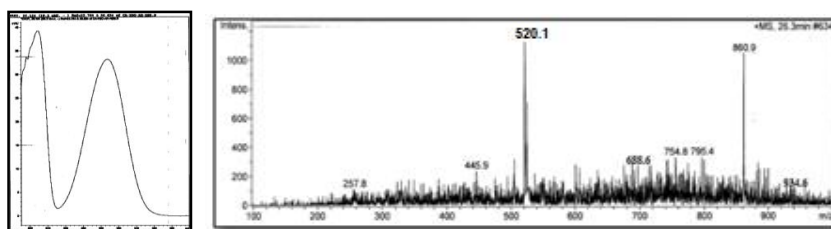


Fig. 3.12.17 DAD and ESI-MS Spectrum of Compound with Code CA-AH9

DAD Spectrum

Two band pattern was exhibited by the compound with code CA-AH9, band I in the region 265nm-350nm while band II in the region 240-220nm. Band II was further split up into two bands band IIa and band IIb. While band IIa appeared only as shoulder on the band IIb. Decrease in intensity of band I relative to band II, resembled flavonols. Double band II was exhibited by the quercetin, with the band IIa appeared only as a shoulder on band IIb. Hypsochromic shift in band I and II along with the increase in the intensity of band I was exhibited by the 3-*O*-glycosylated quercetin. Hypsochromic shift in both bands also manifested the presence of permethylation of quercetin (Campos and Markham 2007). Methylation at the 4' hydroxyl group of quercetin produced no obvious effect on the spectrum of quercetin. By keeping in mind all the above information, identified compound is 3-*O*-glycosylated quercetin-4'-methylether.

ESI-MS Spectrum

Pseudomolecular ion peak appeared on mass spectrum at m/z 935 in positive ion mode. Calculated molecular weight was 902 *amu*. Pseudomolecular ion peak justified with adduct *i.e.*, $[M+MeOH+H]^+$. Base peak at m/z 861 inferred the cleavage of $^{0,3}X_{rha}$ as $[M+MeOH+H-^{0,3}X_{rha}]^+$. Fragment ion peak at m/z 795 manifested the cleavage of rhamnose as $[M+K-rha]^+$. As a result of cleavage of rhamnose, xylose along with terminal rhamnose, peak displayed at m/z 520 *i.e.*, $[M+CH_3CN+H-rha-xyl-rha]^+$. Peak at m/z 349 inferred the loss of glucose, rhamnose, xylose along with terminal rhamnose as $[M+MeOH+H-rha-xyl-rha-glc]^+$ as given in Scheme 3.9.9. So, from above cleavages four sugars were identified.

By keeping in mind all the information obtained from retention time, DAD and ESI-MS spectrum, identified compound is Quercetin-4'-methylether-3-O-[α -L-rhamnopyranosyl-(1 \rightarrow 4)- β -D-xylopyranosyl-(1 \rightarrow 4)- α -L-rhamnopyranosyl-(1 \rightarrow 4)- β -D-glucopyranoside] as given in **Fig. 3.12.18**.

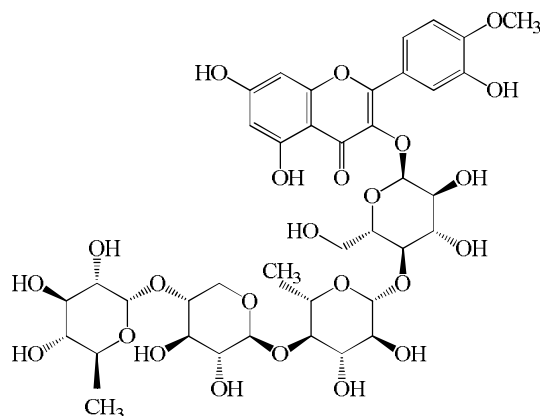
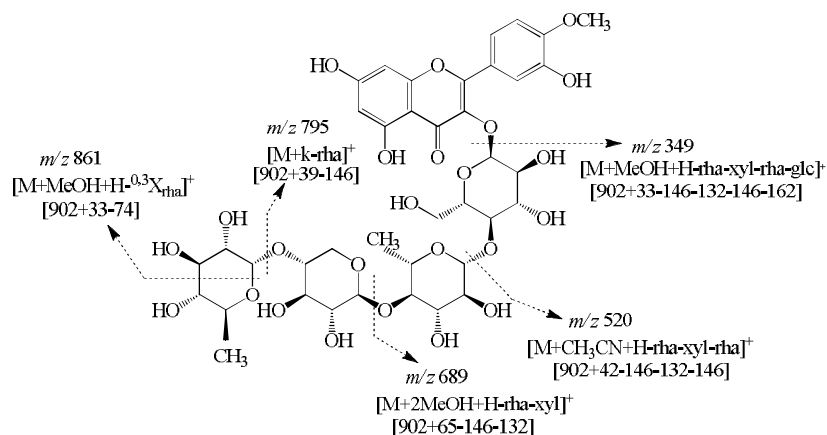


Fig. 3.12.18 Quercetin-4'-methylether-3-O-[α -L-rhamnopyranosyl-(1 \rightarrow 4)- β -D-xylopyranosyl-(1 \rightarrow 4)- α -L-rhamnopyranosyl-(1 \rightarrow 4)- β -D-glucopyranoside] (CA-AH9)



Scheme 3.9.9 Fragmentation Scheme of Quercetin-4'-methylether-3-O-[α -L-rhamnopyranosyl-(1 \rightarrow 4)- β -D-xylopyranosyl-(1 \rightarrow 4)- α -L-rhamnopyranosyl-(1 \rightarrow 4)- β -D-glucopyranoside]

3.13 HPLC-DAD-ESI-MS Analysis of Cannabinoids

3.13.1 C-1

Compound with code C-1 eluted at retention time 46 min. having mobile phase composition of 80% Acetonitrile in deionized water. Retention time of compound was directly related to the proportion of water in a mobile phase. Higher retention time displayed the presence of cannabinoid glycosides. DAD and ESI-MS spectrum was shown in **Fig. 3.17**.

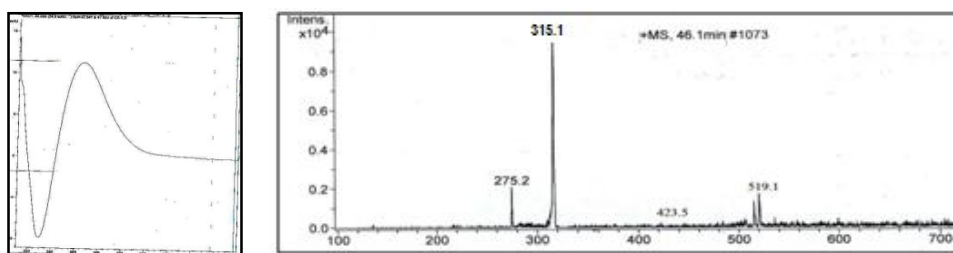


Fig. 3.17 DAD and ESI-MS spectrum of compound with code C-1

DAD Spectrum

Compound with code C-1 displayed two band pattern, band I appeared at 210nm while band II appeared at 275nm. Shape, intensity and λ_{\max} resembled to that of Cannabinoids. Two band patterns were also displayed by phenolic acids. But phenolic acids were appeared at lower retention time. DAD spectrum of compound with code C-1 was also not resembled with flavonoids. Flavonoids also exhibited two band pattern band I in the range of 300-550 nm while band II appeared at 240-285nm **Markham K. R. (1982)**. Retention time, shape and intensity of compound resembled with Cannabicyclol (CBC).

ESI-MS Spectrum

Pseudomolecular ion peak appeared on mass spectrum at m/z 519 in positive ion mode and molecular weight of the compound calculated was 476. Fragment ion peak at m/z 315 manifested the loss of glucose unit with adduct *i.e.*, $[M+H-\text{glc}]^+$. Peak at m/z 316 was also the base peak. Peak at m/z 423 was due to the loss of fragment $^{0,3}\text{X}_{\text{glc}}$ with $2\text{H}_2\text{O}+\text{H}$ adduct as $[M+2\text{H}_2\text{O}+\text{H}-^{0,3}\text{X}_{\text{glc}}]^+$. This fragment also confirmed

the presence of glucose moiety. As a result of cleavage of glucose along with C₅H₁₁, peak appeared at m/z 276 as $[M+MeOH+H-glc-C_5H_{11}]^+$ confirmed the presence of pentyl chain with Cannabicyclol. By consolidating all the information obtained from retention time, DAD spectrum and ESI-MS fragmentation, the identified compound is Cannabichromene-1-*O*- β -D-glucopyranoside as shown in **Fig. 3.17.1**.

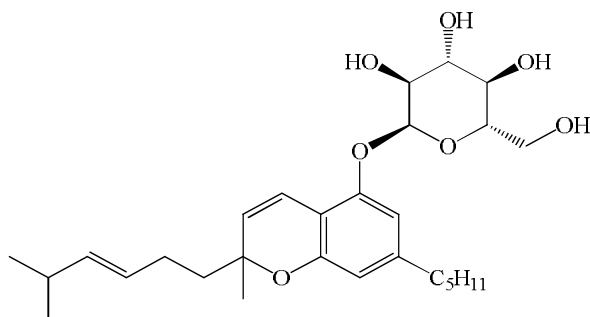
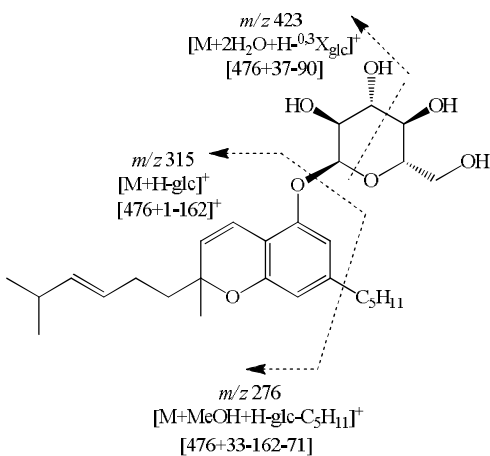


Fig. 3.17.1 Cannabichromene-1-*O*- β -D-glucopyranoside (C-1)



Scheme 3.10.1 Fragmentation Scheme of Cannabichromene-1-*O*- β -D-glucopyranoside

3.13.2 C-2

Compound with code C-2 eluted at retention time 45.706 min. having mobile phase composition 80% acetonitrile in deionized water. Higher elution time manifested the presence of cannabinoid glycosides.

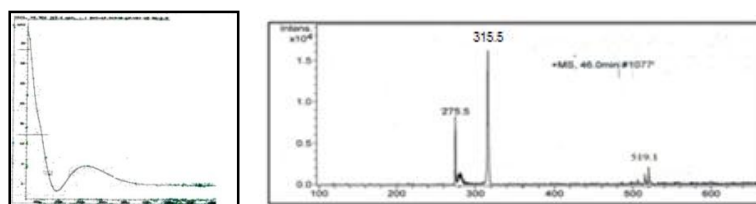


Fig. 3.18 DAD and ESI-MS Spectrum of Compound with code (C-2)

DAD Spectrum

Compound with code C-2 also displayed two band patterns. Higher retention time ruled out the presence of phenolic acids. Two band pattern was also observed by the flavonoids. Band I in the range 300-550 nm while band II in the range 240-285 nm. As there was no band above 300nm that indicated the absence of flavonoids. Shape, intensity and λ_{\max} resembled to that of tetrahydrocannabinol. Band I appeared in the range 210 nm while band II in the range 250nm. Shift of band I from 220nm (original spectrum) to 210 nm and band II from 260nm to 250nm was due to methylation or glycosylation (**Markham 1998**).

ESI-MS Spectrum

Pseudomolecular ion peak appeared on mass spectrum at m/z 519 in positive ion mode and molecular weight of the compound calculated was 476. Fragment ion peak at m/z 315 manifested the loss of glucose unit with adduct *i.e.*, $[M+H-glc]^+$. Peak at m/z 315 was also the base peak. As a result of cleavage of glucose along with C_5H_{11} , peak appeared at m/z 276 confirmed the presence of pentyl chain with the Tetrahydrocannabinol. Compound with code C-2 was only differing from their DAD spectrum, ESI-MS spectrum and the retention time of both compounds was similar. It was reported in literature that retention time of Cannabinoids were quite similar. So, from DAD spectrum results compound with code-2 was Tetrahydrocannabinol. Compound with code C-2 was different from C-1 by DAD spectrum, while retention time and ESI-MS spectrum of both compounds were almost similar. Keeping in view all the information obtained from retention time, DAD spectrum and ESI-MS fragmentation, the identified compound is Tetrahydrocannabinol-1-*O*- β -D-glucopyranoside as shown in **Fig. 3.18.1**.

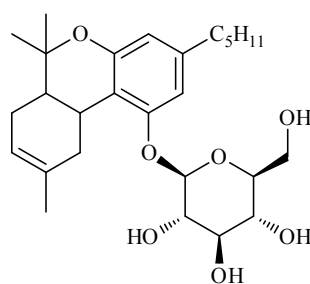
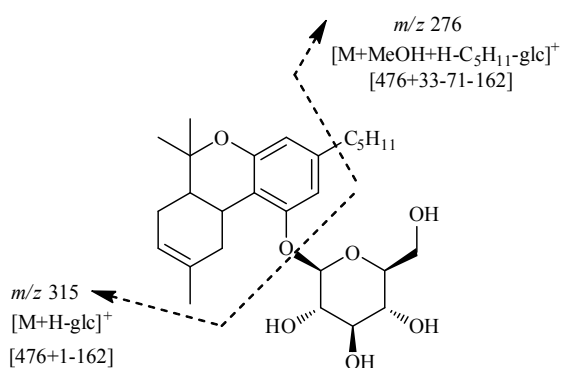


Fig. 3.18.1 Tetrahydrocannabinol-1-*O*- β -D-glucopyranoside (C-2)



Scheme 3.10.2 Fragmentation Scheme of Tetrahydrocannabinol-1-*O*- β -D-glucopyranoside

3.13.3 C-3

Compound with code C-3 eluted at retention time 55.6 min. with mobile phase composition 80% acetonitrile in deionized water. Retention time of compound was directly related to the concentration of water in a mobile phase composition. Compound eluted at higher retention time inferred the presence of cannabinoid glycosides.

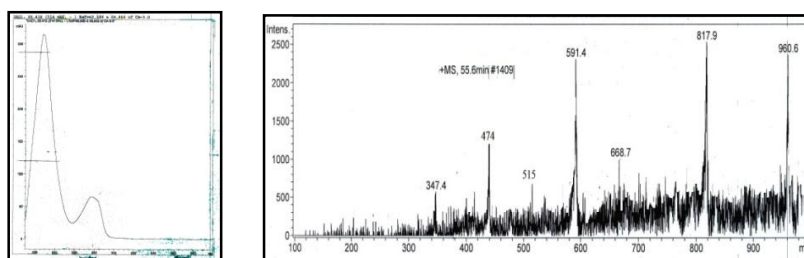


Fig. 3.19 DAD and ESI-MS Spectrum of compound with code (C-3)

DAD Spectrum

Two band pattern was exhibited by the compound with code C-3. Band I appeared at 225nm while band II appeared at 290nm. Phenolic acids also displayed two band patterns like Cannabinoids, but they usually eluted at lower retention time. Flavonoids also exhibited two band pattern, band I in the range 300-550nm while band II in the range 240-285nm. As there was no clear band above 300nm that unveiled the absence of flavonoids. Shape, intensity and λ_{\max} resembled to that of cannabinol (CBN). Hypsochromic shift from 290nm to 275nm in band II was due to glycosylation or methylation (Markham 1998).

ESI-MS Spectrum

Pseudomolecular ion peak exhibited by mass spectrum at m/z 961 in positive ion mode. Molecular weight calculated was 942 *amu*. Pseudomolecular ion peak was justified by adduct as $[M+H_2O+H]^+$. Base peak at m/z 817 was due to the loss of terminal glucose with adduct $2H_2O+H$ *i.e.*, $[M+2H_2O+H-glc]^+$. Fragment ion peak at m/z 667 inferred the loss of terminal glucose along with rhamnose with adduct $MeOH+H$ as $[M+MeOH+H-glc-rha]^+$. As a result of cleavage of terminal glucose, rhamnose and $^{0,3}X_{glc}$ with adduct $2MeOH+H$ *i.e.*, $[M+2MeOH+H-glc-rha-^{0,3}X_{glc}-H_2O]^+$ peak appeared at m/z 591. Loss of terminal glucose, rhamnose and again glucose, peak appeared at m/z 514 *i.e.*, $[M+CH_3CN+H-glc-rha-glc]$. As a result of terminal cleavage of glucose, rhamnose, glucose and another glucose moiety, peak appeared at m/z 347 with adduct $2H_2O+H$ *i.e.*, $[M+2H_2O+H-glc-rha-glc-glc]^+$. By consolidating all the information obtained from retention time, DAD spectrum and ESI-MS fragmentation, identified compound is Cannabinol-1-*O*-[β -D-glucopyranosyl-(1 \rightarrow 4)- α -L-rhamnopyranosyl-(1 \rightarrow 4)- β -D-glucopyranosyl-(1 \rightarrow 4)- β -D-glucopyranoside].

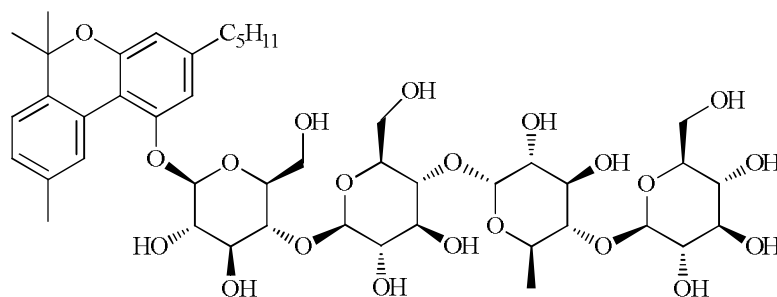
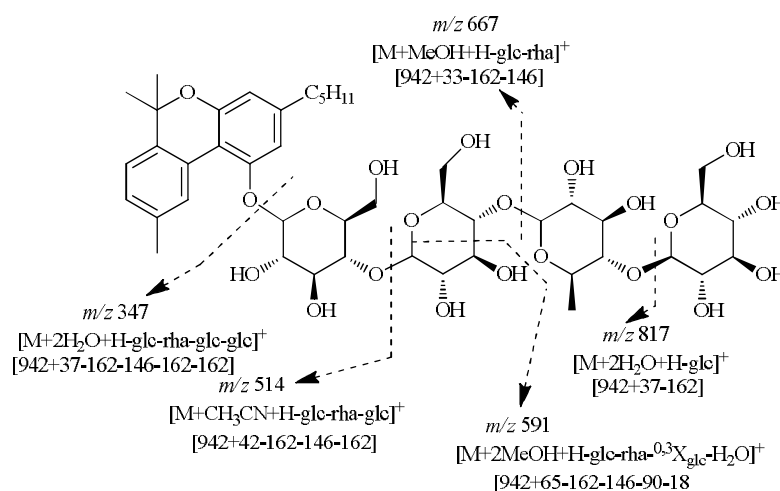


Fig. 3.19.1 Cannabinol-1-*O*-[β -D-glucopyranosyl-(1 \rightarrow 4)- α -L-rhamnopyranosyl-(1 \rightarrow 4)- β -D-glucopyranosyl-(1 \rightarrow 4)- β -D-glucopyranoside] (C-3)



Scheme 3.10.3 Fragmentation Scheme of Cannabinol-1-*O*-[β -D-glucopyranosyl-(1 \rightarrow 4)- α -L-rhamnopyranosyl-(1 \rightarrow 4)- β -D-glucopyranosyl-(1 \rightarrow 4)- β -D-glucopyranoside]

3.13.4 C-4

Compound with code C-4 eluted at retention time 54.9 min. having mobile phase composition 80% acetonitrile in deionized water. Concentration of water in a mobile phase was directly proportional to retention time of compound. Higher retention time inferred the presence of cannabinoid glycosides.

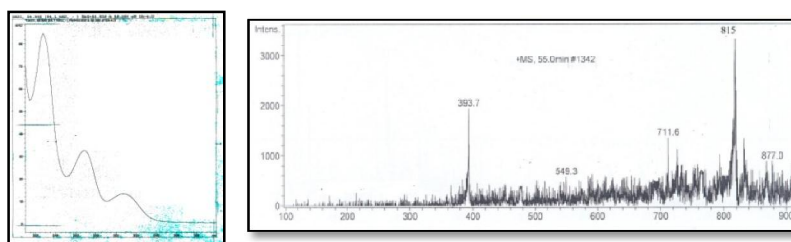


Fig. 3.20 DAD and ESI-MS Spectrum of Compound with code (C-4)

DAD Spectrum

Two band patterns with shoulder were exhibited by compound with code C-4. Such DAD spectrum was not exhibited by phenolic acids and even flavonoids. Shape, intensity and λ_{\max} of this compound matched with Cannabinoids i.e., cannabidiolic acid, cannabinolic acid and cannabigerolic acid. The Cyclization of the non-phenolic part of the Cannabinoids did not influence the absorbance, so DAD spectrum resembled with CBDA, CBNA and CBGA (Hazekamp *et al.*, 2007). From DAD spectrum, CBDA, CBNA and CBGA were not distinguished.

ESI-MS Spectrum

Pseudomolecular ion peak at m/z 877 appeared on mass spectrum with positive ion mode and molecular weight of compound calculated was 840 *amu*. Pseudomolecular ion peak was justified with adduct as $[M+2H_2O+H]^+$. Base peak at m/z 815 manifested the loss of fragment $^{0,3}X_{\text{glc}}$ with adduct $2CH_3CN+H$ along with water loss. Fragment ion peak at m/z 711 betrayed the loss of terminal glucose along with adduct $MeOH+H$ as $[M+MeOH+H-glc]^+$. As a result of loss of terminal glucose along with another glucose moiety, peak appeared at m/z 549 i.e., $[M+MeOH+H-glc-glc]^+$. Cleavage of terminal glucose along with two another glucose moiety loss, peak appeared at m/z 393 i.e., $[M+K-glc-glc-glc]^+$. Aglycone part was cannabinolic acid (CBNA), justified with adduct K. Therefore from ESI-MS fragmentation pattern, identified aglycone part was CBNA. Keeping in mind all the information obtained from above fragmentation, identified compound is Cannabinolic acid-1-*O*- β -D-[glucopyranosyl(1 \rightarrow 4)glucopyranosyl(1 \rightarrow 4)glucopyranoside].

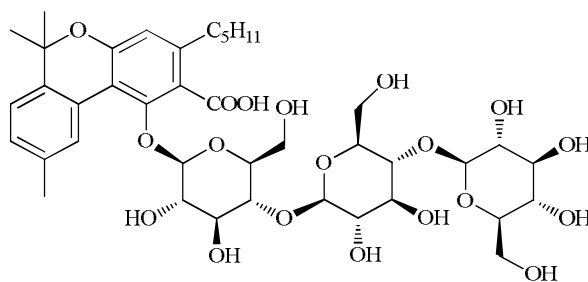
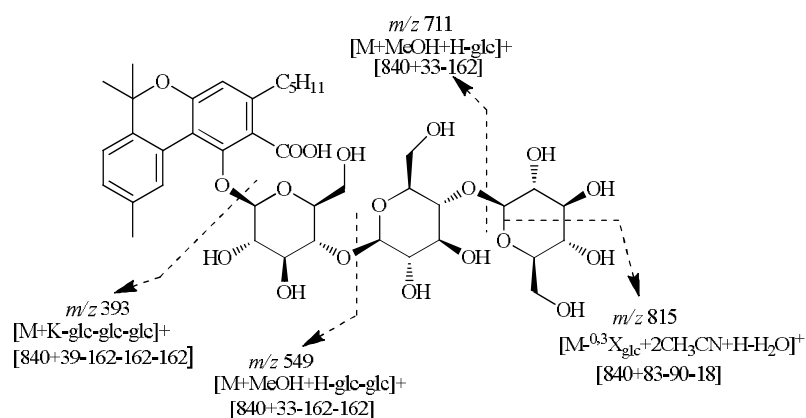


Fig. 3.20.1 Cannabinolic acid-1-*O*- β -
D[glucopyranosyl(1 \rightarrow 4)glucopyranosyl(1 \rightarrow 4)glucopyranoside] (C-4)



Scheme 3.10.4 Fragmentation Scheme of Cannabinolic acid-1-*O*- β -
D[glucopyranosyl(1 \rightarrow 4)glucopyranosyl(1 \rightarrow 4)glucopyranoside]

3.13.5 C-5

Compound with code C-5 eluted at retention time 53.45 min. having mobile phase composition 80% acetonitrile in deionized water. Retention time of compound was directly proportional to the water concentration in a mobile phase. Higher retention time corresponded to the cannabinoid glycosides.

DAD Spectrum

Compound with code C-5 exhibited one band pattern that resembled to Cannabinoids. Band I appeared at 220nm. Shape, intensity and λ_{max} resembled to that of THC, CBD and CBG. The cyclization of non-phenolic part of the Cannabinoids did not influence the UV absorbance except when another aromatic ring or conjugated

double bond was introduced (Hazekamp *et al.*, 2007). Therefore from DAD spectrum THC, CBD and CBG was not distinguished.

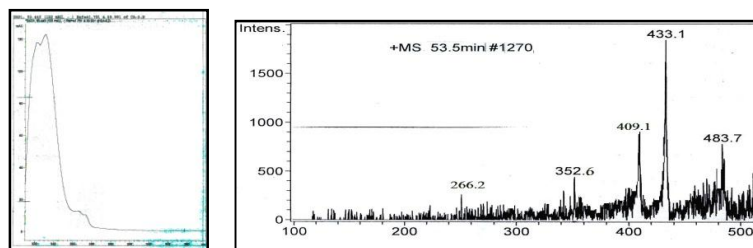


Fig. 3.21 DAD and ESI-MS spectrum of Compound with code (C-5)

ESI-MS Spectrum

Pseudomolecular ion peak appeared at m/z 483 in positive ion mode. Molecular weight of compound calculated was 460 *amu*. Base peak at m/z 433 inferred the cleavage of $^{0,3}X_{\text{rha}}$ with adduct $2\text{CH}_3\text{CN}+\text{H}$ *i.e.*, $[\text{M}+2\text{CH}_3\text{CN}+\text{H}-^{0,3}X_{\text{rha}}-2\text{H}_2\text{O}]^+$. Fragment ion peak at m/z 353 manifested the cleavage of terminal rhamnose with adduct K *i.e.*, $[\text{M}+\text{K}-\text{rha}]^+$. As a result of loss of terminal rhamnose along with C_5H_{11} , peak appeared at m/z 266 as $[\text{M}+\text{Na}-\text{rha}-\text{C}_5\text{H}_{11}]^+$. Aglycone part was justified by adduct K. Aglycone may be CBD and THC, but THC eluted at higher retention time. So, aglycone was THC. By keeping in consideration all the information obtained from retention time, DAD spectrum and ESI-MS fragmentation, identified compound is THC-1-*O*- α -L-rhamnopyranoside

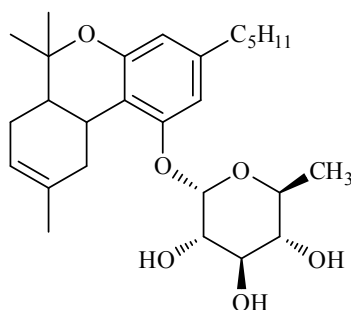
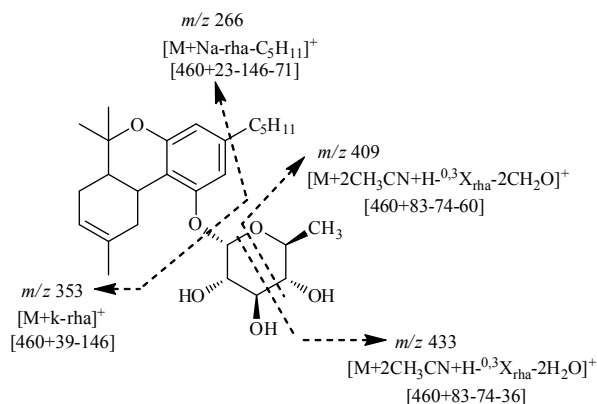


Fig. 3.21 Tetrahydrocannabinol-1-*O*- α -L-rhamnopyranoside (C-5)



Scheme 3.10.5 Fragmentation Scheme of Cannabigerol-1-O- α -L-rhamnopyranoside

3.13.6 C-6

Compound with code C-6 eluted at retention time 55.5 min. having mobile phase composition 80% acetonitrile in deionized water. Higher retention time inferred the presence of cannabinoid glycosides. Retention time of compound was directly proportional to the water concentration in a mobile phase.

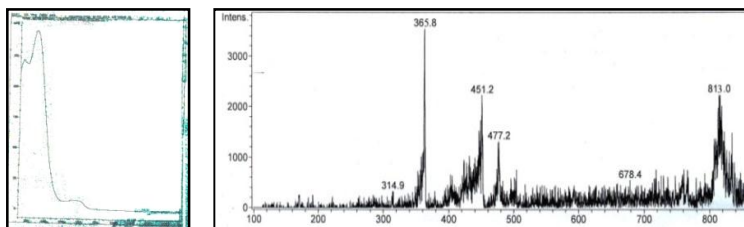


Fig. 3.22 DAD and ESI-MS Spectrum of Compound with code (C-6)

DAD Spectrum

One band pattern was exhibited by the compound with code C-6. One band was also exhibited by phenolic acids, but these acids were eluted out at lower retention time. Shape, intensity and λ_{max} resembled to that of Cannabinoids. Band I appeared at 222nm that resembled to that of THC, CBD and CBG. From DAD spectrum, these three Cannabinoids were not identified. The cyclization of non-phenolic part of Cannabinoids did not influence the UV absorbance. But THC eluted at higher retention time followed by CBD and CBG in Cannabinoids (**Hazekamp *et al.*, 2007**).

ESI-MS Spectrum

Pseudomolecular ion peak appeared at m/z 813 with positive ion mode and molecular weight of compound calculated was 770 *amu*. Fragment ion peak at m/z 677 manifested the cleavage of xylose with K adduct *i.e.*, $[M+K-xyl]^+$. Cleavage of terminal xylose along with glucose moiety, peak appeared at m/z 477 as $[M+H-xyl-glc]^+$. Loss of xylose, glucose along with $^{0,3}X_{glc}$, peak appeared at m/z 451. Base peak at m/z 315 manifested the cleavage of terminal xylose glucose and glucose. Peak at m/z 365 inferred the loss of xylose, glucose and $^{1,5}X_{glc}$. Aglycone part was THC justified with adduct proton. So from above fragmentation one xylose and two glucose moiety were identified. Keeping in mind all the information obtained from retention time, DAD spectrum and ESI-MS fragmentation identified compound is Tetrahydrocannabinol-1-*O*- β -D-[xylopyranosyl(1 \rightarrow 4)glucopyranosyl(1 \rightarrow 4)glucopyranoside) as shown in **Fig. 3.22.1**.

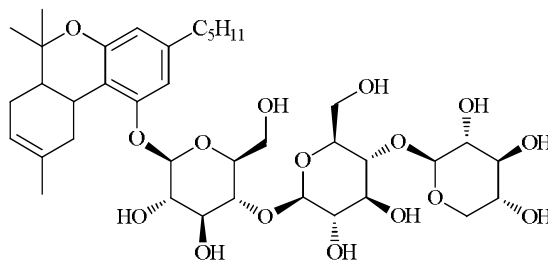
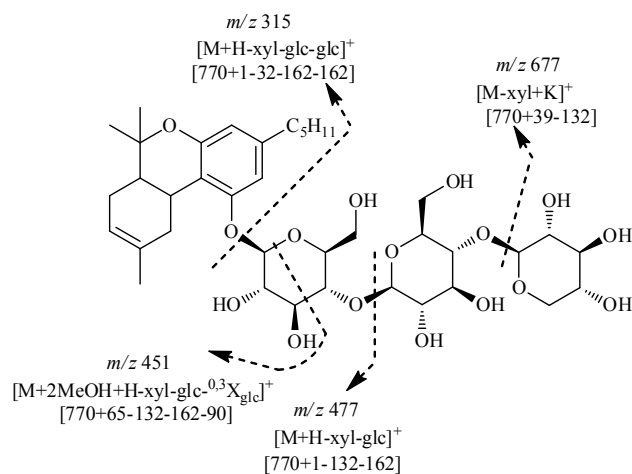


Fig. 3.22.1 Tetrahydrocannabinol-1-*O*- β -D[xylopyranosyl(1 \rightarrow 4)glucopyranosyl(1 \rightarrow 4)glucopyranoside) (C-6)



Scheme 3.10.6 Fragmentation Scheme of Tetrahydrocannabinol-1-*O*- β -D[xylopyranosyl(1 \rightarrow 4)glucopyranosyl(1 \rightarrow 4)glucopyranoside)

3.13.7 C-7

Compound with code C-7 eluted at retention time 55.5min. having mobile phase composition 80% acetonitrile in deionized water. Higher retention time inferred the presence of cannabinoid glycosides.

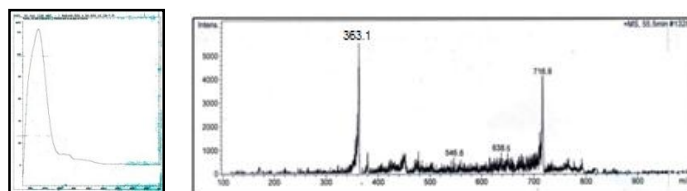


Fig. 3.23 DAD and ESI-MS Spectrum of Compound with code (C-7)

DAD Spectrum

One band pattern was exhibited by the compound with code C-7. One band was also exhibited by phenolic acids, but these acids were eluted out at lower retention time. Shape, intensity and λ_{max} resembled to that of Cannabinoids. Band I appeared at 222nm that resembled to that of THC, CBD and CBG. From DAD spectrum, these three Cannabinoids were not identified. The cyclization of non-phenolic part of Cannabinoids did not influence the UV absorbance. But THC eluted

at higher retention time followed by CBD and CBG in Cannabinoids (**Hazekamp *et al.*, 2007**).

ESI-MS Spectrum

Pseudomolecular ion peak appeared on mass spectrum at m/z 818 in positive ion mode and molecular weight calculated was 784 *amu*. Fragment ion peak at m/z 639 inferred the loss of terminal rhamnose with adduct H as $[M+H-rha]^+$. As a result of cleavage of terminal rhamnose and second molecule of rhamnose, peak appeared at m/z 547 *i.e.*, $[M+3H_2O+H-rha-rha]^+$. Base peak at m/z 363 manifested the cleavage of terminal rhamnose, second molecule of rhamnose and glucose with adduct $[M+MeOH+H-rha-rha-glc]^+$. Keeping in mind all the information obtained from retention time, DAD spectrum and ESI-MS spectrum identified compound is Tetrahydrocannabinol-1-*O*-[α -L-rhamnopyranosyl-(1 \rightarrow 4)- α -L-rhamnopyranosyl-(1 \rightarrow 4)- β -D-glucopyranoside].

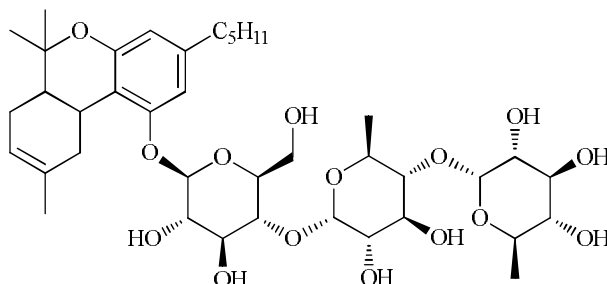
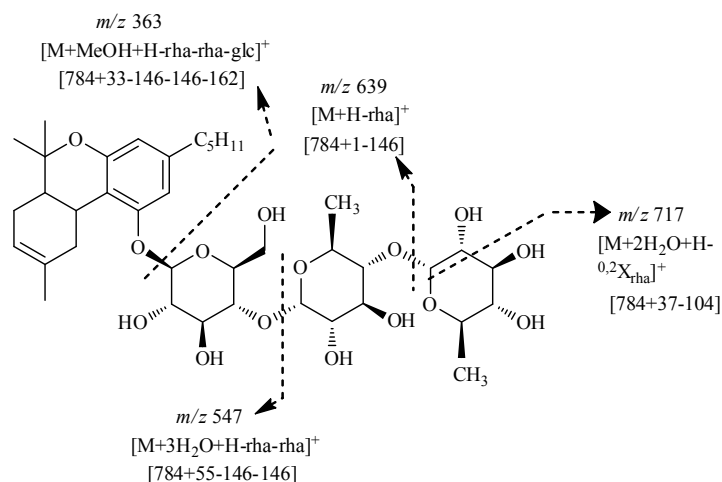


Fig. 3.23.1 Tetrahydrocannabinol-1-*O*-[α -L-rhamnopyranosyl-(1 \rightarrow 4)- α -L-rhamnopyranosyl-(1 \rightarrow 4)- β -D-glucopyranoside] (C-7)



Scheme 3.10.7 Fragmentation Scheme of Tetrahydrocannabinol-1-*O*-[α -L-rhamnopyranosyl-(1 \rightarrow 4)- α -L-rhamnopyranosyl-(1 \rightarrow 4)- β -D-glucopyranoside]

3.13.8 C-8

Compound with code C-8 did not contain any Cannabinoids that was determined from their DAD and ESI-MS spectrum.

3.13.9 C-9

Compound with code C-9 eluted at retention time 55.6 min. having mobile phase composition 80% Acetonitrile in deionized water. Higher retention time inferred the presence of cannabinoid glycosides.

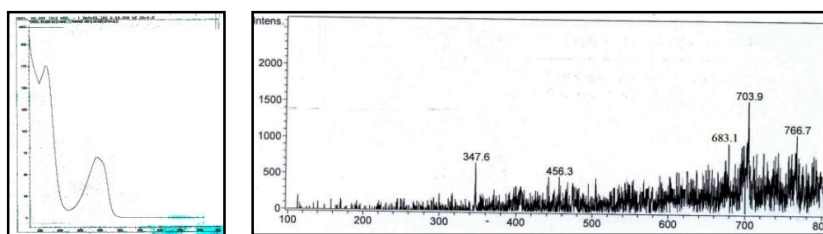


Fig. 3.24 DAD and ESI-MS Spectrum of compound with code (C-9)

DAD Spectrum

Two band pattern was exhibited by compound with code C-9. Phenolic acids also exhibited the two band pattern, but they usually eluted at lower retention time.

Flavonoids also exhibited two band pattern, band I in the range 300-550nm, band II at 240-285nm. But in this spectrum, there was no band above 300nm that unveiled the absence of flavonoids. Band I of compound with code C-9 appeared at 220nm, while band II at 278nm. Shape, intensity and λ_{\max} of this compound resembled to that of Cannabinol. Hypsochromic shift of band from 290nm (original spectrum) to 278nm was due to glycosylation or methylation.

ESI-MS Spectrum

Pseudomolecular ion peak exhibited by mass spectrum at m/z 766 in positive ion mode and molecular weight of compound calculated was 764 *amu*. Fragment ion peak at m/z 683 was due to the cleavage of terminal rhamnose with adduct $[M+2\text{MeOH}+\text{H-rha}]^+$. As a result of cleavage of terminal rhamnose along with glucose, peak appeared at m/z 457 with proton adduct. Cleavage of terminal rhamnose, glucose and rhamnose, peak appeared at m/z 347 *i.e.*, $[M+2\text{H}_2\text{O}+\text{H-rha-glc-rha}]^+$. From all above fragmentation pattern, three sugars were identified two rhamnose and one glucose. By keeping in mind all the information obtained from retention time, DAD and ESI-MS fragmentation, the identified compound is Cannabinol-1-*O*-[α -L-rhamnopyranosyl-(1 \rightarrow 4)- β -D-glucopyranosyl-(1 \rightarrow 4)- α -L-rhamnopyranoside]

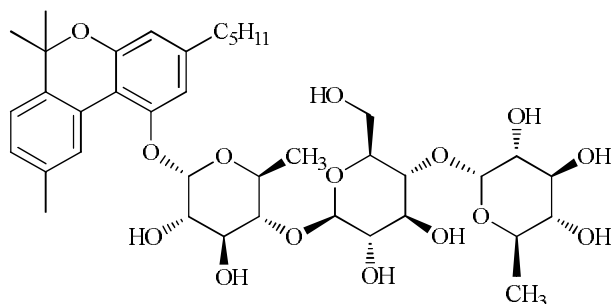
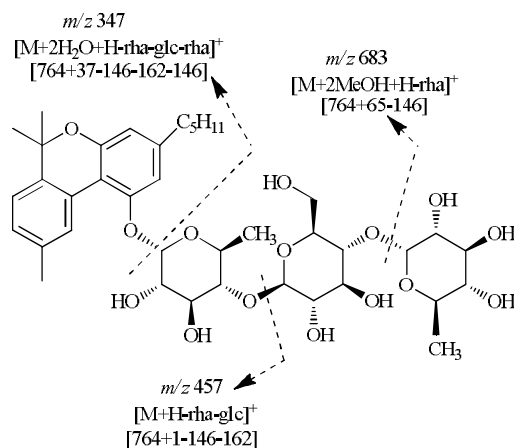


Fig. 3.24.1 Cannabinol-1-*O*-[α -L-rhamnopyranosyl-(1 \rightarrow 4)- β -D-glucopyranosyl-(1 \rightarrow 4)- α -L-rhamnopyranoside] (C-9)



Scheme 3.10.8 Cannabinol-1-*O*-[α -L-rhamnopyranosyl-(1 \rightarrow 4)- β -D-glucopyranosyl-(1 \rightarrow 4)- α -L-rhamnopyranoside]

CODE	Retention time	Identified compound
C-1	44.520	Cannabichromene-1- <i>O</i> - β -D-glucopyranoside
C-2	45.706	Tetrahydrocannabinol-1- <i>O</i> - β -D-glucopyranoside
C-3	55.6	Cannabinol-1- <i>O</i> -[β -D-glucopyranosyl-(1 \rightarrow 4)- α -L-rhamnopyranosyl-(1 \rightarrow 4)- β -D-glucopyranosyl-(1 \rightarrow 4)- β -D-glucopyranoside]
C-4	54.9	Cannabinolic acid-1- <i>O</i> -[β -D-glucopyranosyl-(1 \rightarrow 4)- β -D-glucopyranosyl-(1 \rightarrow 4)- β -D-glucopyranoside]
C-5	53.45	Tetrahydrocannabinol-1- <i>O</i> - β -D-rhamnopyranoside
C-6	55.9	Tetrahydrocannabinol-1- <i>O</i> -[β -D-xylopyranosyl-(1 \rightarrow 4)- β -D-glucopyranosyl-(1 \rightarrow 4)- β -D-glucopyranoside]
C-7	55.5	Tetrahydrocannabinol-1- <i>O</i> -[α -L-rhamnopyranosyl-(1 \rightarrow 4)- α -L-rhamnopyranosyl-(1 \rightarrow 4)- β -D-glucopyranoside]
C-9	55.6	Cannabinol-1- <i>O</i> -[α -L-rhamnopyranosyl-(1 \rightarrow 4)- β -D-glucopyranosyl-(1 \rightarrow 4)- α -L-rhamnopyranoside]

Table 3.7 List of Isolated Cannabinoids

3.14 Column Chromatographic Results

To isolate the colored compounds from aqueous layer of acid hydrolysis of *C. sativa* roots, column chromatography was performed by using analytical grade cellulose and water as a mobile phase. No separation of colored band was observed in the column under shorter and longer wavelength of UV light. Just one band appeared in the column that inferred that separation was not perfect with cellulose as stationary phase and water as mobile phase. By using cellulose as stationary phase and eluent as water, flow rate was very slow. By changing the stationary phase from cellulose to silica gel, flow rate was improved 5ml/min. Two bands were observed under shorter wavelength (254nm).

3.14.1 Cannabinoids Isolation Results

Sample loaded on analytical grade TLC plate and eluted with solvent *n*-hexane:diethyl ether (1:1), *n*-hexane:ethylacetate (9:1), MeOH:CHCl₃. Then observe the TLC in ordinary light. Following bands were observed as shown in Fig.

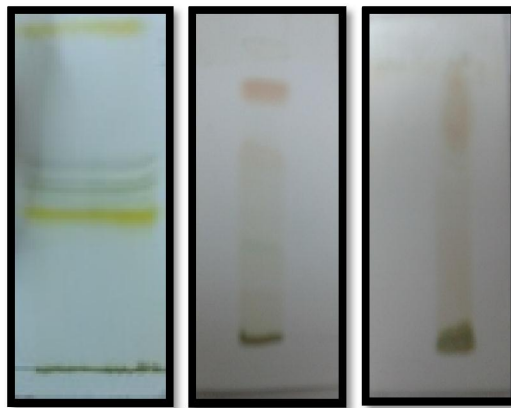


Fig. 3.13 TLC Plates Using three Different Solvents

(a) *n*-Hexane : Diethylether (1:1) (b) *n*-Hexane : Ethylacetate (9:1) (c) MeOH : CHCl₃ (9:1)

TLC in solvent *n*-Hexane : Diethylether (1:1) exhibited the beautiful bands of different colors. About 6-7 bands were appeared in this solvent system under ordinary light. While second solvent system *n*-Hexane : Ethylacetate (9:1) did not exhibited perfect bands as observed in first solvent system. Just one pink color was cleared at

the top of TLC, that inferred the imperfect separation. While the third solvent system showed poor separation having no clear band was observed. So, *n*-Hexane : Diethylether (1:1) was selected as superb solvent system for the separation of cannabinoids. Beautiful colored streaks were observed under ordinary light as shown in **Fig. 3.13**.

Preparative thin layer chromatography was performed for the isolation of Cannabinoids by using *n*-hexane and diethyl ether (1:1) as mobile phase on self made silica gel plates. After elution with binary solvents, separated bands were observed on the chromatographic plates displaying different florescent under ordinary light as well as under shorter wavelength (254nm).

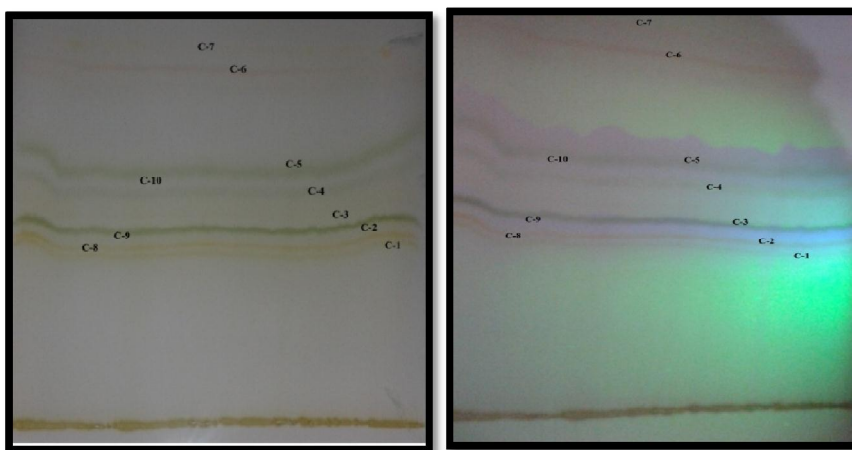


Fig. 3.14 Preparative TLC on Silica Gel Plates

(a) Viewed under visible light (b) Viewed under shorter UV wavelength (254nm)

Ten different colored bands were observed, coded as C-1 for light yellow color band considered as first band, C-2 displayed thick dark colored yellow band, C-3 exhibited thick dark green band, C-4 showed light green band with medium thickness, above C-4 band was band with maximum thickness having dark green color with code C-5, band with code C-6 appeared light pink in color, band at top of TLC appeared with code C-7 with dark yellow color. These all colors were observed with ordinary light. When band was observed under shorter UV wavelength (254nm), three new bands were observed. Band with code C-8, appeared between C-1 and C-2 displayed light blue color. Band with code C-9, observed

between C-2 and C-3 exhibited dark blue color. While the band coded as C-10 expressed the dark purple color as shown in **Fig. 3.14**.




After the identification of bands, these are scrapped off the plate with spatula or with a tubular scrapper connected to a vacuum collector. But scrapper connected with vacuum collector was not very useful because the purified product was in direct contact with the stream of air and risk of autoxidation. These scrapped products were then eluted out with *n*-hexane solvent and then stored in glass collecting vials with codes C-1, C-2, C-3, C-4, C-5, C-6, C-7, C-8, C-9 and C-10 as shown in **Fig. 3.15**.



Fig. 3.15 Products obtained after PTLC

3.14.2 Results of Duquenois Levine reagents

Duquenois reagent was used to identify the Cannabinoids. By the addition of Duquenois Levine reagent, Cannabinoids appeared blue color. Results were shown in **Table 3.7**.

Codes	Colors	Duquenois Levine reagents	
C-1	Light pink color	Negative	
C-2	Pink color	Negative	
C-3	Green color	Negative	








C-4	Light blue color	Negative	
C-5	Light blue	Positive	
C-6	Bluish violet color	Positive	
C-7	Light pink	Negative	
C-8	Light blue	Positive	
C-9	Light yellow	Negative	
C-10	Light blue	Positive	

Table 3.8 Detection of Cannabinoids by Duquenois Levine reagent

Duquenois Levine reagent reacted with Δ^9 -THC, CBN and CBD to produced a violet to purple colour. C-1, C-2, C-3, C-4, C-7, C-9 gave negative results with Duquenois Levine reagent. While C-5, C-6, C-8 and C-10 displayed positive results with the formation of violet to purple color as shown in **Fig. 3.16**. These colors unveiled the presence of Cannabinoids especially tetrahydrocannabinol, cannabinol and Cannabidiol. Intensity of colors displayed by these samples was also dependent

on the concentration of samples. If sample was diluted, intensity of color displayed by reagent was low. Sample with code 6 displayed intense color, that manifested the presence of concentrated Cannabinoids.



Fig. 3.16 Results of Duquenois Levine Reagent Test

3.15 Conclusions

A growing interest in *Cannabis* as a source of medicinal compounds has emerged during the last few years. Several crude preparations or synthetic drugs derived from *Cannabis* are under development or in the clinical pipeline for distribution on the market. The roots of *Cannabis* were scientifically overlooked. Although the stem, leaves, flowers and seeds have received an overwhelming amount of attention, almost nothing was so far published on the phytochemical constituents of roots. The present study was used to unveil these hidden phytochemical constituents of *C. sativa* roots.

According to results obtained, the preliminary research on extraction methodologies unveiled the presence of volatile compounds *i.e.*, Cannabinoids, Esters, Benzene derivatives, Steroids, Bicyclic compounds and Hydrocarbons.

Acid and alkaline hydrolytic cleavages followed by co-chromatography aided in the identification of three sugars *i.e.*, glucose, rhamnose and xylose and five phenolic acids *i.e.*, Salicylic acid, Syringic acid, *p*-Hydroxybenzoic acid, 2,5-Dihydroxybenzoic acid and Gallic acid, which strengthened the subsequent task of identifying the compound with GC-MS and LC-DAD-ESI-MS.

A generally straightforward and propelled technique was used for the preparative isolation of Cannabinoids. *n*-Hexane and Diethyl-ether was used as eluent for this method. THC, CBN and CBD were detected by using Duquenois Levine

reagent. Nine Cannabinoid glycosides were first time isolated by using this method. Isolated Cannabinoids were then identified by using LC-DAD-ESI-MS.

LC coupled with DAD-ESI-MS in positive ion mode successfully furnished concrete evidences for the identification of 25 Cannabinoids and flavonoid glycosides. Ethanolic extract revealed the presence of three phenolic acids (*p*-Hydroxy benzoic acid, Syringic acid and Gallic acid) and four Cannabinoid glycosides. While one important flavonoid glycoside *i.e.*, Luteolin-4-*O*-[β -D-xylopyranosyl-(1 \rightarrow 4)- β -D-rhamnopyranoside] and two important Cannabinoid glycosides *i.e.*, $\Delta^{(8)}$ -Tetrahydrocannabinol-1-*O*-[β -D-xylopyranosyl-(1 \rightarrow 4)- β -D-glucopyranosyl-(1 \rightarrow 4)- β -D-glucopyranosyl-(1 \rightarrow 4)- β -D-rhamnopyranoside] and Tetrahydrocannabivarinic acid -C4-1-*O*-[β -D-glucopyranosyl-(1 \rightarrow 4)- β -D-glucopyranosyl-(1 \rightarrow 4)- β -D-xylopyranoside] were also identified from acetone extract.

From GC-MS analyses 29 volatile phytochemical constituents with structural variation was first time identified. Retention times of Cannabinoids in GC-MS were quite similar, but their separation is good enough to distinguish them. As the high temperature is applied in GC, that causes the decarboxylation of acidic Cannabinoids to neutral Cannabinoids. So, from GC-MS analyses only neutral Cannabinoids could be identified. GC-MS analyses of ethanolic extract indicated two important Cannabinoids *i.e.*, Cannabinol, methyl derivative of Cannabidivarin and one steroid (Lanosterol). One important psychoactive Cannabinoid $\Delta^{(9)}$ -THC, esters and hydrocarbons were unveiled from the *n*-Hexane extract. From acetone extract another important anti-psychotic Cannabinoid *i.e.*, Cannabidiol was identified. Two novel compounds cobalt (ii) bis(O,O'-diethyldithiophosphate) and iodoctane were identified from the roots.

Use of LC-DAD-ESI-MS made it possible to identify both acidic and neutral Cannabinoids. Two acidic Cannabinoids *i.e.*, THCA and THVA glycosides could be identified from ethanolic extract. Hence, GC-MS and HPLC-MS have been proven to be a quick, efficient identification and quantification techniques. This comprehensive study of roots provided a solid evidence for the utilization of roots for drug discovery and medicinal purposes. *C. sativa* absorbs and accumulates heavy metals in the roots,

therefore roots are considered to be the good candidate for phytoremediation of soils contaminated with metals. To cutshort, this study provided a detailed picture of chromatographic and spectroscopic study of *C. sativa* roots.

References

- Abraham R. E., Barrow C. J. and Puri M. (2013).** Relationship to reducing sugar production and scanning electron microscope structure to pretreated hemp hurd biomass (*Cannabis sativa*). *Biomass and Bioenergy*, vol. 58, pp. 180-187.
- Ahmed S. A., Ross S. A., Slade D., Radwan M. M., Zulfiqar F., Matsumoto R. R., Xu Y-T., Viard E., Speth R. C., Karamyan V. T. and ElSohly M. A. (2008).** Cannabinoid ester constituents from high-potency *Cannabis sativa*. *Journal of Natural Products*, vol. 71, pp. 536-542.
- Arru L., Rognoni S., Baroncini M., Bonatti P. M. and Perata P. (2004).** Copper localization in *Cannabis sativa* L. grown in a copper-rich solution. *Euphytica*, vol. 140, pp. 33-38.
- Atoui A. K., Mansouri A., Boskou G. and Kefalas P. (2005).** Tea and herbal infusions: their antioxidant activity and phenolic profile. *Food chemistry*, vol. 89, pp. 27-36.
- Aviello G., Romano B., Borrelli F., Capasso R., Gallo L., Piscitelli F., Marzo V. D. and Izzo A. A. (2012).** Chemopreventive effect of the non-psychotropic phytocannabinoid cannabidiol on experimental colon cancer. *Journal of Molecular Medicine*, vol. 90, pp. 925-934.
- Behnaz B., Mikael S. and Lena B. (2013).** Manufacture and characterisation of thermoplastic composites made from PLA/hemp co-wrapped hybrid yarn prepregs. *Applied Science and Manufacturing*, vol. 50, pp. 93-101.
- Bloomquist E. R. (1971).** Marijuana : The Second Trip (Revised Edn.). *Glenco Press*, pp. 1-11.
- Borrellia F., Fasolino I., Capassoa R., Maiello F., Orlandoc P., Battistab G., Paganoa E., Marzod V. D. and Izzoa A. A. (2013).** Beneficial effect of the non-psychotropic plant cannabinoid cannabigerol on experimental inflammatory bowel disease. *Biochemical Pharmacology*, vol. 85, pp. 1306-1316.

-
- Calvaruso G., Pellerito O., Notaro A. and Giuliano M. (2012).** Cannabinoid associated cell death mechanisms in tumor models. *International Journal Oncology*, vol. 41, pp. 407.
- Campos A. C., Ortega Z., Palazuelos J., Fogaca M. V., Aguiar D. C., Alonso J. D., Gutierrez S. O., Villa H. V., Moreira F. A., Guzman M., Roperh I. G. and Guimaraes F. S. (2013b).** The anxiolytic effect of cannabidiol on chronically stressed mice depends on hippocampal neurogenesis: involvement of the endocannabinoid system. *Research on Applied Neurosciences*, vol. 16, pp. 1407-1419.
- Campos A. C., Soares V. P., Carvalho M. 15C. C., Ferreira F. R., Vicente M. A., Brandão M. L., Zuardi A. W., Zangrossi H. and Guimarães F. S. (2013a).** Involvement of serotonin-mediated neurotransmission in the dorsal periaqueductal gray matter on cannabidiol chronic effects in panic-like responses in rats. *Psychopharmacology*, vol. 226, pp. 13-24.
- Campos M. G. and Markham K. R. (2007).** Structure information from HPLC and online measured absorption spectra: Flavones, Flavonols and Phenolic acids. *Coimbra*, pp. 17-30.
- Cota D., Marsicano G., Lutz B., Vicennati V., Stalla G. K., Pasquali R. and Pagotto U. (2003).** Endogenous cannabinoid system as a modulator of food intake. *International Journal of Obesity*, vol. 27, pp. 289-301.
- Deiana and Serena (2013).** Medical use of *Cannabis*. Cannabidiol: A new light for schizophrenia? *Drug Testing and Analysis*, vol. 5, pp. 46-51.
- Docimo T., Consonni R., Coraggio I. and Mattana M. (2013).** Early Phenylpropanoid Biosynthetic Steps in *Cannabis sativa*. Link between Genes and Metabolites. *International Journal of Molecular Sciences*. vol. 14, pp. 13626-13644.
- Elsohly M. A. (2006).** Marijuana and the Cannabinoids. *Humana Press*, pp. 87-90.

-
- Elsohly M. A. and Slade D. (2005).** Chemical constituents of marijuana. The complex mixture of natural Cannabinoids. *Life Sciences*, vol. 78, pp. 539-548.
- Fitzgerald K. T., Bronstein A. C. and Newquist K. L. (2013).** Marijuana Poisoning. *Topics in Companion Animal Medicine*, vol. 28, pp. 8-12.
- Fusari P., Rovellini P. and Folegatti L. (2013).** Oil and flour of *Cannabis sativa* L. multiscreening analysis of mycotoxins, phthalates, polycyclic aromatic hydrocarbons, metals and pesticide residues. *Rivista Italiana Delle Sostanze Grasse*, vol. 90, pp. 9-19.
- Gagnea S. J., Stouta J. M., Liua E., Boubakira Z., Clarka S. M. and Pagea J. E. (2012).** Identification of olivetolic acid cyclase from *Cannabis sativa* reveals a unique catalytic route to plant polyketides. *Proceedings of the National Academy of Sciences of the United States of America*, vol. 109, pp. 12811-12816.
- Gamage T. F. and Lichtman A. H. (2012).** The Endocannabinoid system: role in energy regulation. *Pediatric blood and cancer*, vol. 58, pp. 144-148.
- Garcia S. G., Hospido A., Feijoo G. and Moreira M. T. (2012).** Life cycle assessment of hemp hurds use in second generation ethanol production. *Biomass and Bioenergy*, vol. 36, pp. 268-279.
- Greaves J. and Roboz J. (2014).** Mass Spectrometry for the Novice. *CRC press Taylor and Francis Group*, pp. 15-19.
- Haney A. and Bazzaz F.A. (1970).** Some ecological implications of the distribution of hemp (*Cannabis sativa* L.) in the United States of America. *The Botany and Chemistry of Cannabis*, pp. 39-48.
- Harrison J. H. (1957).** The experimental modification of sex expression in flowering plants. *Biological Reviews*, vol. 32, pp. 1-51.
- Hazekamp A., Peltenburg A., Verpoorte R. and Giroud C. (2007).** Chromatographic and spectroscopic data of cannabinoids from *Cannabis*

sativa L. *Journal of Liquid Chromatography and Related Technologies*, vol. 28, pp. 2361-2382.

Hazekamp A., Simonsa R., Loomana A. P., Sengers M., Zwedena R. V. and Verpoortea R. (2004). Preparative isolation of cannabinoids from *Cannabis sativa* by centrifugal partition chromatography. *Journal of Liquid Chromatography and Related Technologies*, vol. 27, pp. 2421-2439.

Hillestad A., Wold J. K. and Paulsen B. S. (1977). Structural studies of water soluble glycoproteins from *Cannabis sativa* L. *Carbohydrate Research*, Vol. 57, pp. 135-144.

Holland B. J., Francis P. S., Li B., Tsuzuki T., Adcock J. L., Barnett N. W. and Conlan X. A. (2012). Chemiluminescence detection of cannabinoids and related compounds with acidic potassium permanganate. *Drug Testing and Analysis*, vol. 4, pp. 675-679.

Hong Y., Zhou Y., Wang Y., Xiao S., Liao D. J., and Zhao Q. (2013). PPAR gamma mediates the effects of WIN55, 212-2, synthetic cannabinoid, on the proliferation and apoptosis of the BEL-7402 hepatocarcinoma cells. *Molecular Biology Reports*, vol. 40, pp. 6287-6293.

Huang N., Siegel M. M., Kruppa G. H. and Laukien F. H. (1999). Automation of a fourier transform ion cyclotron resonance mass spectrometer for acquisition, analysis and e-mailing of high resolution exact mass electrospray ionization mass spectral data. *Journal of American Society Mass spectrometry*, vol. 10, pp. 1166-1173.

Huang Y., Chen L., Feng L., Guo F. and Li Y. (2013). Characterisation of total phenolic constituents from the stems of *Spatholobus suberectus* using LC-DAD-MSⁿ and their inhibitory effect on human neutrophil elastase activity. *Molecules*, vol. 18, pp. 7549-7556.

Husseini L., Leussink V. I., Warnke C., Hartung H. P. and Kieseier B. C. (2012). Cannabinoids for symptomatic therapy of Multiple Sclerosis. *Nervenarz*, vol. 83, pp. 695.

-
- Ibrahim A. K., Radwan M. M., Ahmed S. A., Slade D., Ross S. A., Elsohly M. A. and Khan I. A. (2010).** Microbial metabolism of cannflavin A and B isolated from *Cannabis sativa*. *Phytochemistry*, vol. 71, pp. 1014-1019.
- Ilias Y., Rudaz S., Mathieu P., Christen P. and Veuthey J. L. (2005).** Extraction and analysis of different *Cannabis* samples by headspace solid-phase microextraction combined with gas chromatography-mass spectrometry. *Journal of Separation Science*, vol. 28, pp. 2293-2300.
- Jaraboa R., Fuentea E., Montea M. C., Savastano H., Mutjéc P. and Negroa C. (2012).** Use of cellulose fibers from hemp core in fiber-cement production. Effect on flocculation, retention, drainage and product properties. *Industrial Crops and Products*. vol. 39, pp. 89-96.
- Kreugera E., Siposb B., Zacchib G., Svenssonc S. E. and Björnssona L. (2011).** Bioconversion of industrial hemp to ethanol and methane: The benefits of steam pretreatment and co-production. *Bioresource Technology*, vol. 102, pp. 3457-3465.
- Lachenmeier D. W., Kroener L., Musshoff F. and Madea B. (2004).** Determination of cannabinoids in hemp food products by use of headspace solid-phase microextraction and gas chromatography-mass spectrometry. *Analytical and Bioanalytical Chemistry*, vol. 378, pp. 183-189.
- Lavoie J. M. and Beauchet R. (2012).** Biorefinery of *Cannabis sativa* using one- and two-step steam treatments for the production of high quality fibres. *Industrial Crops and Products*, vol. 37, pp. 275-283.
- Lin L-Z. and Harnly J. M. (2007).** A screening method for identification of glycosylated Flavonoids and other phenolic components using a standard analytical approach for all plant materials. *Journal of Agricultural Food Chemistry*, vol. 51, pp. 1084-1096.
- Linger P., Ostwald A. and Haensler J. (2005).** *Cannabis sativa* L. growing on heavy metal contaminated soil: growth, cadmium uptake and photosynthesis. *Biologia Plantarum*, vol. 49, pp. 567-576.

-
- Lopesa C. F. B., Angelisa B. B., Purdentea H. M., Souzaa B. V.G., Cardosob S. V. and Ribeiroa R. L. M. A. (2012).** Concomitant consumption of marijuana, alcohol and tobacco in oral squamous cell carcinoma development and progression: Recent advances and challenges. *Archives of Oral Biology*, vol. 57, pp. 1026-1033.
- Macedo M. P., Kosmann C. and Roberto P-L. J. (2013).** Origin of samples of *Cannabis sativa* through insect fragments associated with compacted hemp drug in South America. *Revista Brasileira De Entomologia*, vol. 57, pp. 197-201.
- Mansouri H., Salari F. and Asrar Z. (2013).** Ethephon application stimulates cannabinoids and plastidic terpenoids production in *Cannabis sativa* at flowering stage. *Industrial Crops and Products*, vol. 46, pp. 269-273.
- Markham K. R. (1982).** Techniques of Flavonoid Identification. *Academic Press INC. (LONDON) LTD*, pp. 52-60.
- Marrota L., Lefeuvrea A., Pontoire B., Bourmauda A. and Baley C. (2013).** Analysis of the hemp fiber mechanical properties and their scattering. *Industrial Crops and Products*, vol. 51, pp. 317-327.
- Mecha M., Feliú A., Iñigo P. M., Mestre L., Salinas F. J. C. and Guaza C. (2013).** Cannabidiol provides long-lasting protection against the deleterious effects of inflammation in a viral model of Multiple Sclerosis: A role for A2A receptor. *Neurobiology of Disease*, vol. 59, pp. 141-150.
- Müller-Vahl K. R. (2013).** Treatment of Tourette syndrome with Cannabinoids. *Behavioural Neurology*, vol. 27, pp. 119-124.
- Novotny M., Lee M. L., Low C. E. and Raymond A. (1976).** Analysis of marijuana samples from different origins by high resolution gas-liquid chromatography for forensic application. *Analytical Chemistry*, vol. 48, pp. 24-29.

-
- Pan X., Niu G. and Liu H. (2003).** Microwave-assisted extraction of tea polyphenols and tea caffeine from green tea leaves. *Chemical Engineering and Processing*, vol. 42, pp. 129-133.
- Pavia D. L., Lampman G. M., Kriz G. S. and Vyvyan J. R. (2011).** Introduction to Spectroscopy. *Cengage learning Publisher*, 4th Edn. , pp. 367-394.
- Pelt B. V. (2008).** Characterization of medicinal properties of *Cannabis sativa* L. roots. *Humana press*, pp. 3-11.
- Petrova S., Benesova D. and Soudek P. (2012).** Enhancement of metalloids phytoextraction by *Cannabis sativa* L. *Journal of Food Agriculture and Environment*, vol. 10, pp. 631-641.
- Pisanti S., Malfitano A. M. Grimaldi C. and Bifulco M. (2009).** Use of cannabinoid receptor agonists in cancer therapy as palliative and curative agents. *Best Practice and Research Clinical Endocrinology and Metabolism*, vol. 23, pp. 117-131.
- Politia M., Peschela W., Wilsona N., Zloh M., Prietoea J. M. and Heinricha M. (2008).** Direct NMR analysis of cannabis water extracts and tinctures and semi-quantitative data on Δ^9 -THC and Δ^9 -THC-acid. *Phytochemistry*, vol. 69, pp. 562-570.
- Puangsin B., Fujisawa S., Kuramae R. Saito T. and Isogai A. (2013).** TEMPO-Mediated oxidation of hemp bast holocellulose to prepare cellulose nanofibrils dispersed in water. *Journal of Polymers and the Environment*, vol. 21, pp. 555-563.
- Radwan M. M., Ross S. A., Slade D., Ahmed S. A., Zulfiqar F. and ElSohly M. A. (2008).** Isolation and characterisation of new *Cannabis* constituents form high potency variety. *Planta Medica*, vol. 74, pp. 267-272.
- Rehman M. S., Rashida N., Saif A., Mahmood T. and Hana J-I (2013).** Potential of bioenergy production from industrial hemp (*Cannabis sativa*): Pakistan

perspective. *Renewable and Sustainable Energy Reviews*, vol. 18, pp. 154-164.

Ross S. A., ElSohly H. N., ElKashoury E. A. and ElSohly M. A. (1996). Fatty acids of *Cannabis seeds*. *Phytochemical Analysis*, Vol. 7, pp. 279-283.

Ross S. A., ElSohly M. A., Sultana G. N. N., Mehmedic Z., Hossain C. F. and Chandra S. (2005). Flavonoid glycosides and Cannabinoids from the pollen of *Cannabis sativa* L. *Phytochemical Analysis*, vol. 16, pp. 45-48.

Rothschild M., Bergstrom G. and Wangberg SA. (2005). *Cannabis sativa* volatile compounds from pollen and entire male and female plants of two variants, Northern Lights and Hawaiian Indica. *Botanical Journal of the Linnean Society*, vol. 147, pp. 387-397.

Russo and Ethan B. (2011). Taming THC: potential *Cannabis* synergy and phytocannabinoid terpenoid entourage effects. *British Journal of Pharmacology*, vol. 163, pp. 1344-1364.

Rustichelli C., Ferioli V., Baraldi M., Zanolli P. and Gamberini G. (1998). Analysis of Cannabinoids in Fiber Hemp Plant Varieties (*Cannabis sativa* L.) by High-Performance Liquid Chromatography. *Chromatographia*, vol. 48, pp. 215-222.

Shi G., Liu C., Cui M., Ma Y. and Cai Q. (2011). Cadmium tolerance and bioaccumulation of 18 hemp accessions. *Applied Biochemistry and Biotechnology*, vol. 168, pp. 163-173.

Steiner W. E., Clowers B. H. and Hill H. H. (2003). Rapid separation of phenylthiohydantoin amino acids: ambient pressure ion mobility mass spectrometry (IMMS). *Analytical and Bioanalytical Chemistry*, vol. 375, pp. 99-102.

Stott C. G. and Guy GW. (2004). Cannabinoids for the pharmaceutical industry. *Euphytica*, vol. 140, pp. 83-93.

-
- Sun X., and Dey S. K. (2012).** Endocannabinoid Signaling in Female Reproduction. *ACS Chemical Neuroscience*, vol. 3, pp. 349-355.
- Tang C-H., Wang X-S., and Yang X-Q. (2009).** Enzymatic hydrolysis of hemp (*Cannabis sativa* L.) protein isolate by various proteases and antioxidant properties of the resulting hydrolysates. *Food Chemistry*, vol. 114, pp. 1484-1490.
- Tomita K., Machmudah S., Quitain A. T., Sasaki M., Fukuzato R. and Gotob M. (2013).** Extraction and solubility evaluation of functional seed oil in supercritical carbon dioxide. *Journal of Supercritical Fluid*, vol. 79, pp. 109-113.
- Trofin I. G., Vlad C. C. and Dabija G. (2011).** Influence of Storage Conditions on the Chemical Potency of Herbal *Cannabis*. *Revista De Chimie.*, vol. 62, pp. 639-645.
- Turner J. C. and Mahlberg P. G. (1982).** Simple high performance liquid chromatographic method for separating acidic and neutral Cannabinoids in *Cannabis sativa* L. *Journal of Chromatography*, vol. 253, pp. 295-303.
- Watson J. T. and Sparkman O. D. (2009).** Introduction to mass spectrometry, instrumentation, applications and strategies for data interpretation. *Wiley*, pp. 831-832.
- Wohlfarth A., Mahler H. and Auwaerter V. (2011).** Rapid isolation procedure for Δ^9 -Tetrahydrocannabinolic acid A (THCA) from *Cannabis sativa* using two flash chromatography systems. *Journal of Chromatography B-Analytical Technologies in the Biomedical and Life Sciences*, vol. 879, pp. 3059-3064.
- Yang R., Sua S., Lia M., Zhangb J., Haob X. and Zhang H. (2010).** One-pot process combining transesterification and selective hydrogenation for biodiesel production from starting material of high degree of unsaturation. *Bioresource Technology*, vol. 101, pp. 5903-5909.

Zampori L., Dotelli G. and Vernelli V. (2013). Life Cycle assessment of hemp cultivation and use of hemp-based thermal insulator materials in buildings. *Environmental and Science Technologies*, vol. 47, pp. 7413-7420.

Zulfiqara F., Rossa S. A., Sladea D., Ahmeda S. A., Radwana M. M., Alia Z., Khana I. A. and ElSohlya M. A. (2012). Cannabisol, a novel $\Delta^{(9)}$ -THC dimer possessing a unique methylene bridge, isolated from *Cannabis sativa*. *Tetrahedron Letters*, vol. 53, pp. 3560-3562.